

AD-A103 377

ARMY ELECTRONICS RESEARCH AND DEVELOPMENT COMMAND WS--ETC F/G 20/6  
LIDAR OBSERVATIONS AT 0.7 MICROMETER AND 10.6 MICROMETER WAVELENGTH--ETC(U)

JUL 80 J S RANDHAWA

UNCLASSIFIED ERADCOM/ASL-DR-80-0004

NL

1 of 1  
404  
10332

9

END  
DATE FILMED  
10-81  
DTIC

ADA103377

ERAD-80  
ASL-DR-80-0004

AD

Reports Control Symbol  
OSD-1366

LIDAR OBSERVATIONS AT 0.7  $\mu$ M AND 10.6  $\mu$ M WAVELENGTHS  
DURING DUSTY INFRARED TEST I (DIRT-I).

ADDITIONAL RESULTS

11 JUL 80

12 83

9  
12  
By  
J. S. RANDHAWA

DMC FILE COPY



US Army Electronics Research and Development Command  
ATMOSPHERIC SCIENCES LABORATORY

White Sands Missile Range, NM 88002

81 8 27 004

410663

## NOTICES

### Disclaimers

The findings in this report are not to be construed as an official Department of the Army position, unless so designated by other authorized documents.

The citation of trade names and names of manufacturers in this report is not to be construed as official Government indorsement or approval of commercial products or services referenced herein.

### Disposition

Destroy this report when it is no longer needed. Do not return it to the originator.

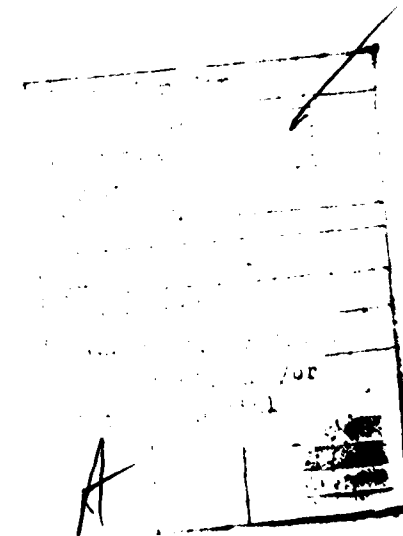
SECURITY CLASSIFICATION OF THIS PAGE (When Data Entered)

REPORT DOCUMENTATION PAGE		READ INSTRUCTIONS BEFORE COMPLETING FORM
1. REPORT NUMBER ASL-DR-80-0004	2. GOVT ACCESSION NO. AD-A103 377	3. RECIPIENT'S CATALOG NUMBER
4. TITLE (and Subtitle) LIDAR OBSERVATIONS AT 0.7μm AND 10.6μm WAVELENGTHS DURING DUSTY INFRARED TEST I (DIRT-I) Additional Results	5. TYPE OF REPORT & PERIOD COVERED R&D Technical Data Report	
7. AUTHOR(s) J. S. Randhawa	6. PERFORMING ORG. REPORT NUMBER	
9. PERFORMING ORGANIZATION NAME AND ADDRESS Atmospheric Sciences Laboratory White Sands Missile Range, NM 88002	10. PROGRAM ELEMENT, PROJECT, TASK AREA & WORK UNIT NUMBERS DA Task 1L162111AH71	
11. CONTROLLING OFFICE NAME AND ADDRESS US Army Electronics Research and Development Command Adelphi, MD 20783	12. REPORT DATE July 1980	
14. MONITORING AGENCY NAME & ADDRESS (if different from Controlling Office)	13. NUMBER OF PAGES 83	
16. DISTRIBUTION STATEMENT (of this Report)  Approved for public release; distribution unlimited.	15. SECURITY CLASS. (of this report)  UNCLASSIFIED	
17. DISTRIBUTION STATEMENT (of the abstract entered in Block 20, if different from Report)	15a. DECLASSIFICATION/DOWNGRADING SCHEDULE	
18. SUPPLEMENTARY NOTES		
19. KEY WORDS (Continue on reverse side if necessary and identify by block number) Lidar Obscuration Smoke clouds	Transmission Dust clouds	
20. ABSTRACT (Continue on reverse side if necessary and identify by block number) Two wavelength lidar measurements were made during the Dusty Infrared Test-I (DIRT-I) program conducted at White Sands Missile Range (WSMR) in October 1978. This report contains the additional results obtained during the test but not published in an earlier report.		

SECURITY CLASSIFICATION OF THIS PAGE(When Data Entered)

## CONTENTS

1. INTRODUCTION.....	5
2. EXPERIMENT.....	5
3. DATA.....	5
4. CONCLUSIONS.....	6



## 1. INTRODUCTION

The Dusty Infrared Test I (DIRT-I) was held at White Sands Missile Range (WSMR) in October 1978 to evaluate various techniques to measure physical and optical properties of battlefield dust. Since lidar technique represents one of the most promising techniques, two lidar systems: 10.6 $\mu$ m wavelength (ASL-lidar) and 0.7 $\mu$ m Ruby lidar system (Mark IX), were operated over a common 2-km optical path during this test. Primary lidar backscatter data for both wavelengths were recorded on magnetic tape by using Mark IX lidar data system<sup>1</sup> while independent 10.6 $\mu$ m lidar transmission data were recorded on strip chart in the ASL lidar van. Photographs were also taken every 30 to 60 seconds during each event of range-resolved 10.6 $\mu$ m backscatter amplitude data (A-Scope presentation). In an earlier report<sup>2</sup> a few results were described along with the experimental setup, calibration and operating procedures, and analysis technique. This report contains the rest of the results obtained during the test.

## 2. EXPERIMENT

The two lidar systems were positioned as shown in figure 1. Static TNT charges, artillery rounds, live artillery barrages, and an oil and rubber fire generated dust and smoke cloud in a test zone midway (1 km) between the lidar systems and a beam-stop lidar target.<sup>3</sup> Specifications for the 10.6 $\mu$ m lidar are given in table 1. Table 2 is an inventory and summary of the data collected during the DIRT-I program. In addition to the above data, television video records (video tape) of the lidar optical path were made during each event.

## 3. DATA

Data gathered by the two lidar systems are presented in figures 2 through 74. Data from October 2 through October 12 show only 10.6 $\mu$ m lidar backscatter and transmission, with the exception of event C-2 which shows the difference between the Ruby and CO<sub>2</sub> optical depths. Data taken on October 13 and 14 are presented under three categories for each event: (a) 10.6 $\mu$ m backscatter, (b) percent transmission as observed by the two-wavelengths system, and (c) optical depth difference (Ruby and CO<sub>2</sub>).

<sup>1</sup>E. E. Uthe and R. J. Allen, 1975, "A Digital Read Time Lidar Data Recording, Processing, and Display System," Optical and Quantum Electronics, 7:121

<sup>2</sup>Jan E. Van der Laan, 1979, Lidar Observations at 0.7 $\mu$ m and 10.6 $\mu$ m Wavelengths during Dusty Infrared Test-I (DIRT-I), ASL-CR-79-0001-2, US Army Atmospheric Sciences Laboratory, White Sands Missile Range, NM

<sup>3</sup>James D. Lindberg, 1979, Measured Effects of Battlefield Dust and Smoke on Visible, Infrared and Millimeter Wavelength Propagation: A Preliminary Report on Dusty Infrared Test-I (DIRT-I), ASL Technical Report 0021, White Sands Missile Range, NM

#### 4. CONCLUSIONS

Results of the DIRT-I program as presented in the earlier report indicate that the broad particle size distribution present in the dust generated at White Sands produces little if any wavelength-dependent transmission effects. The few observed exceptions, where greater 10.6 $\mu$ m transmission is indicated, generally can be explained by the presence of wavelength-dependent smoke (which was also generated by the detonations) along the optical path.

TABLE 1. ASL LIDAR SPECIFICATIONS

System Component	Specification	Comments
<u>Transmitter</u>		
Manufacturer	Lumonics Research Ltd., Model TEA-101-2	
Type	CO <sub>2</sub>	
Wavelength	10.6 μm	
Beam diameter	3.1 cm	
Beam divergence	1.2 mrad	
Operation	pulsed	
Energy	250 mJ	
Pulsewidth	75 ns (FWHM)	
PRF (maximum)	1 pps	No nitrogen gas mix
<u>Receiver</u>		
Telescope	12-inch (30 cm), Newtonian	
Field of view	1.23 mrad	
Detector	Honeywell Associates; HgCdTe photodiode; * $D = 1.3 \times 10^{10} \text{ cmHz}^{1/2} \text{W}^{-1}$ ; 100 MHz BW	LN <sub>2</sub> -cooled
Postamplifier	Linear: 26 dB gain, 100 MHz BW  Log: tangential sensitivity -111 dBr; ±0.5 dB linearity over 80-dB range; 15-ns rise time	

TABLE 2. LIDAR DATA INVENTORY

Date	Event	Data*					Comments
		1	2	3	4	5	
Oct. 2	A-1	X	✓	✓	✓	✓	X = not available; Mark IX not on site
	A-2	X	✓	✓	✓	✓	✓
	A-3	X	✓	✓	✓	✓	✓
	A-4	X	✓	✓	✓	✓	✓ = data available
Oct. 3	B-1	+	✓	✓	✓	✓	+
	B-2	+	✓	✓	✓	✓	✓
	B-3	+	✓	✓	✓	✓	✓
	B-4	+	✓	✓	✓	✓	✓
	B-5	+	✓	✓	✓	✓	✓
	B-6	+	✓	✓	✓	✓	✓
	B-7	+	✓	✓	✓	✓	✓
	B-8	+	✓	✓	✓	✓	✓
Oct. 5	C-1	✓	✓	✓	✓	✓	
Oct. 6	D-1	✓	✓	✓	✓	✓	X = not available;
	D-2	✓	✓	✓	✓	✓	ASL lidar digitizer
	D-3	✓	✓	✓	✓	✓	malfunction
	D-4	✓	✓	✓	✓	✓	X
Oct. 10	C-2	✓	✓	✓	✓	✓	
Oct. 11	E-1	✓	✓	✓	✓	✓	
	E-2	✓	✓	✓	✓	✓	
	E-3	✓	✓	✓	✓	✓	
	E-4	✓	✓	✓	✓	✓	
Oct. 12	F-1	✓	✓	✓	✓	✓	X = not available
	F-2	✓	✓	✓	✓	✓	ASL lidar digitizer
	F-3	✓	✓	✓	✓	✓	malfunction
	F-4	-X	-X	-X	-X	-X	-X (F-4) = live 155
Oct. 13	F-5	✓	✓	✓	✓	✓	mm rounds missed test
	F-6	✓	✓	✓	✓	✓	zone
	F-7	✓	✓	✓	✓	✓	
	F-8	✓	✓	✓	✓	✓	
Oct. 14	E-5	✓	✓	✓	✓	✓	
	E-6	✓	✓	✓	✓	✓	
	E-7	✓	✓	✓	✓	✓	
	E-8	✓	✓	✓	✓	✓	
	E-9	✓	✓	✓	✓	✓	
	E-10	✓	✓	✓	✓	✓	
Oct. 14	G-1	✓	✓	X	✓	✓	

- \* 1. Digitized 0.7 and 10.6  $\mu\text{m}$  range-resolved backscatter data; 9-track magnetic tape.
- 2. 10.6  $\mu\text{m}$  target return amplitude data; strip chart recordings.
- 3. 10.6  $\mu\text{m}$  digitized target return data; IBM card/tape format.
- 4. 10.6  $\mu\text{m}$  energy output; strip chart recordings.
- 5. 10.6  $\mu\text{m}$  range-resolved backscatter; (A-scope) photographs; polaroid sequence.

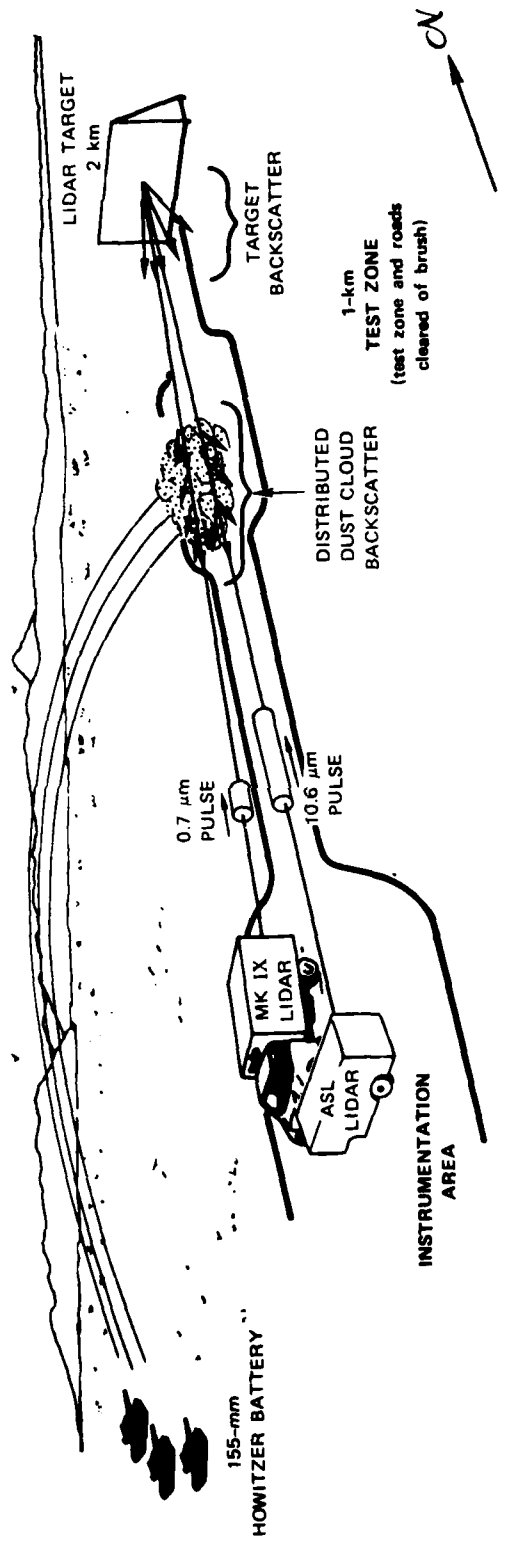


Figure 1. Experimental configuration for two-wavelength lidar observations - DIRT-1.

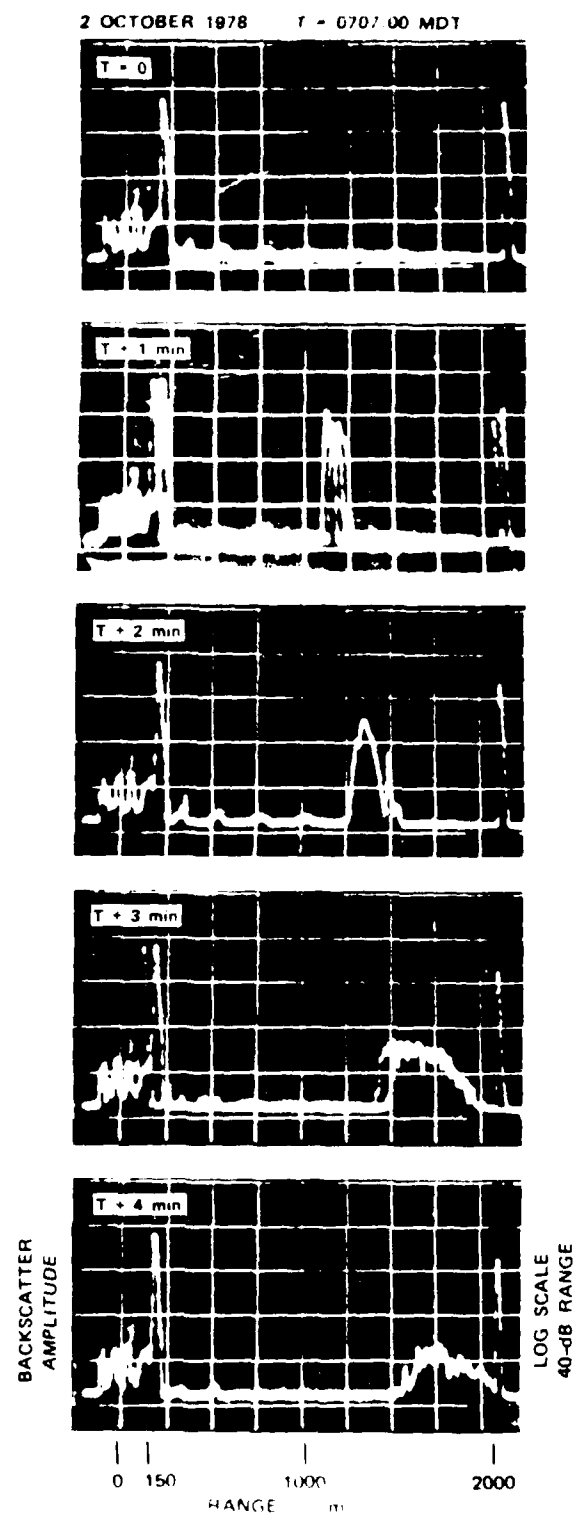


Figure 2. Event A-1 10,  $n_r$ , backscatter data.

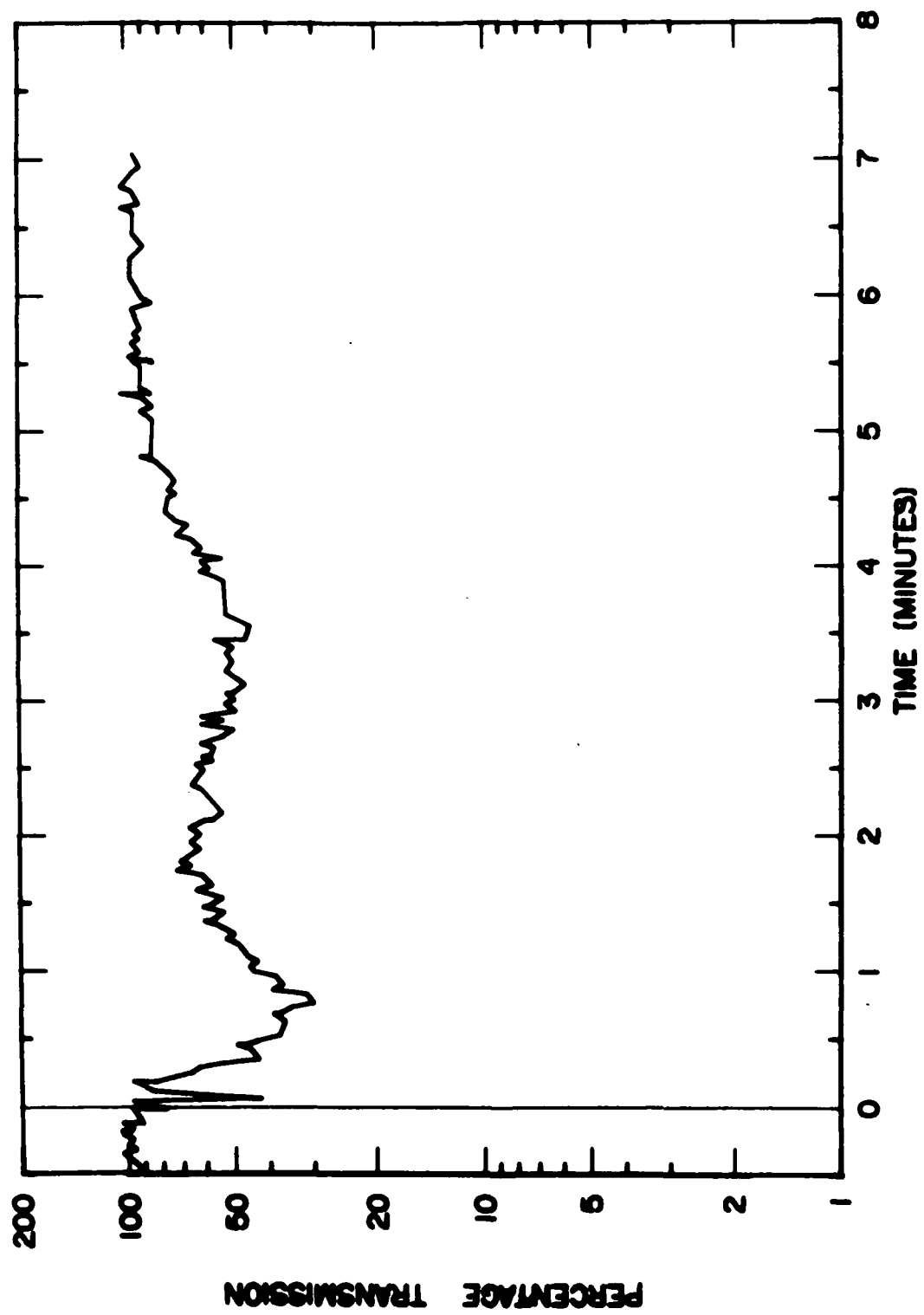


Figure 3. Event A-1 10.6 $\mu$ m transmission.

2 OCTOBER 1978 T = 0716 30 MDT

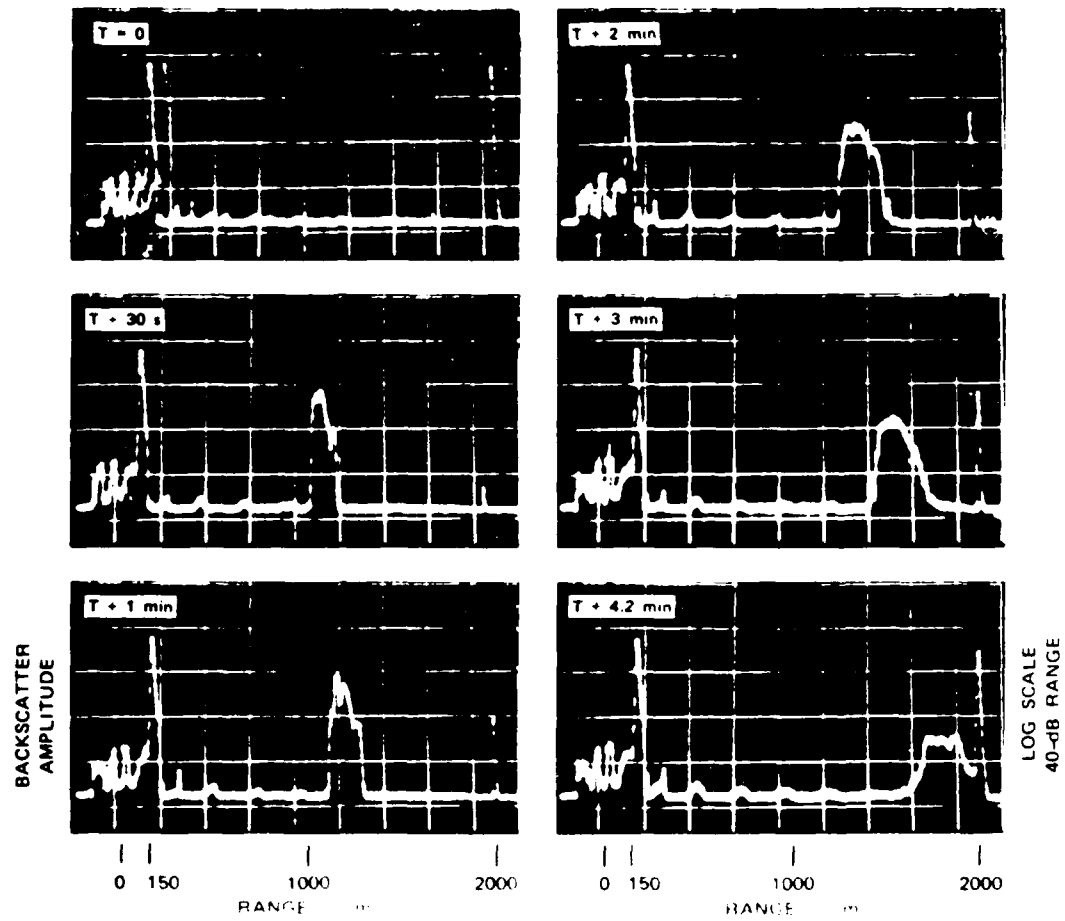


Figure 4. Event A-2 10.6  $\mu\text{m}$  backscatter data.

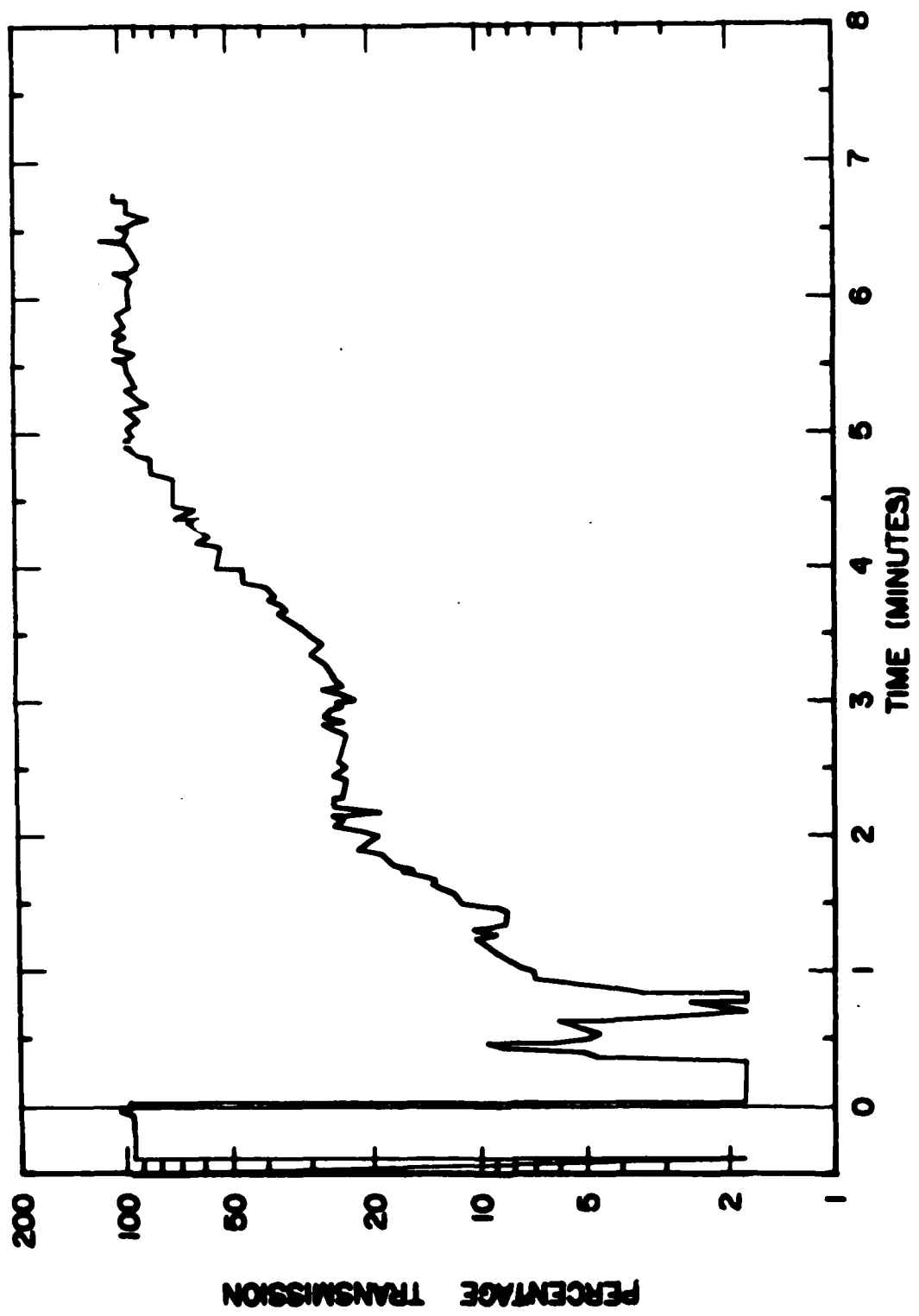


Figure 5. Event A-2  $10.6\mu\text{m}$  transmission.

2 OCTOBER 1978 T = 0729 00 MOT

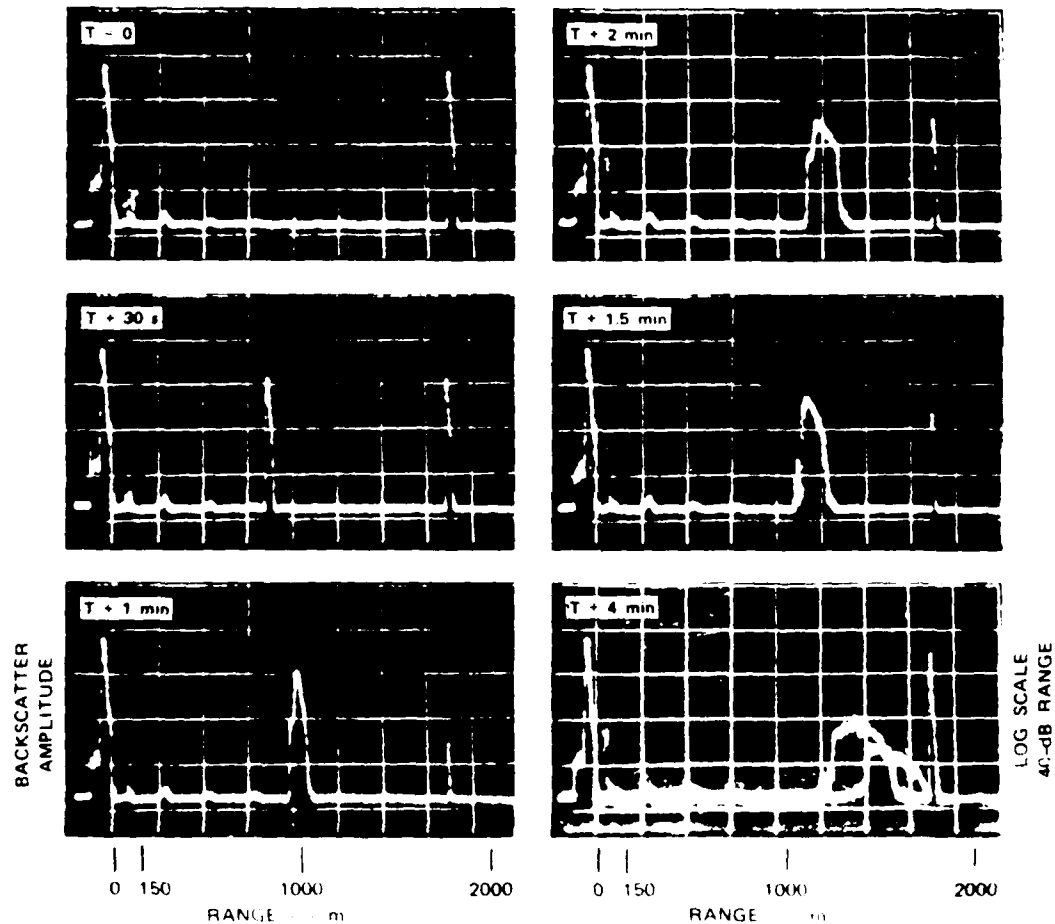


Figure 6. Event A-3 10.6 cm backscatter data.

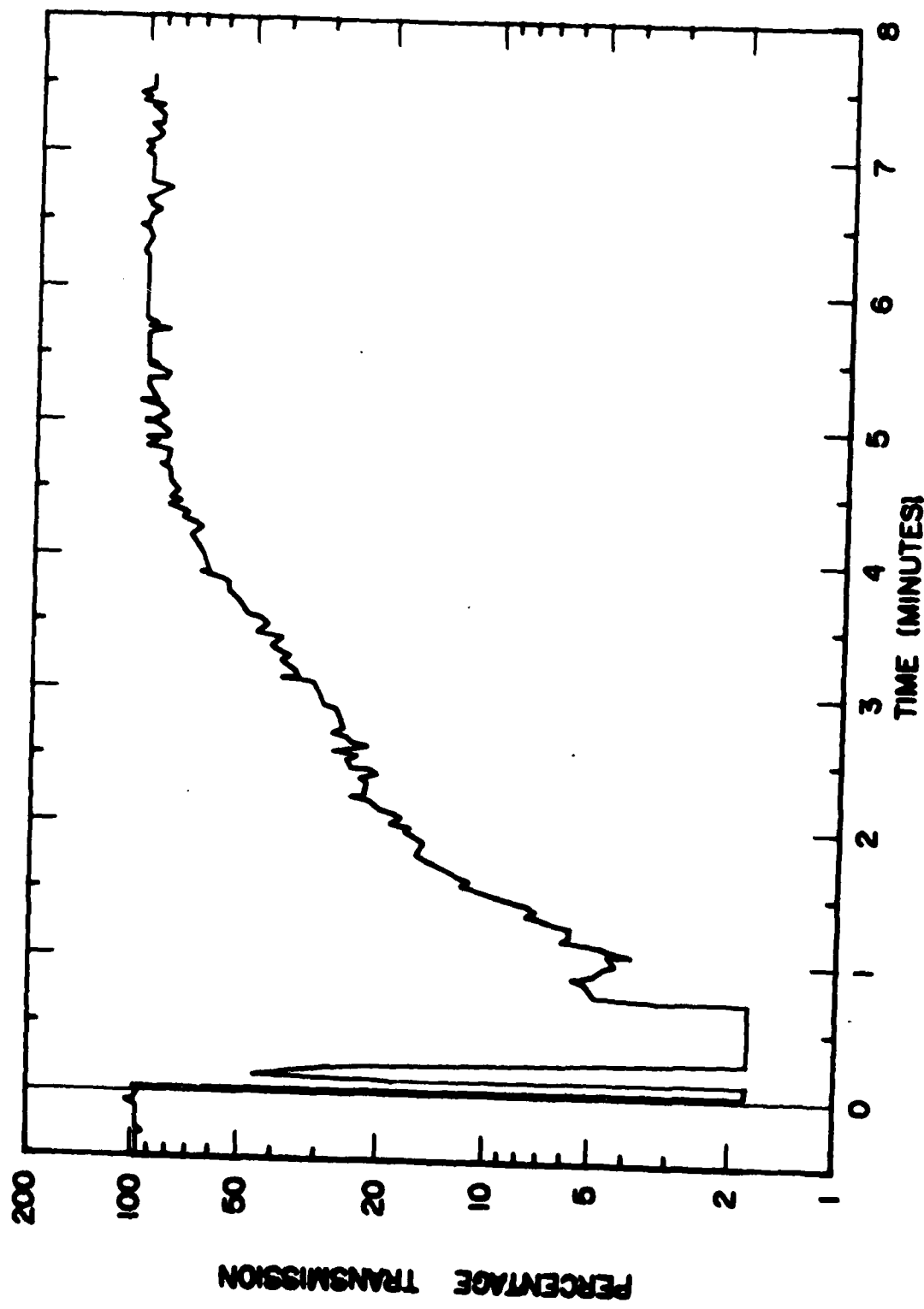


Figure 7. Event A-3 10.6 $\mu$ m transmission.

2 OCTOBER 1978 T = 0739 50 MDT

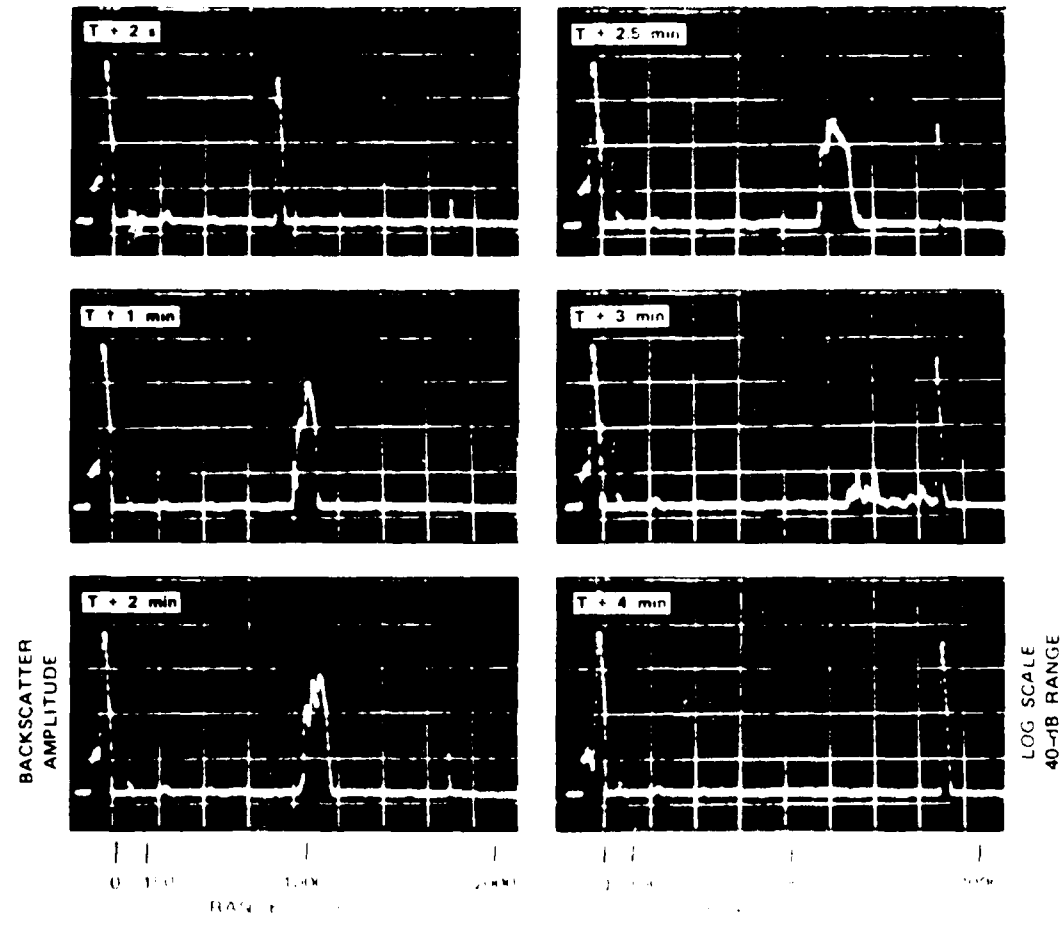


Figure 8. (From Fig. 4) A 4-10.6  $\mu$ m  $\times$  1000  $\mu$ m  $\times$  1000  $\mu$ m

3 OCTOBER 1978 T = 0710.00 MDT

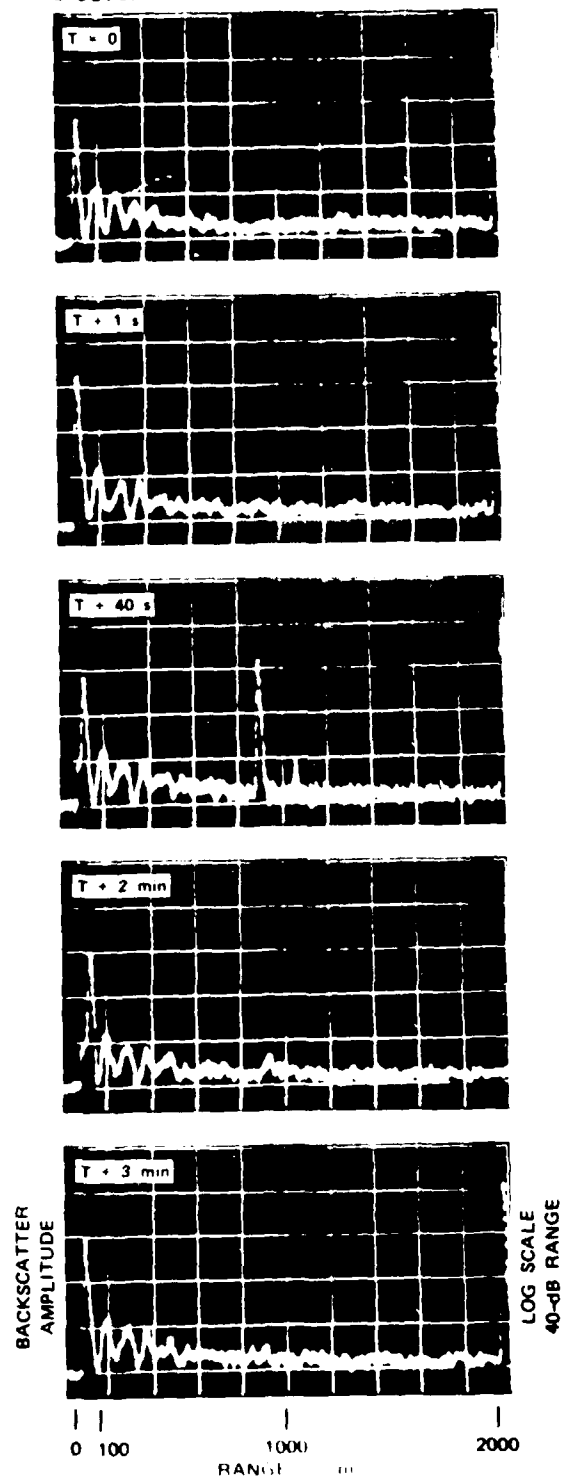


Figure 9. Event B-1 10,000 m - backscatter data.

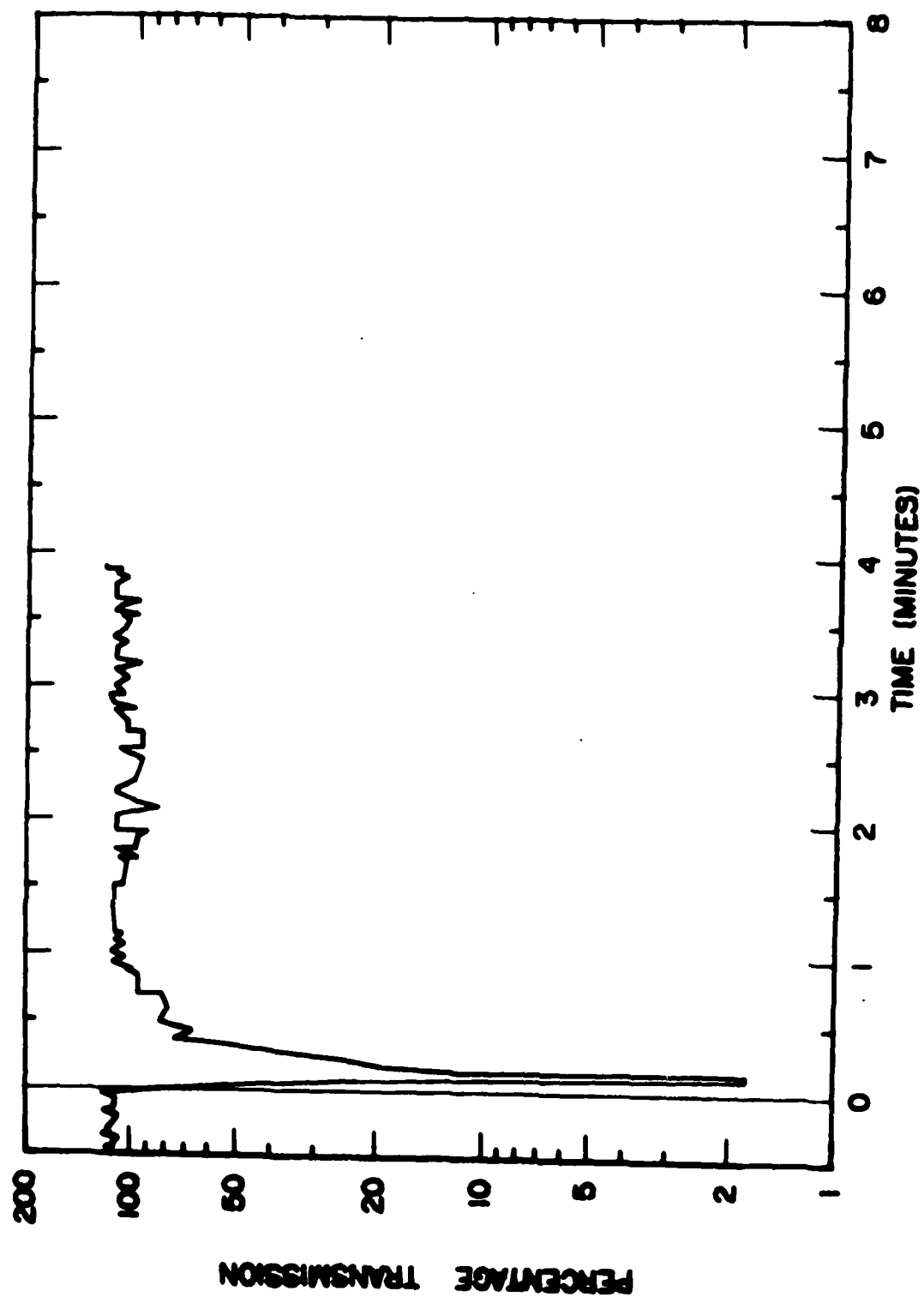


Figure 10. Event B-1 10.6  $\mu$ m transmission.

3 OCTOBER 1978      T = 0723 (0730) ZLT

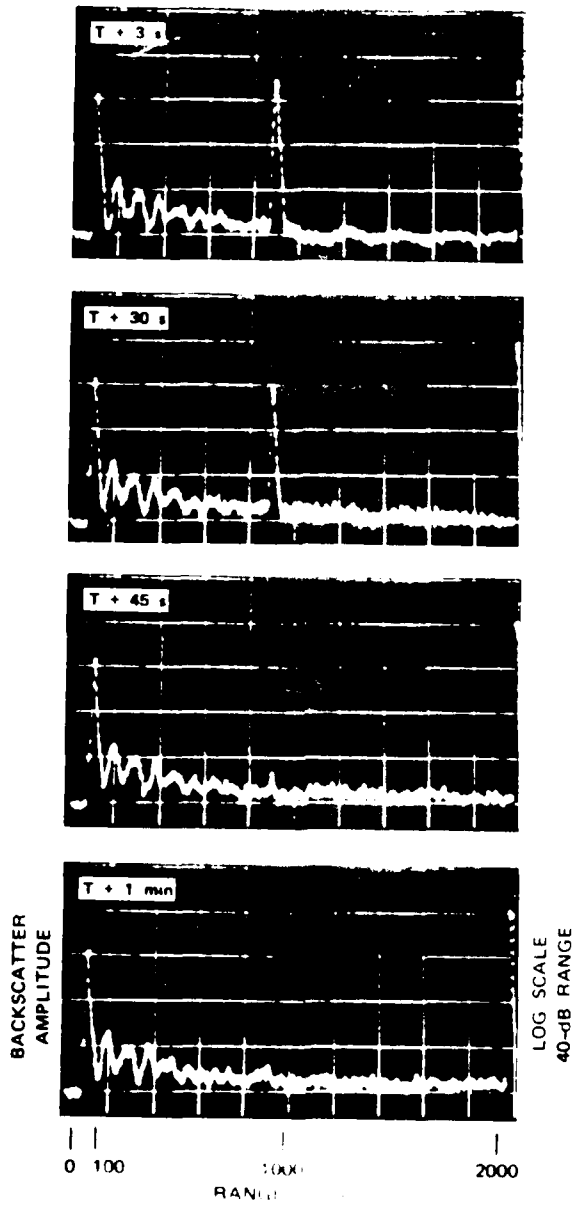


Figure 11. Event B-2. Seismometer backscatter data.

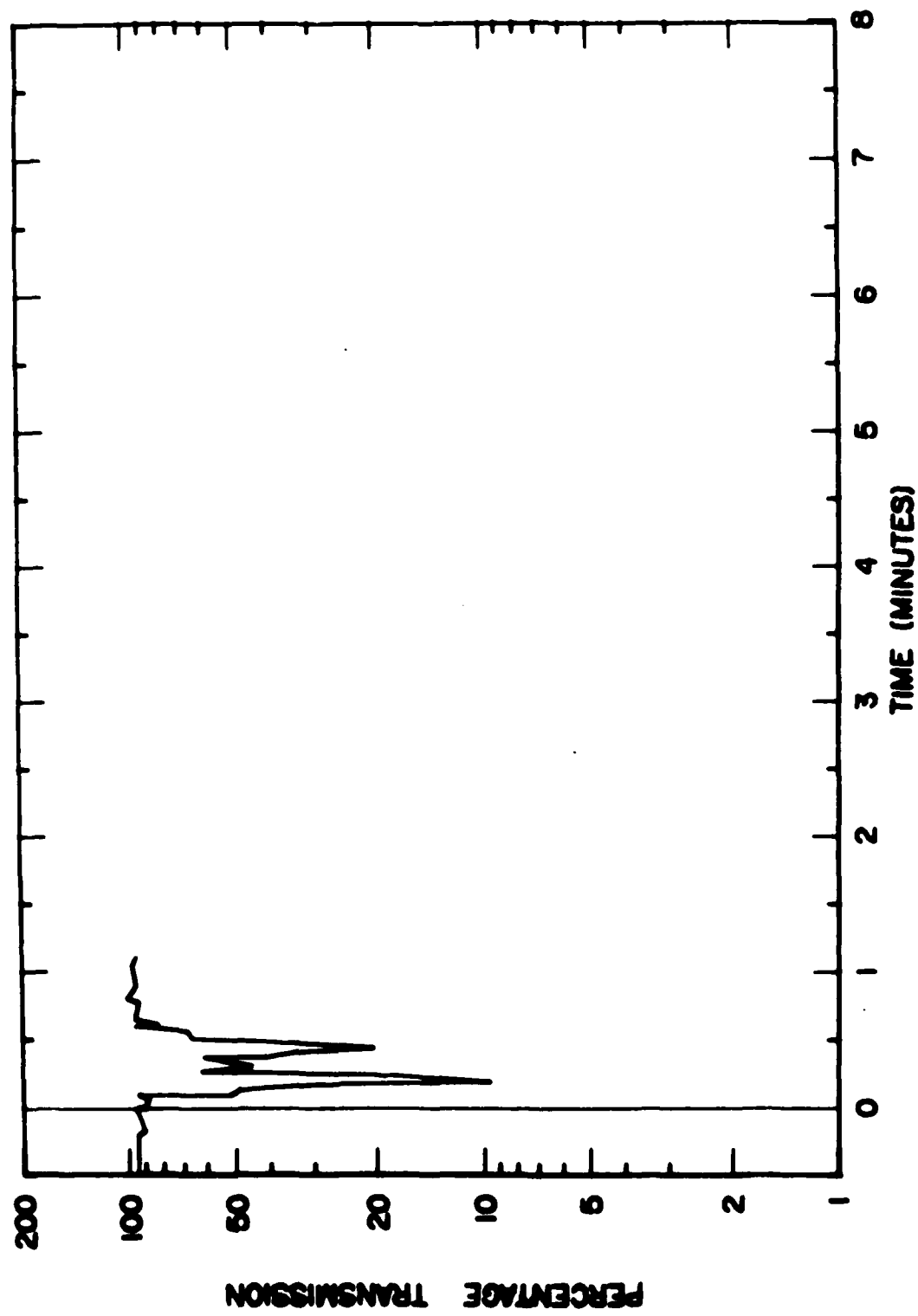


Figure 12. Event B-2 10.6 $\mu$ m transmission.

3 OCTOBER 1978 T = 0731.00 MDT

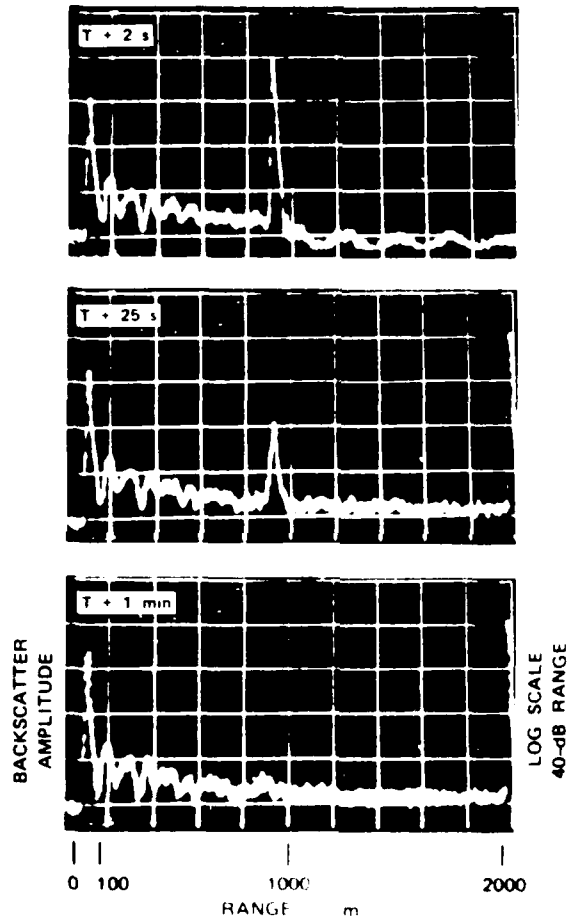


Figure 13. Event B-3 10.6 $\mu$ m backscatter data.

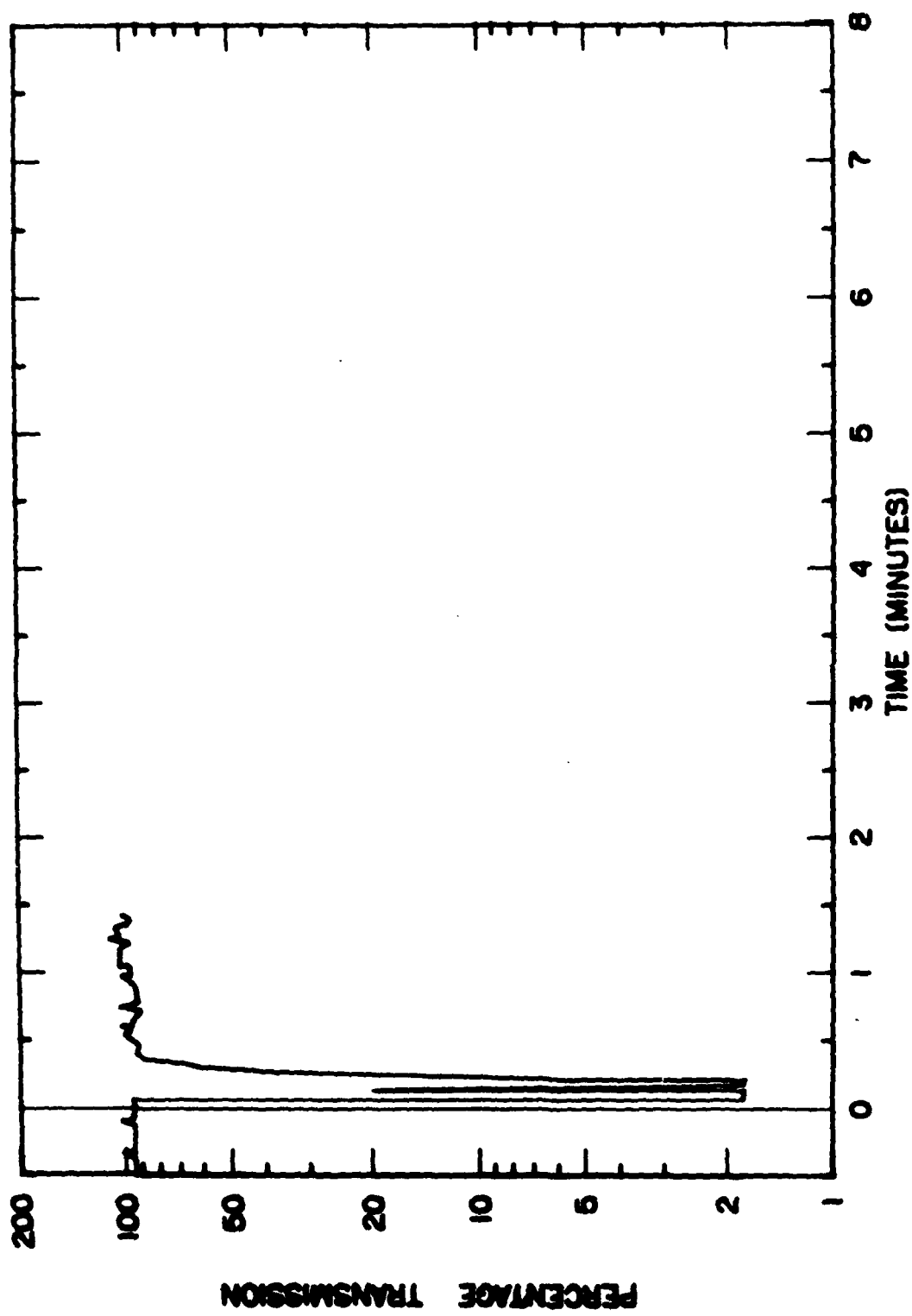


Figure 14. Event B-3  $10.6\text{ }\mu\text{m}$  transmission.

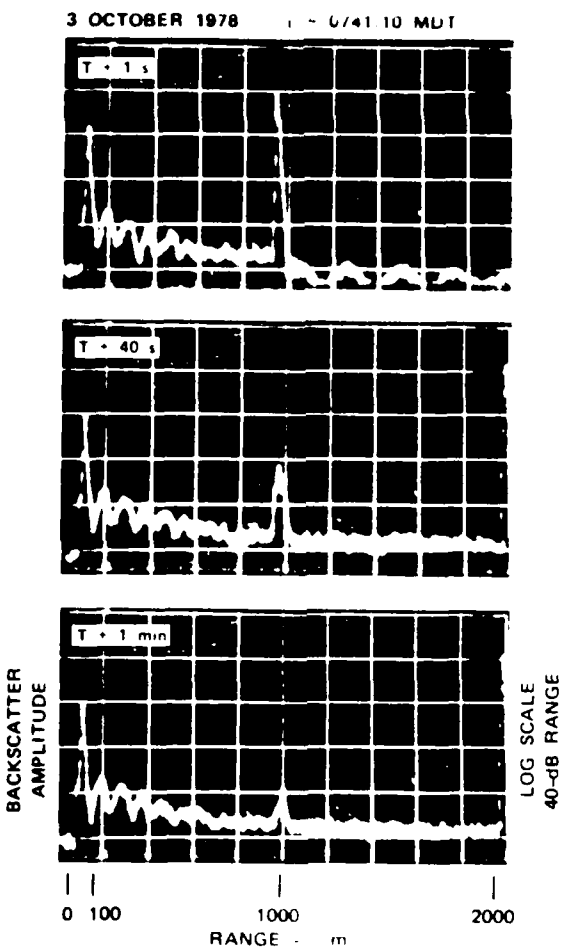


Figure 15. Event B-4 10.6  $\mu$ m backscatter data.

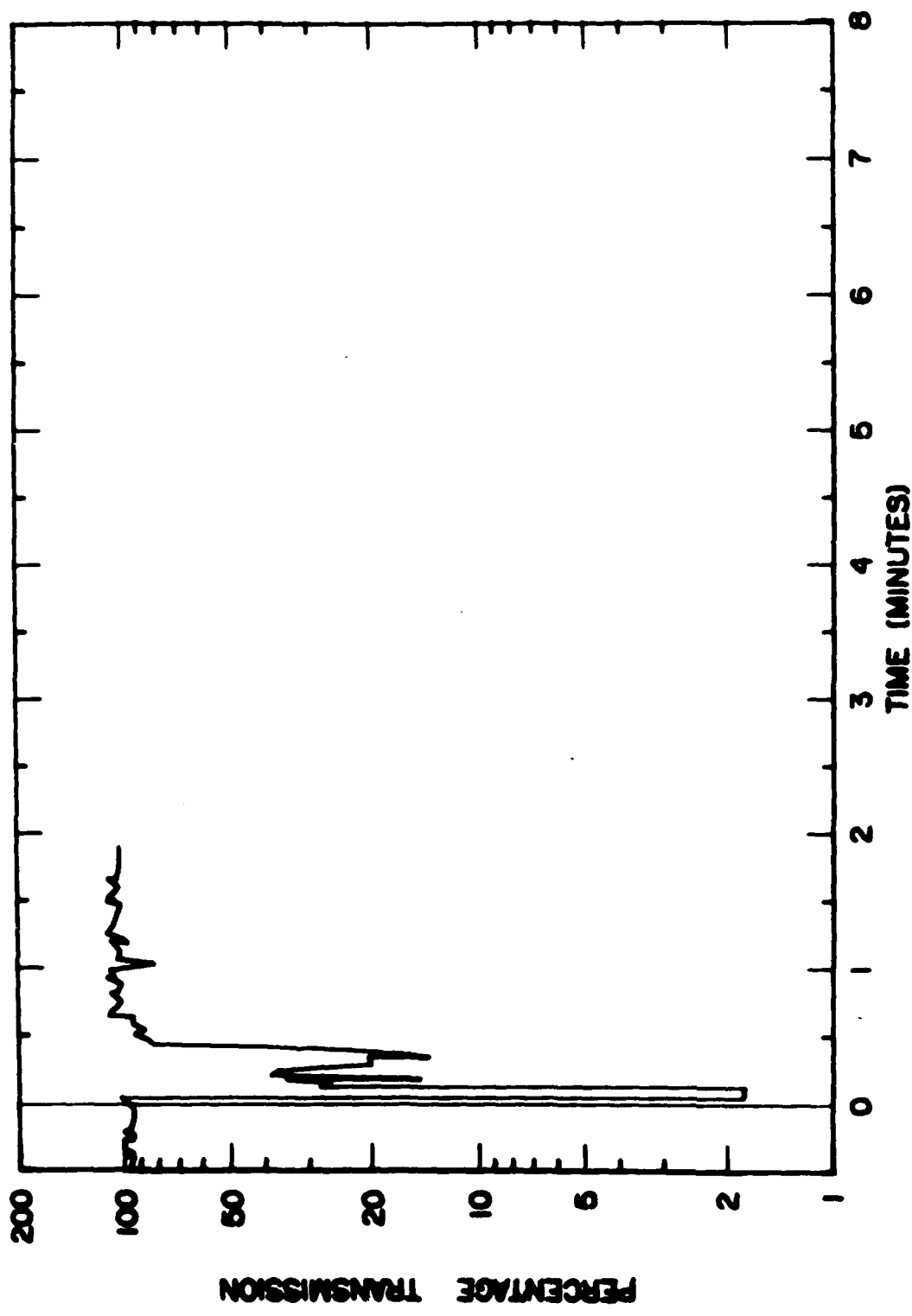
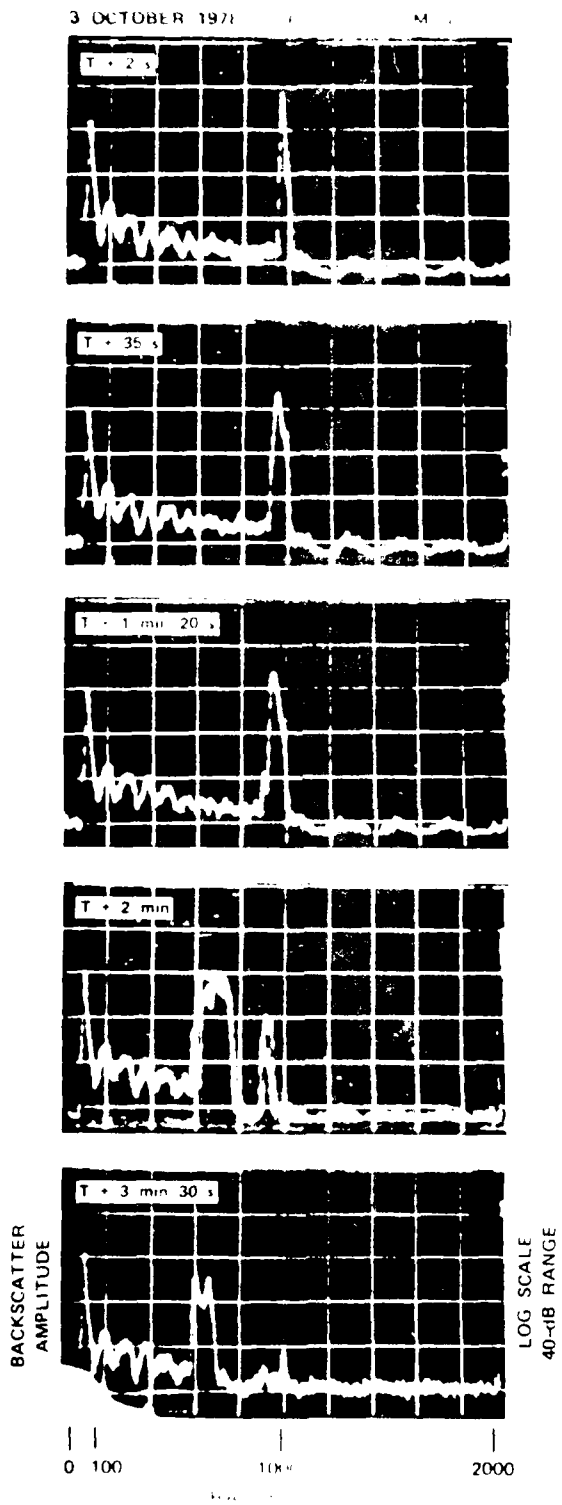


Figure 16. Event B-4  $10.6 \mu\text{m}$  transmission.



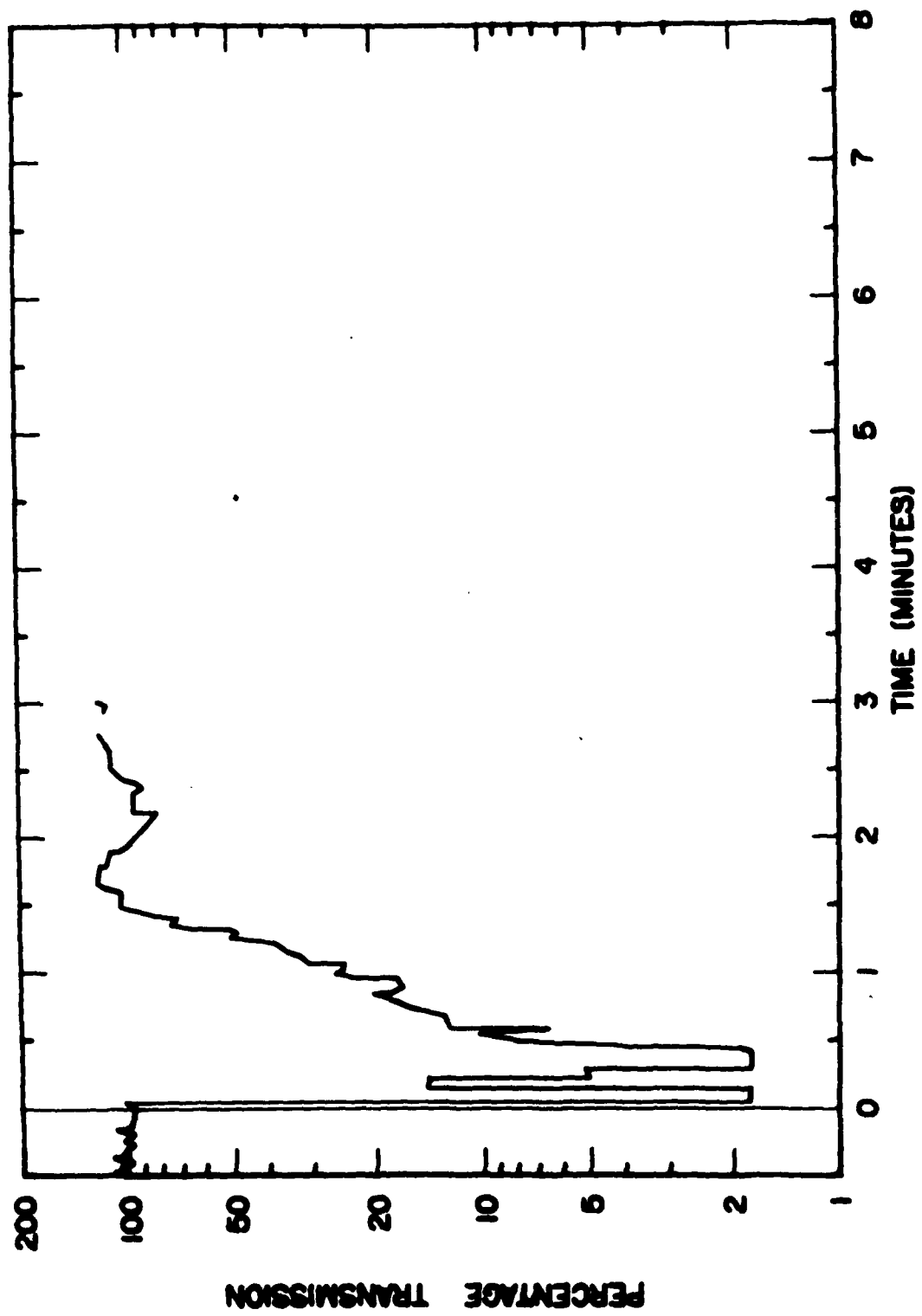


Figure 18. Event B-5 10.6 $\mu$ m transmission.

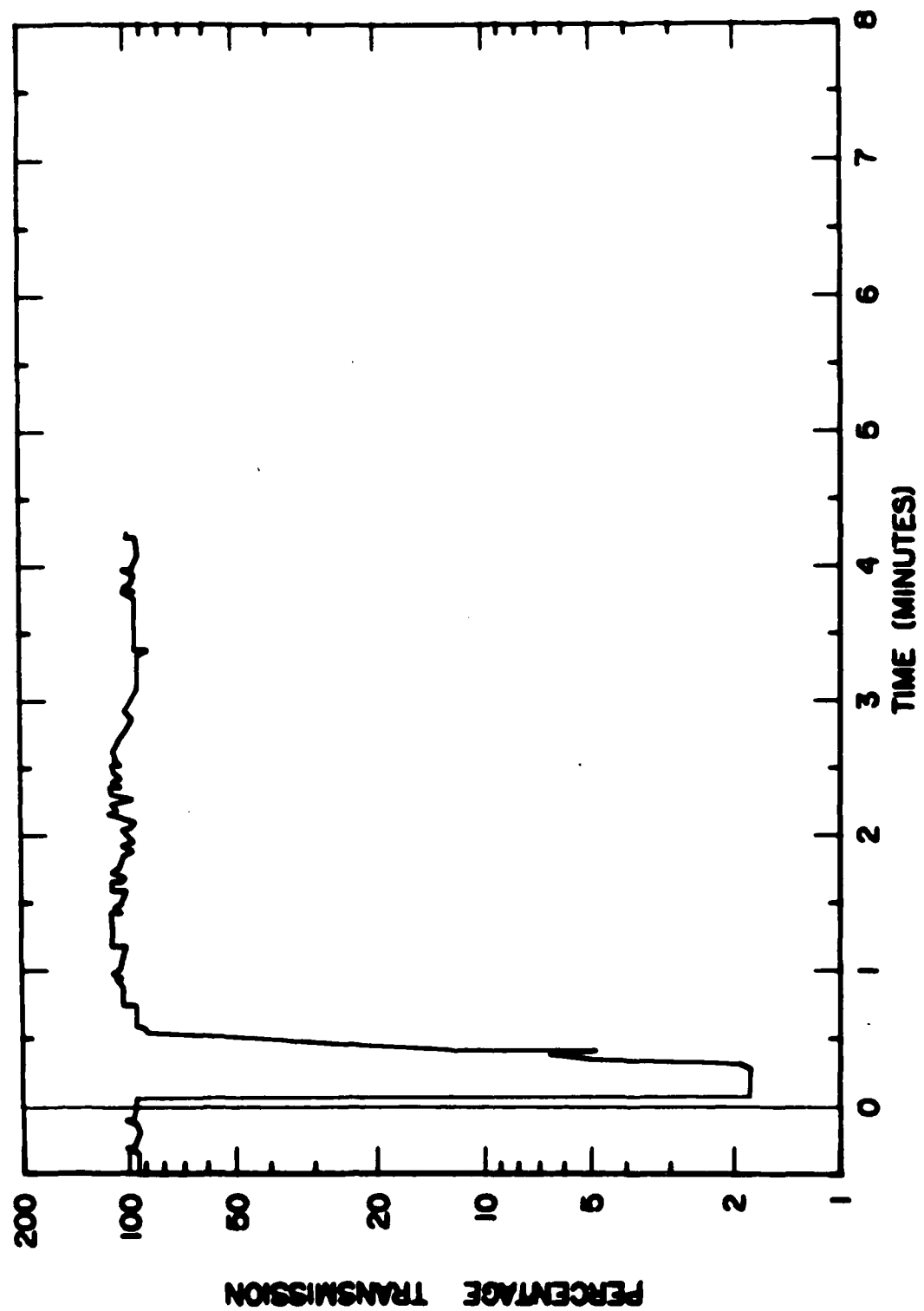


Figure 19. Event B-6 10.6  $\mu$ m transmission.

3 OCTOBY 9:18 T = 0815:00 MST

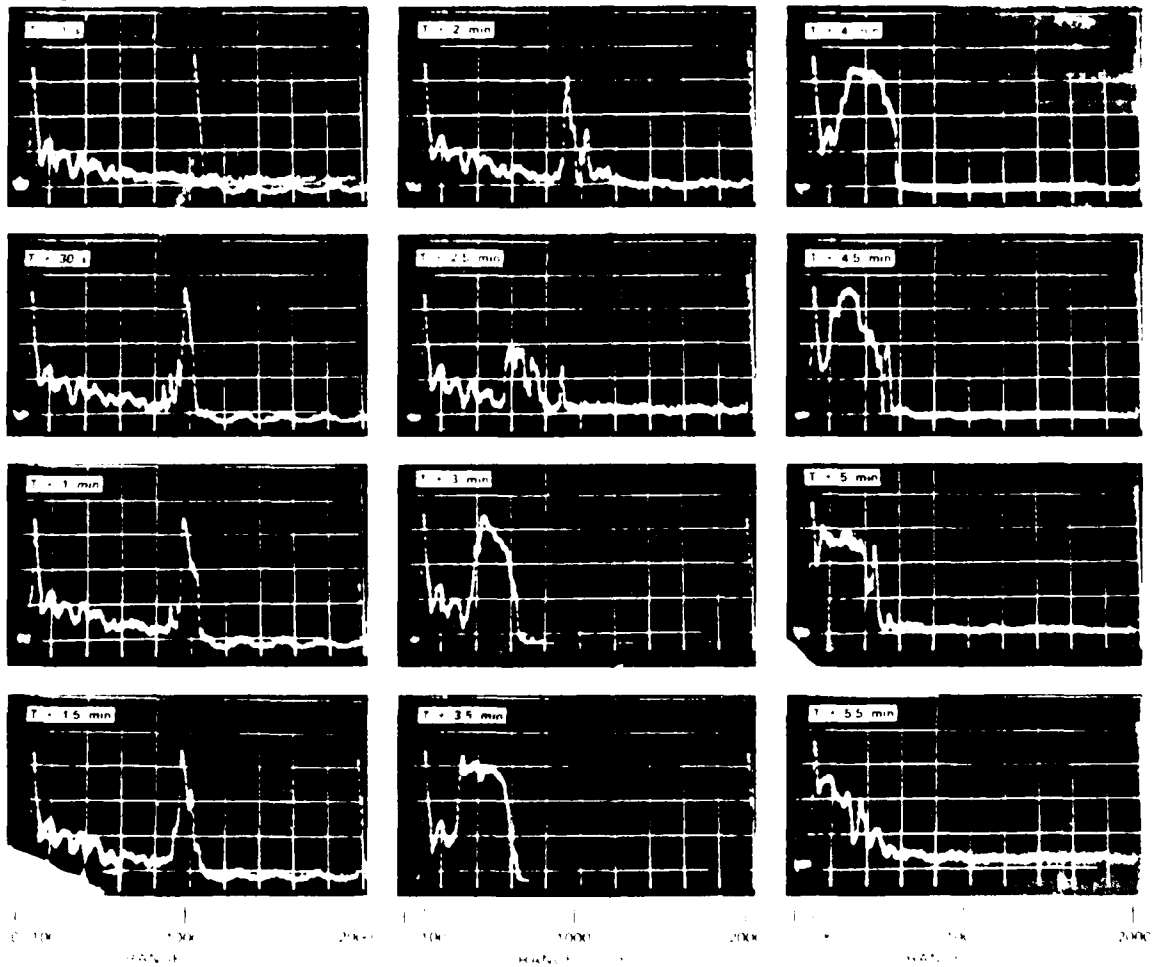


Fig. 1. Heart rate variability in a normal subject during a 10-min period of quiet rest.

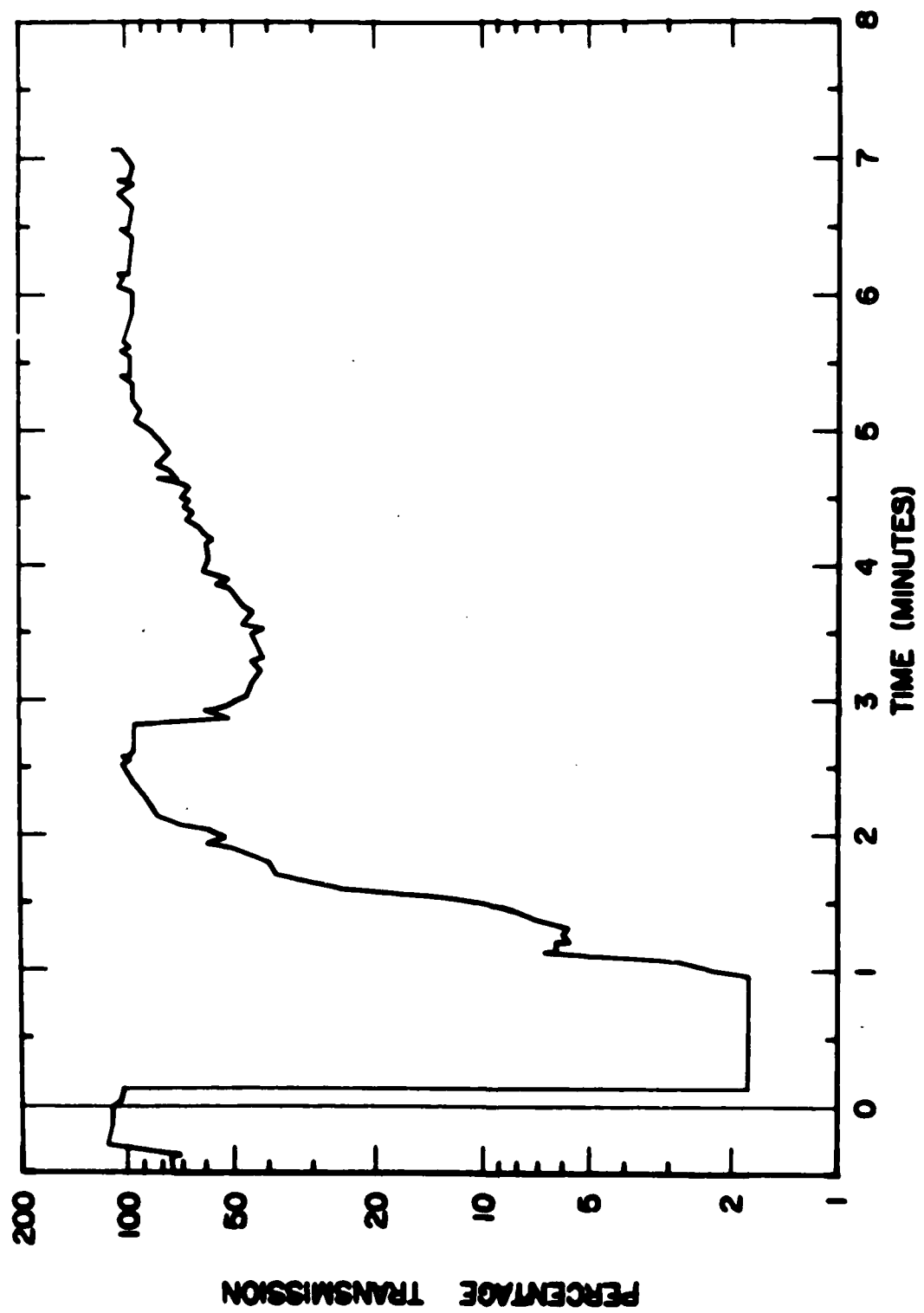
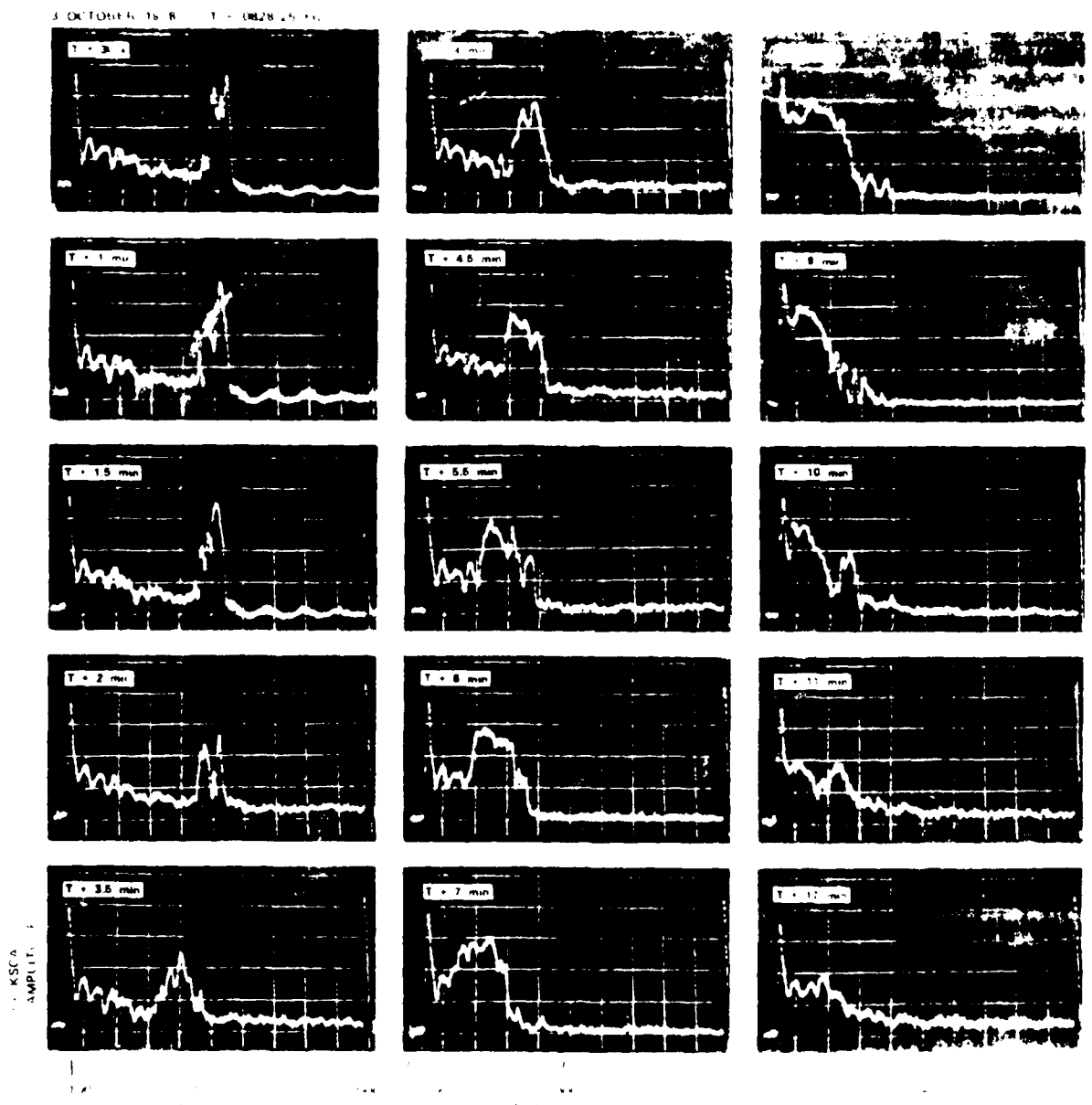


Figure 21. Event B-7 10.6 $\mu$ m transmission.



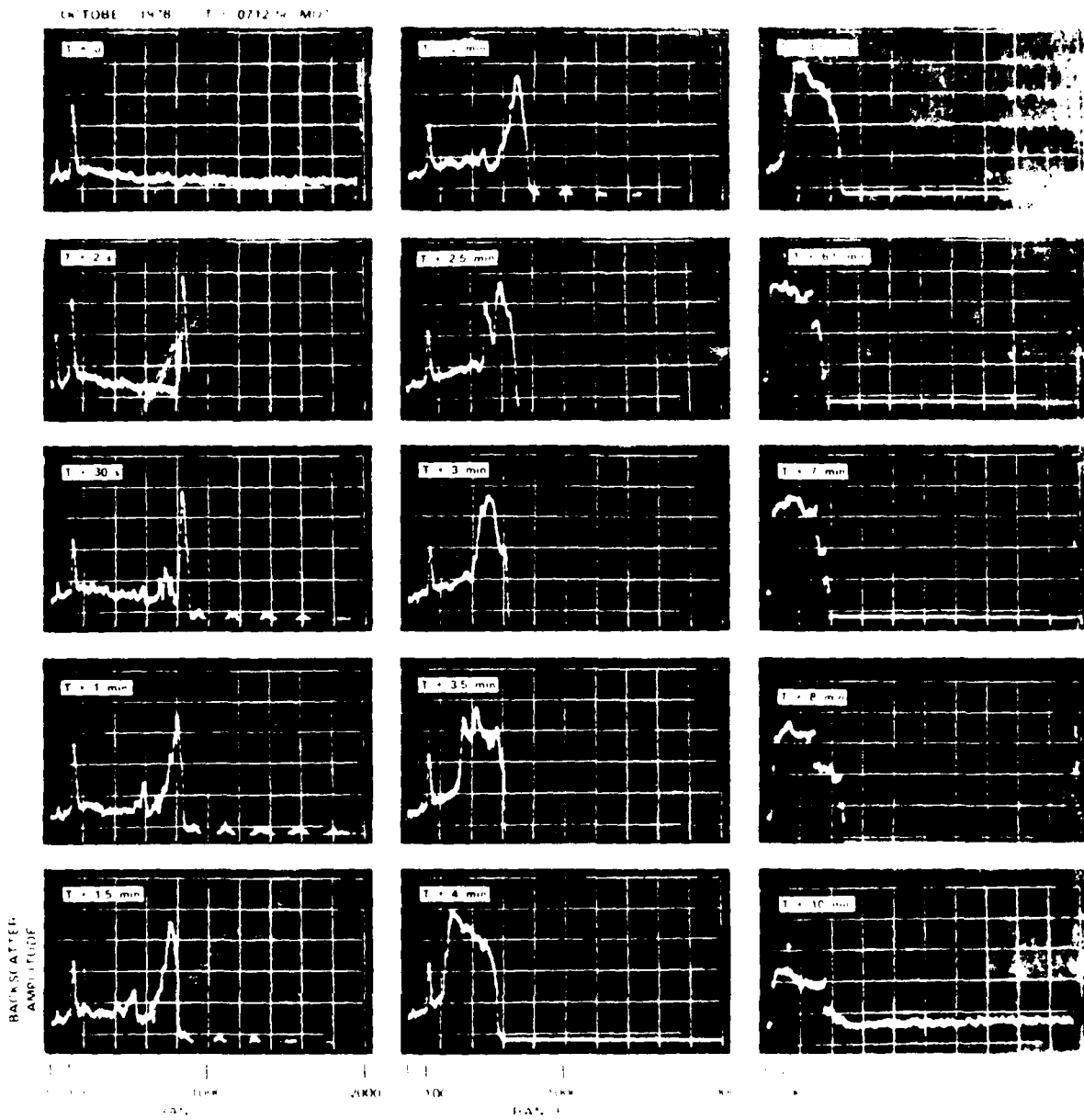


Fig. 1. Backscatter amplitude plots showing the evolution of the signal over time.

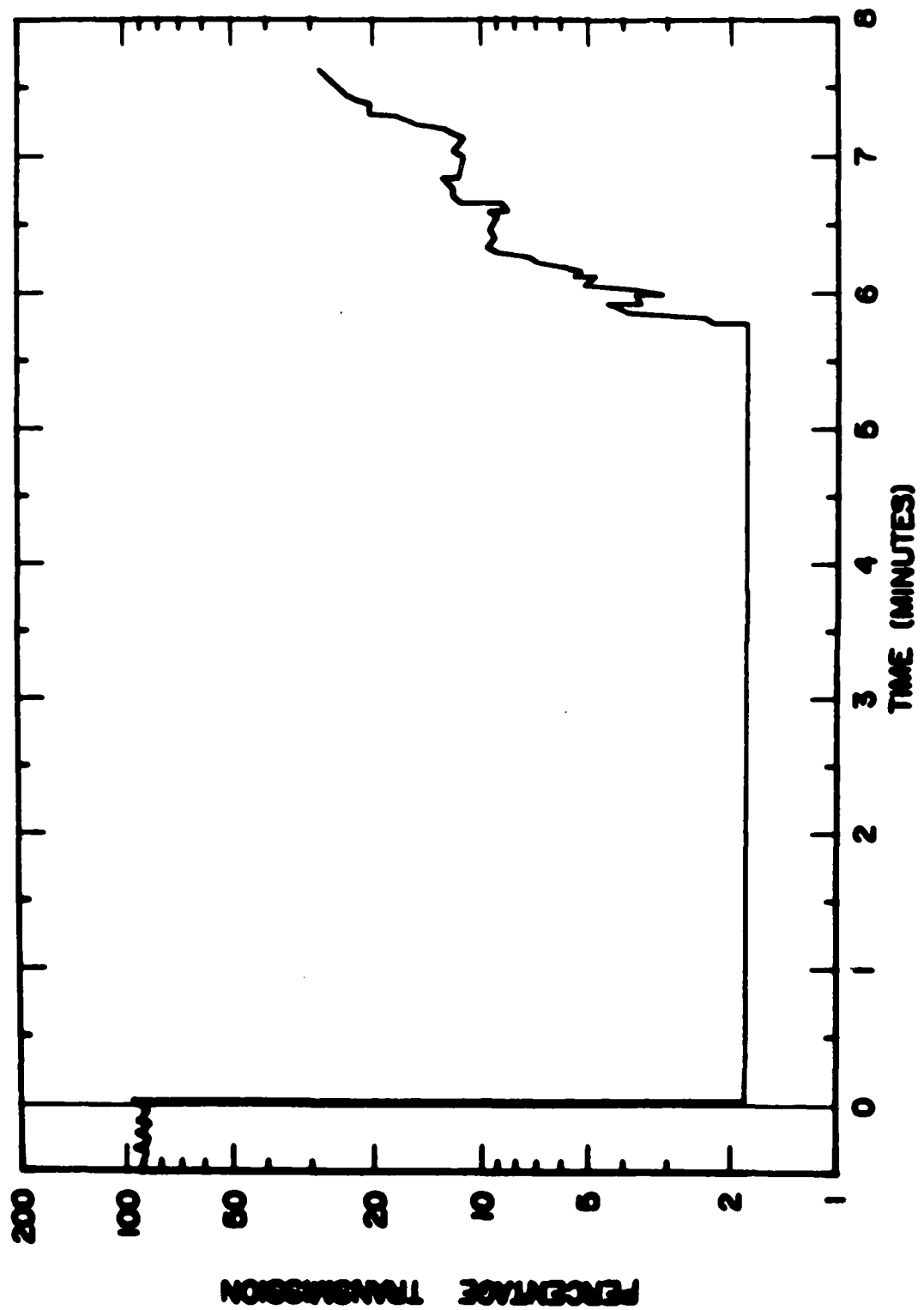


Figure 24. Event C-1 10.6 $\mu$ m transmission.

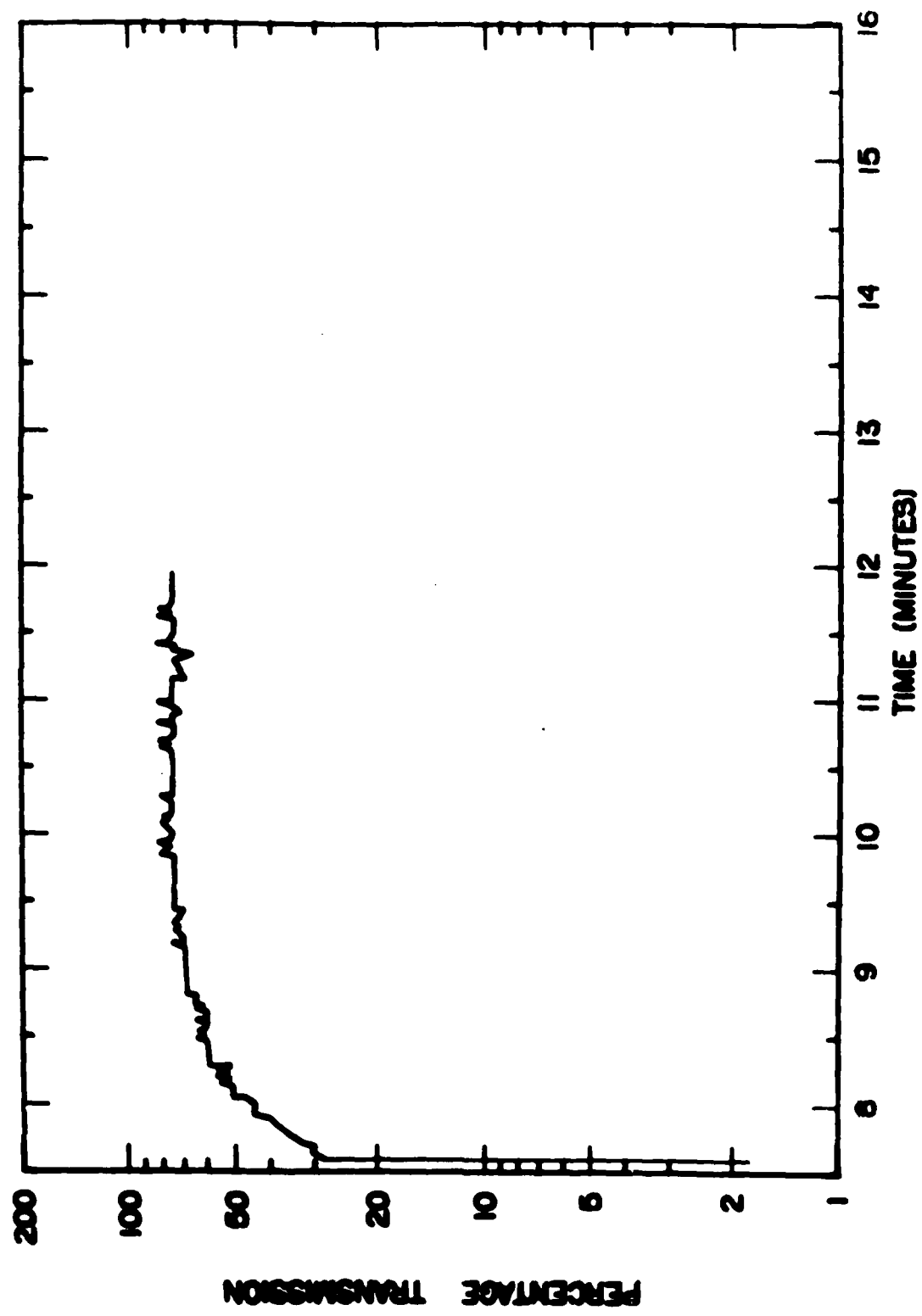
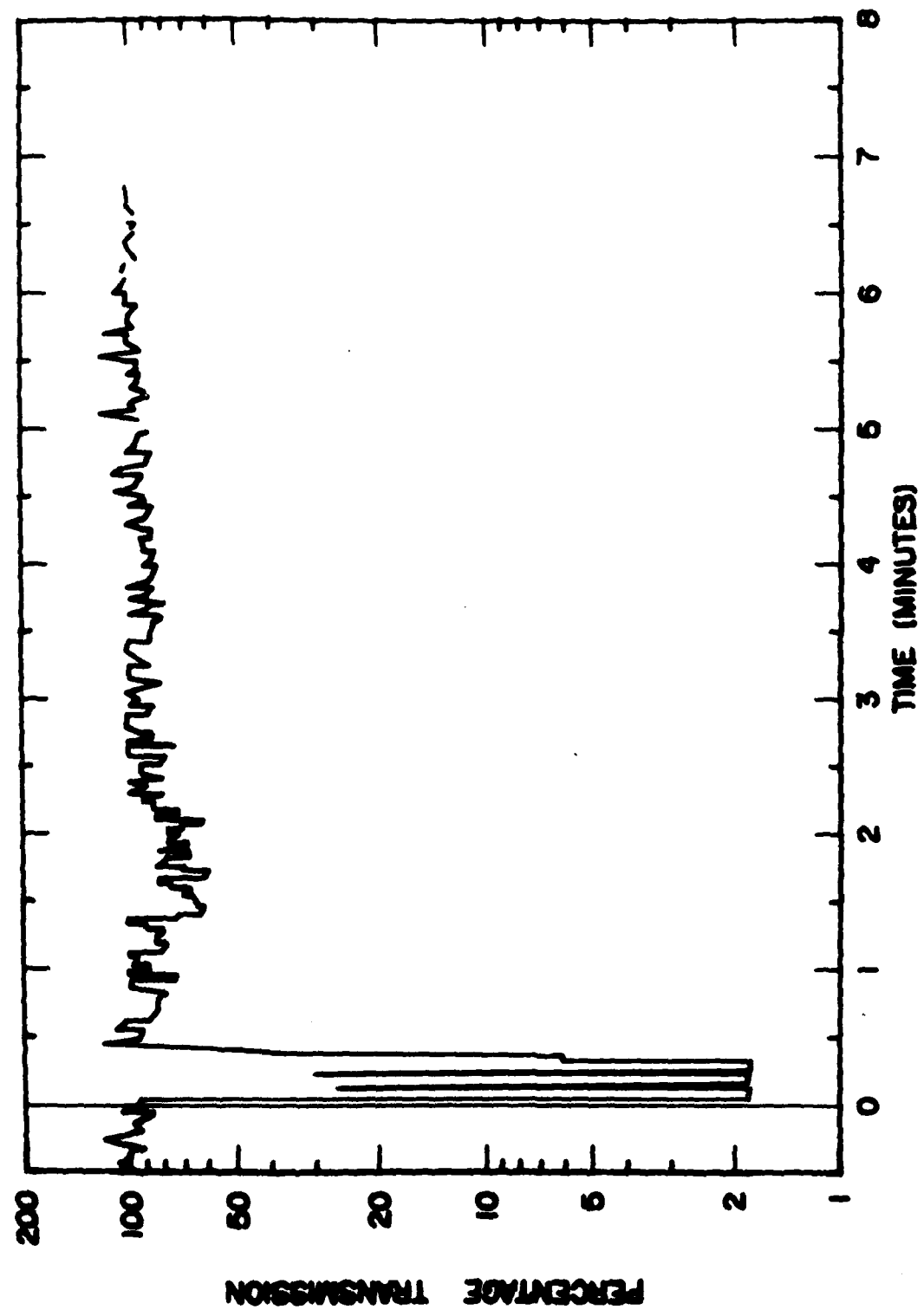


Fig. 25 (cont)



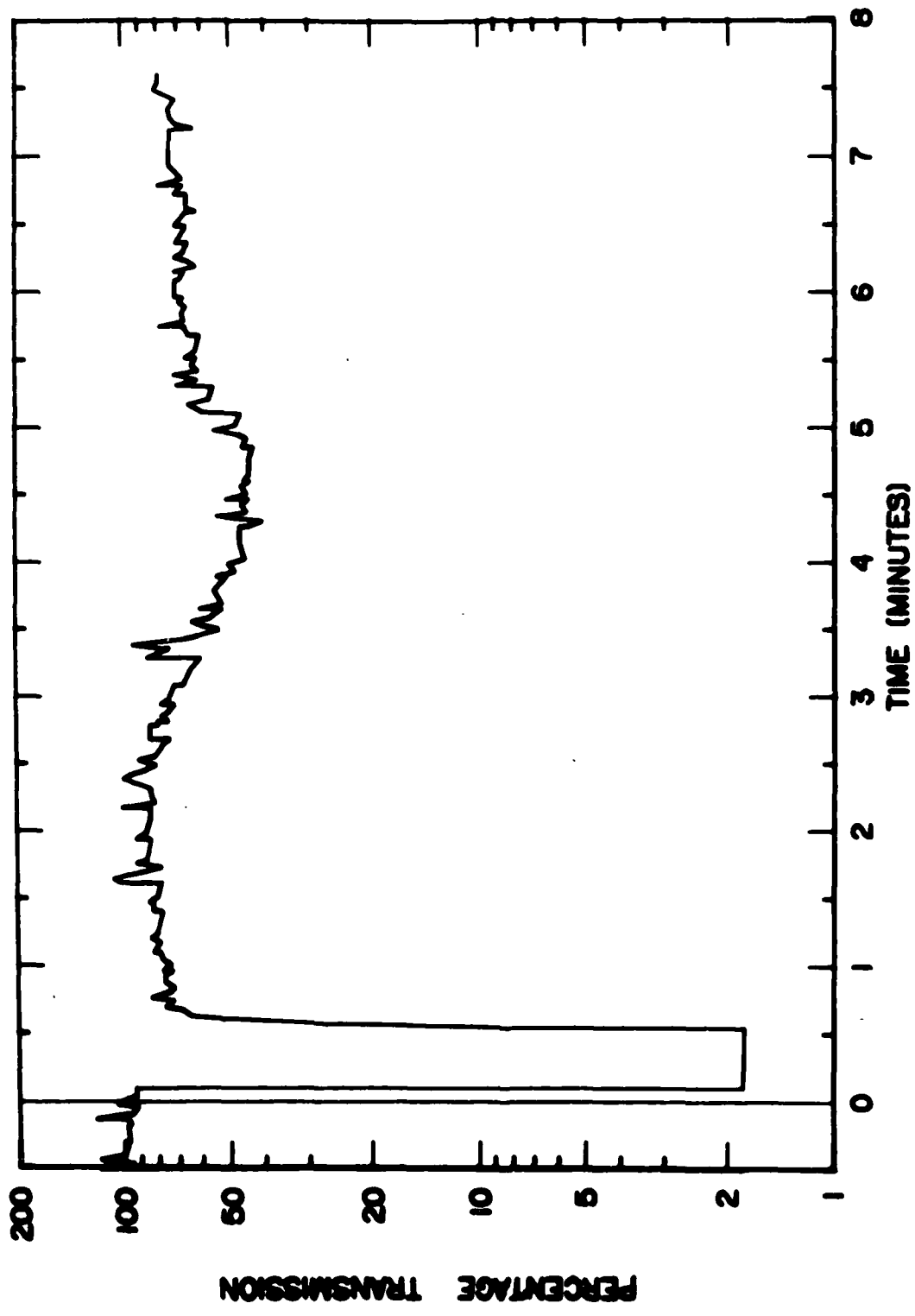


Figure 27. Event D-2 10.6 $\mu$ m transmission.

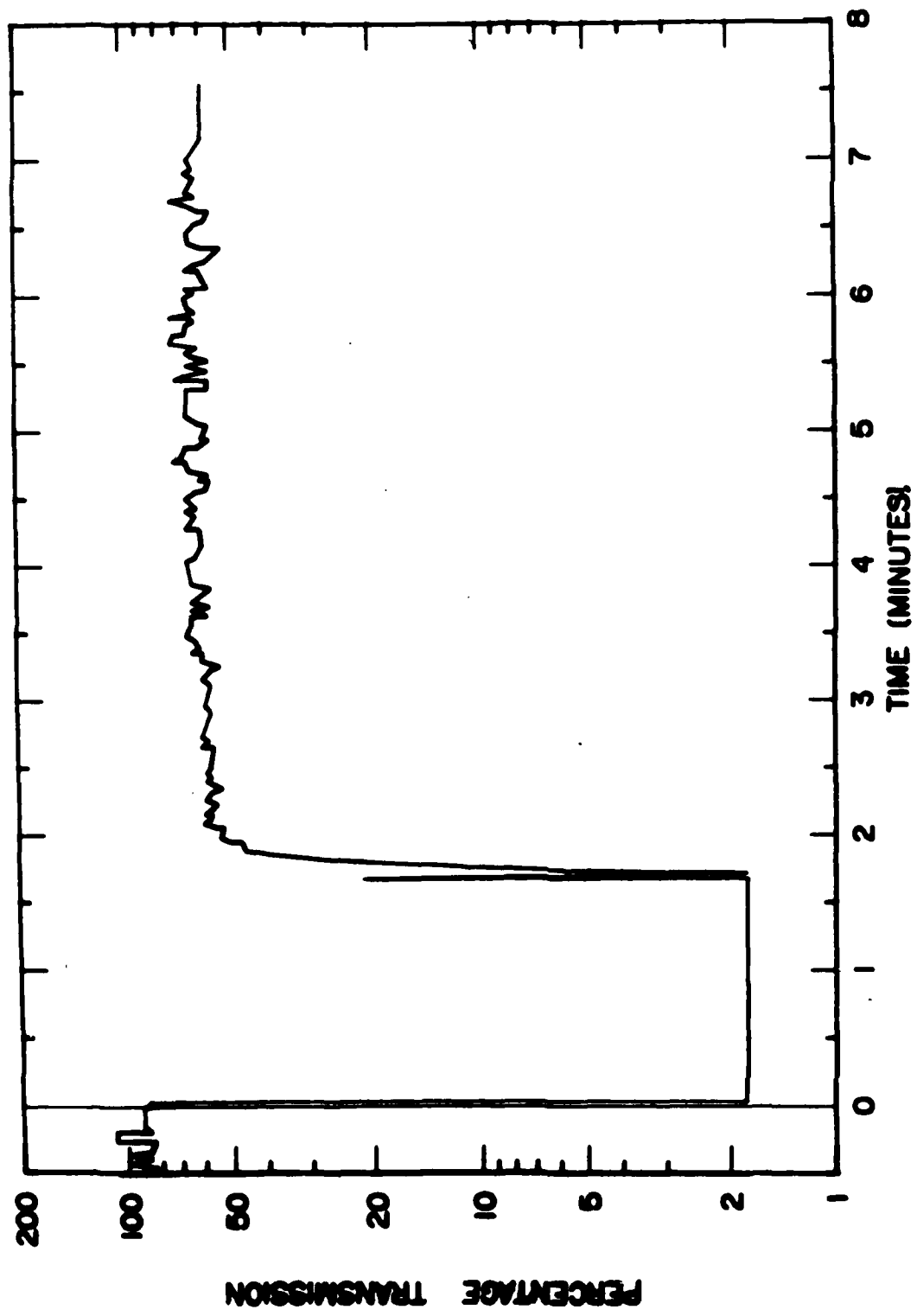


Figure 28. Event D-3 10.6 $\mu$ m transmission.

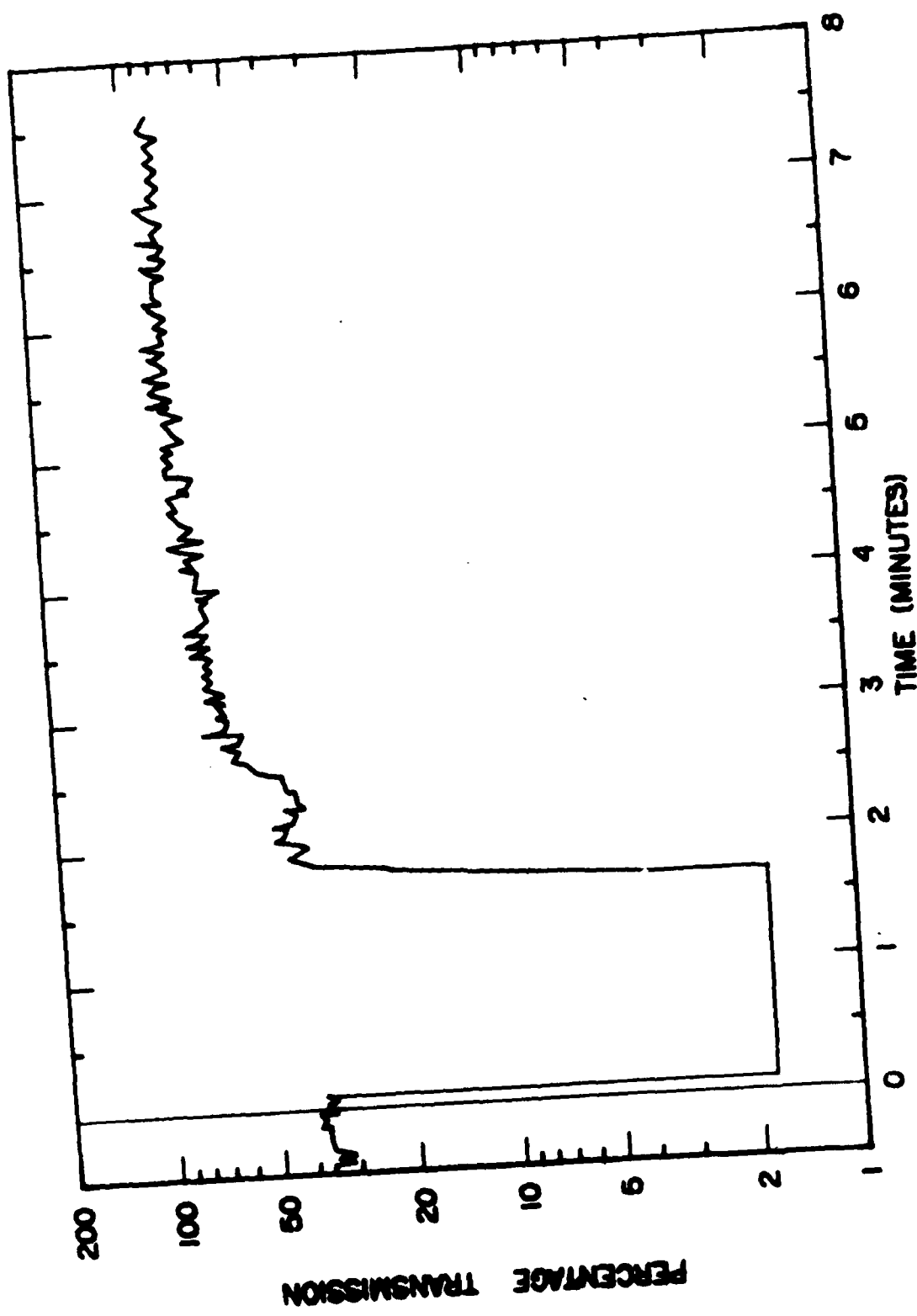
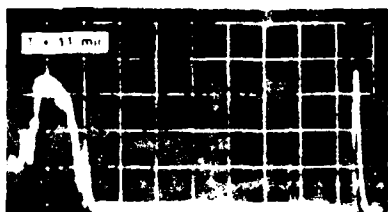
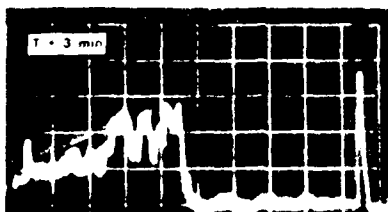
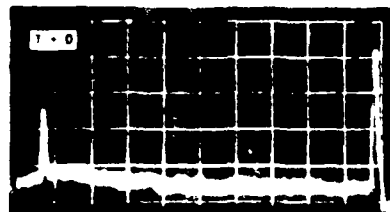


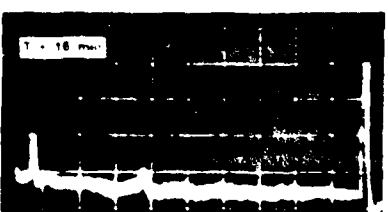
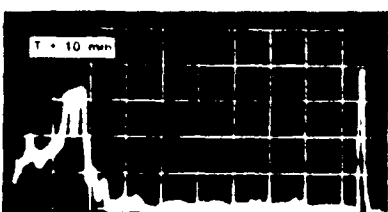
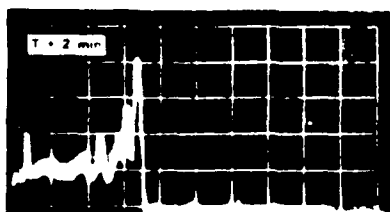
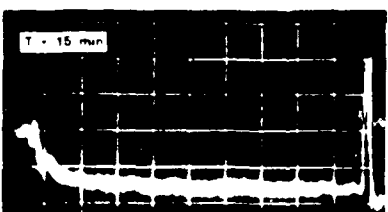
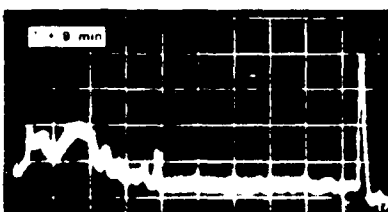
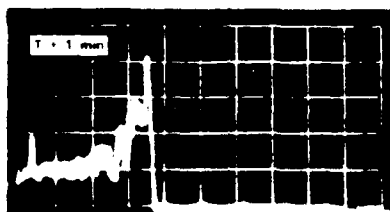
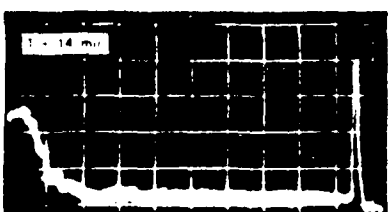
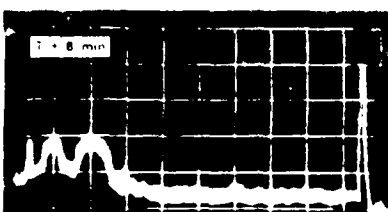
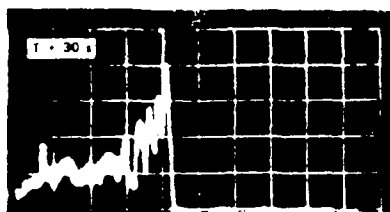
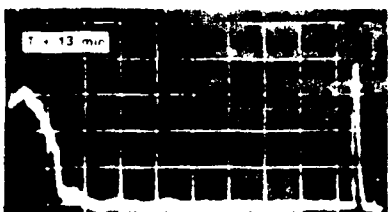
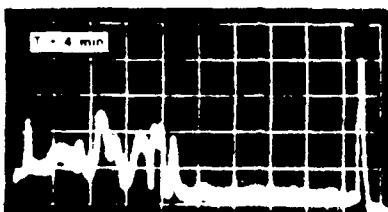
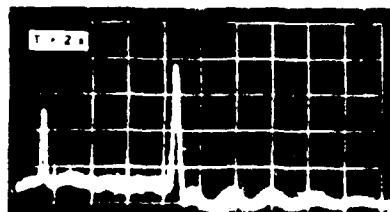
Figure 29. Event D-4 10.6 $\mu$ m transmission.

10 OCTOBER 1977 2 1400 MET

NATIONAL SECURITY



114. 54. 41. 6



Digitized by srujanika@gmail.com

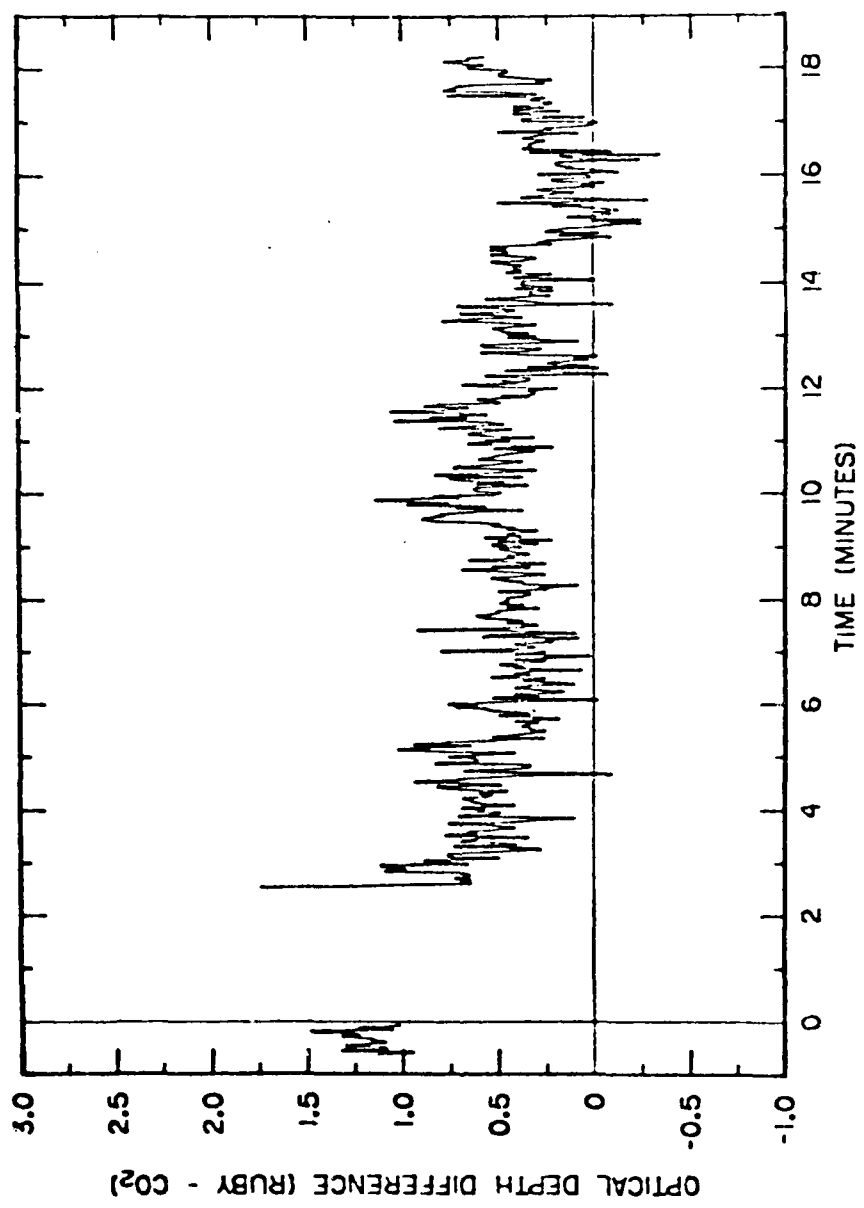


Figure 31. Difference between Ruby and  $\text{CO}_2$  optical depths (Ruby -  $\text{CO}_2$ ).

11 OCTOBER 1978 7:45 a.m. Zulu

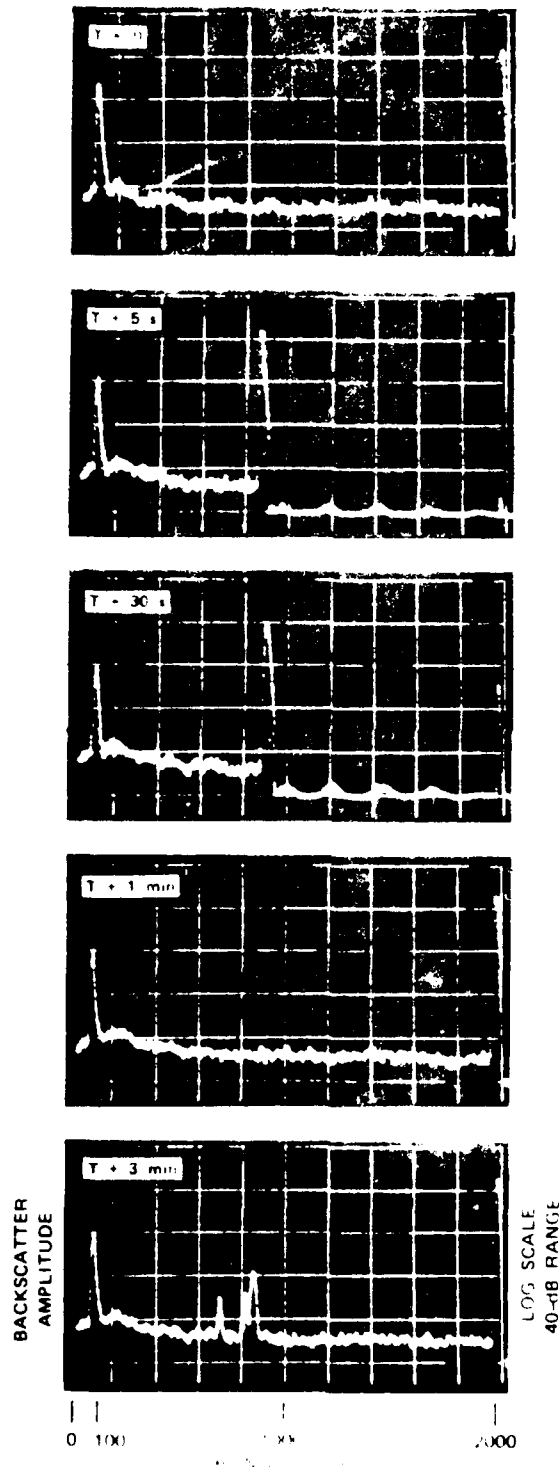


Figure 3. Sonar backscatter amplitude data.

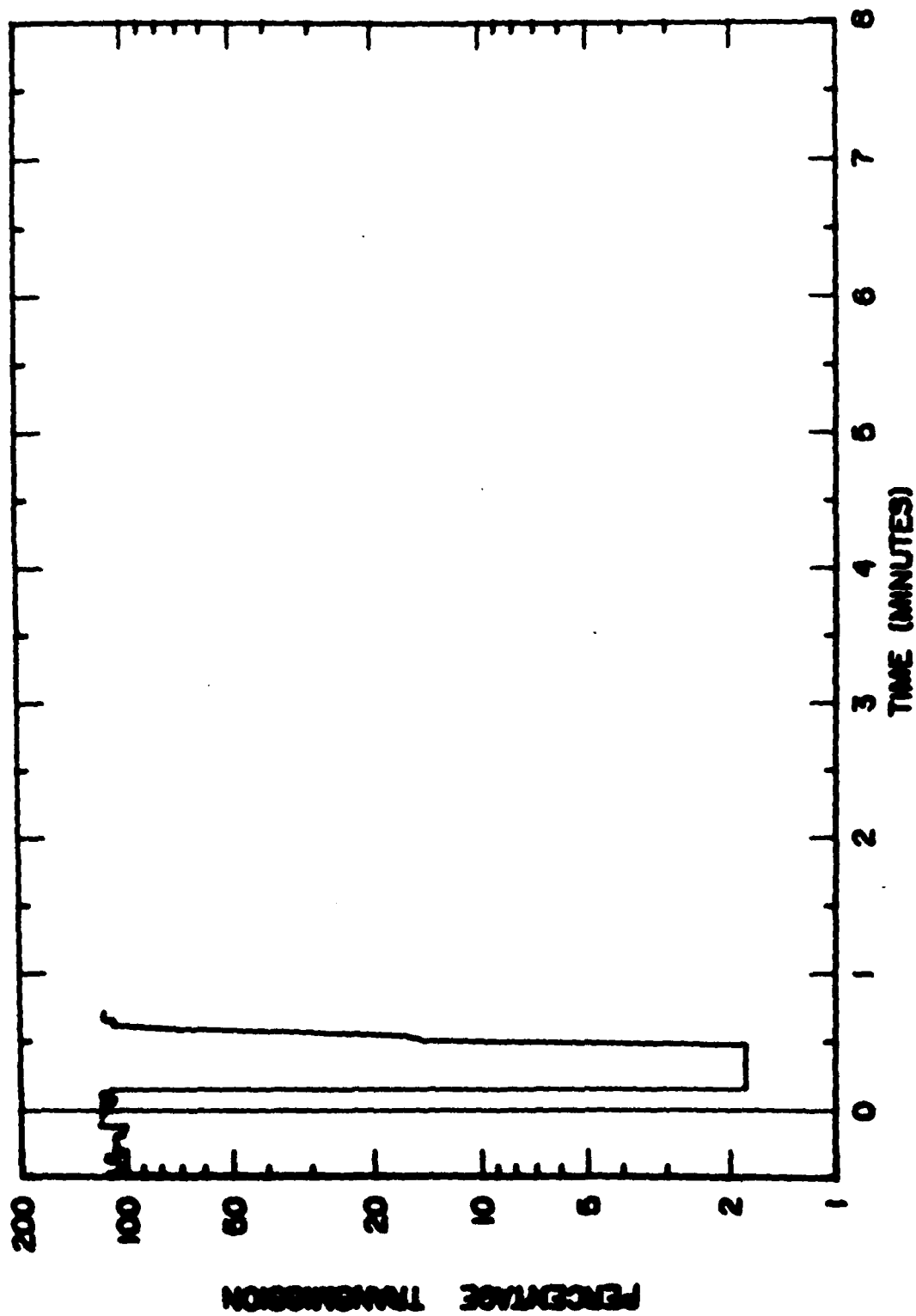


Figure 33. Event E-1 10.6 $\mu$ m transmission.

11 OCTOBER 1978 T = 0.5710 MDT

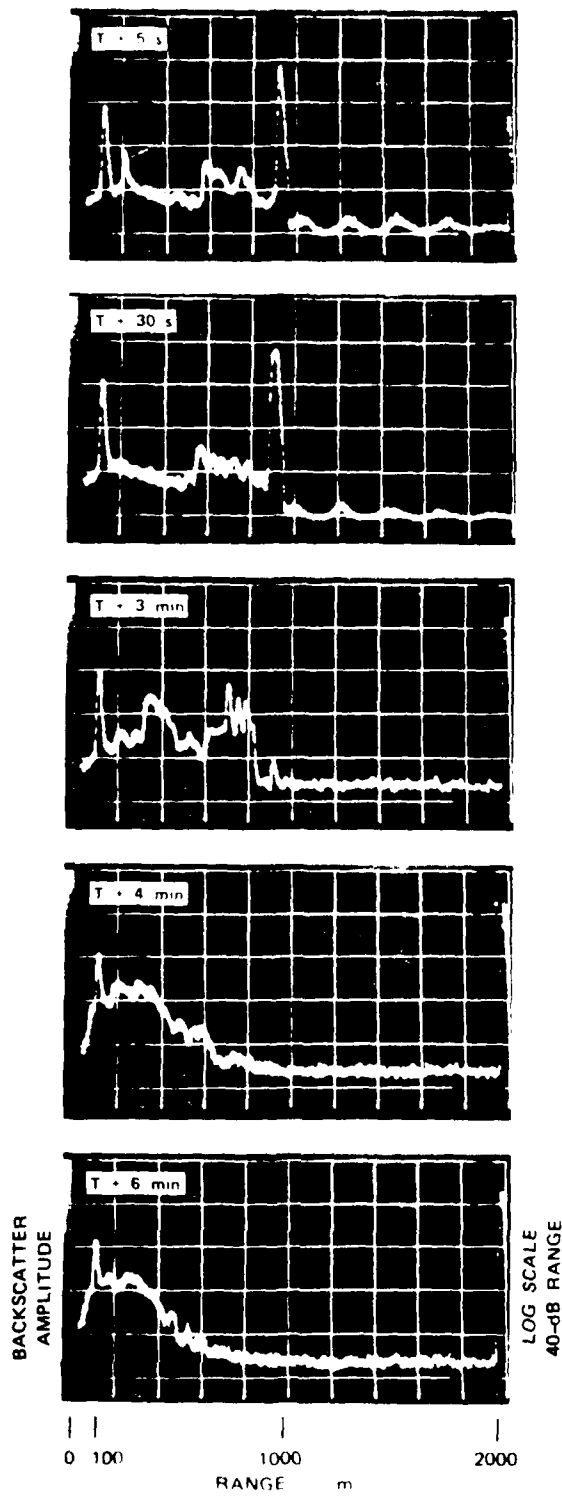


Figure 34. Event E-2 (10.6  $\mu$ m) backscatter data.

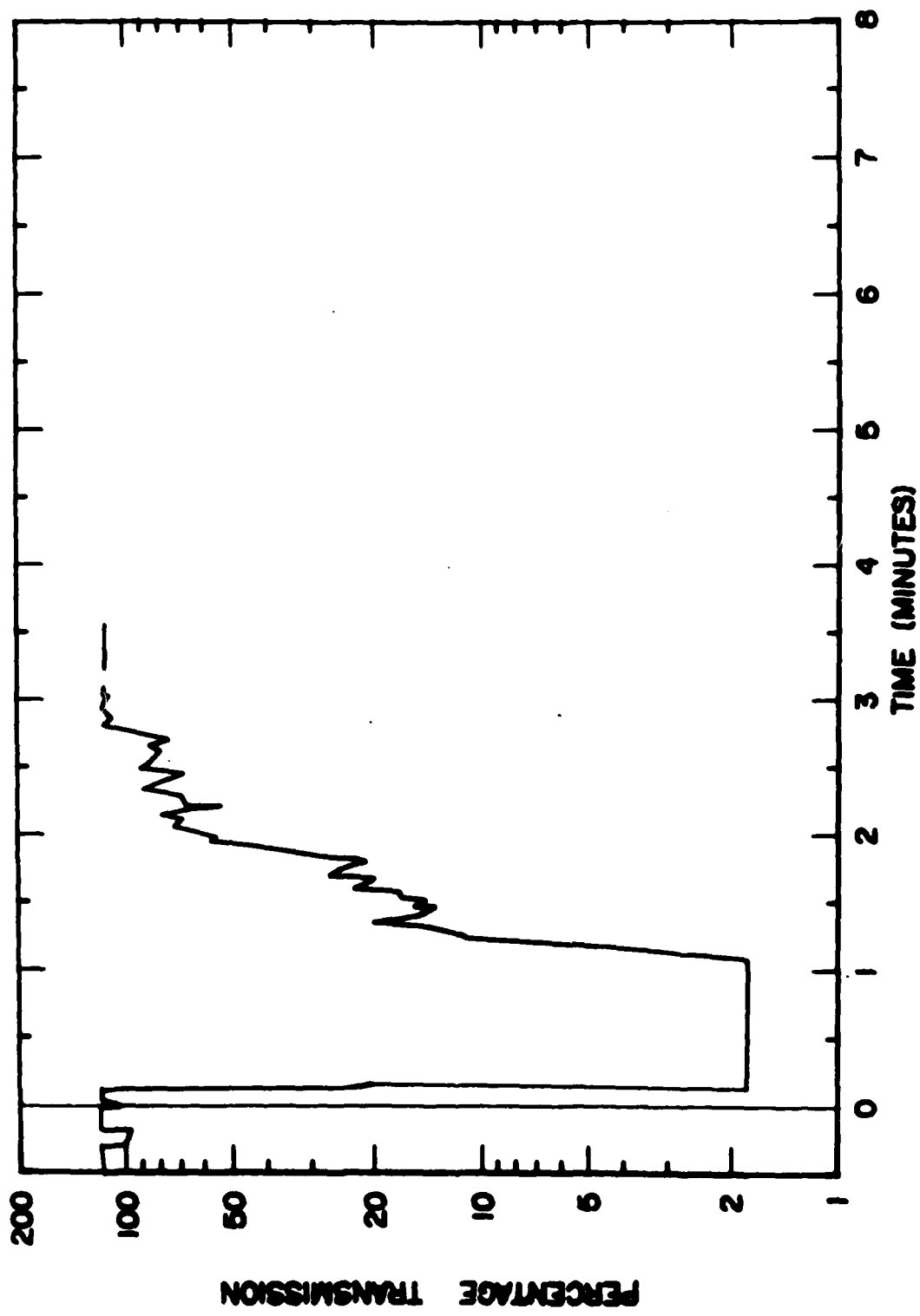


Figure 35. Event E-2 10.6  $\mu\text{m}$  transmission.

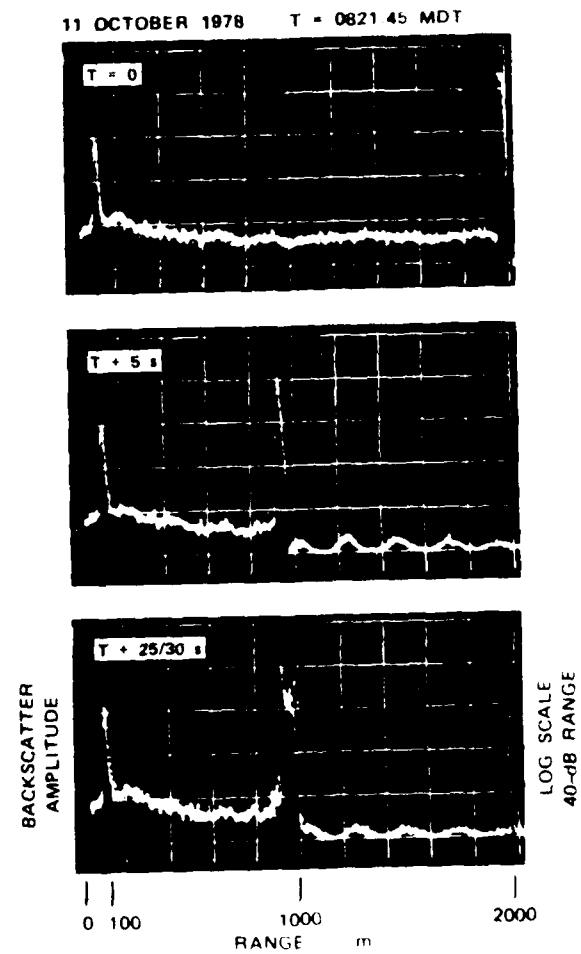


Figure 36. Event E-3 - 10.6  $\mu$ m backscatter data.

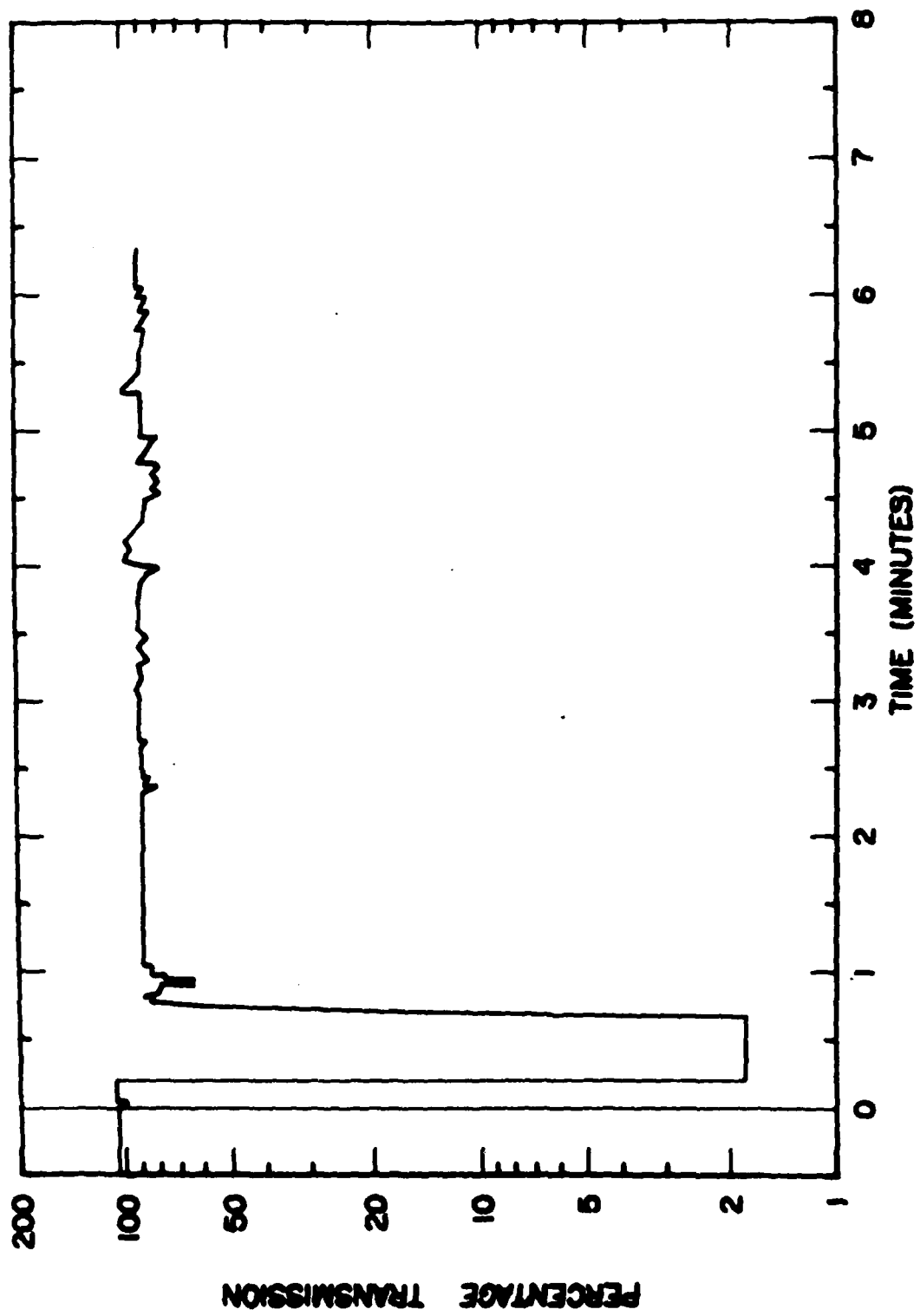


Figure 37. Event E-3 10.6 $\mu$ m transmission.

11 OCTOBER 1978 T = 0829 05

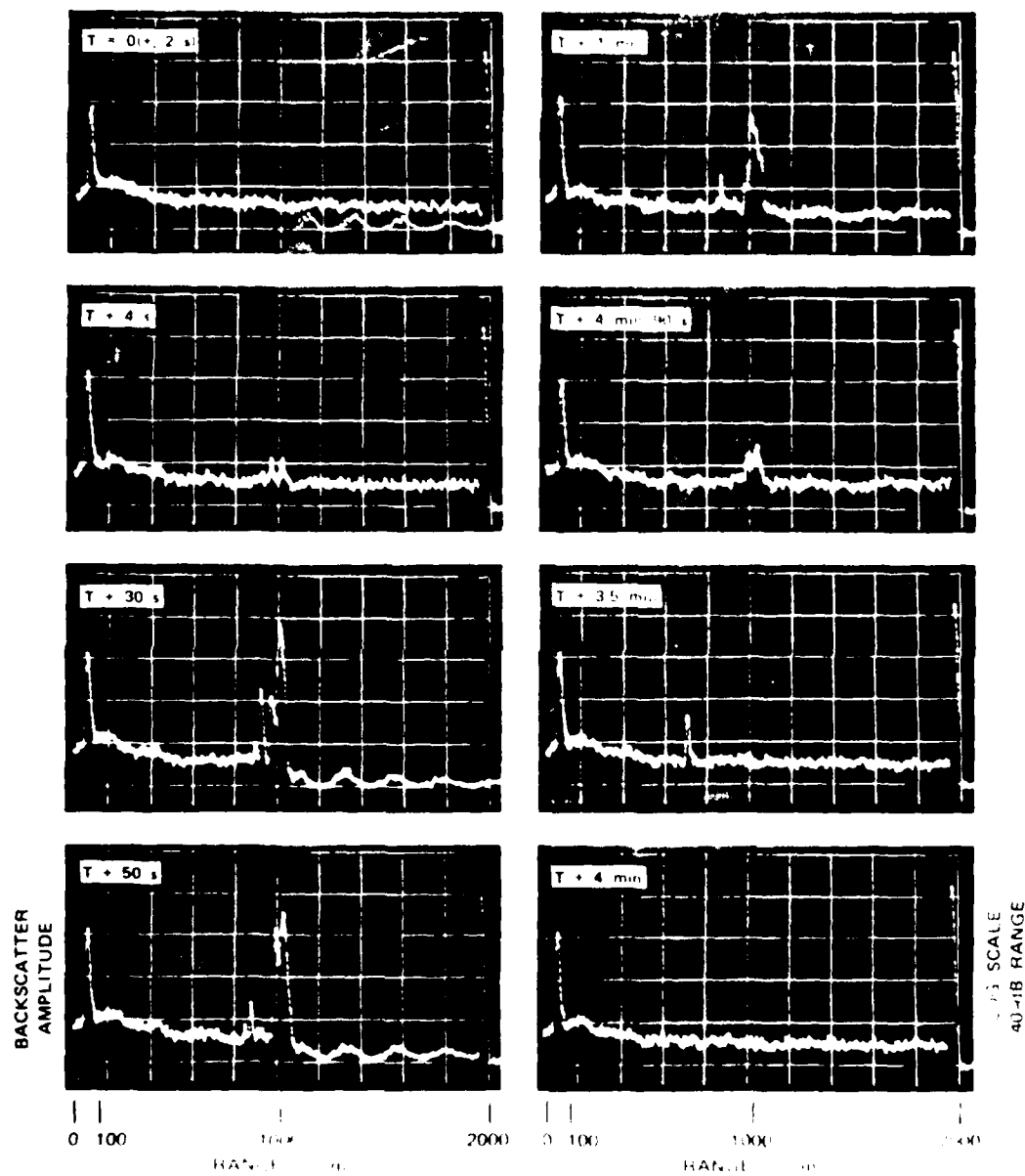


FIGURE 1. BACKSCATTER PPI (T = 0 to T = 4 min) FOR THE 1000 m DIA. DOME.

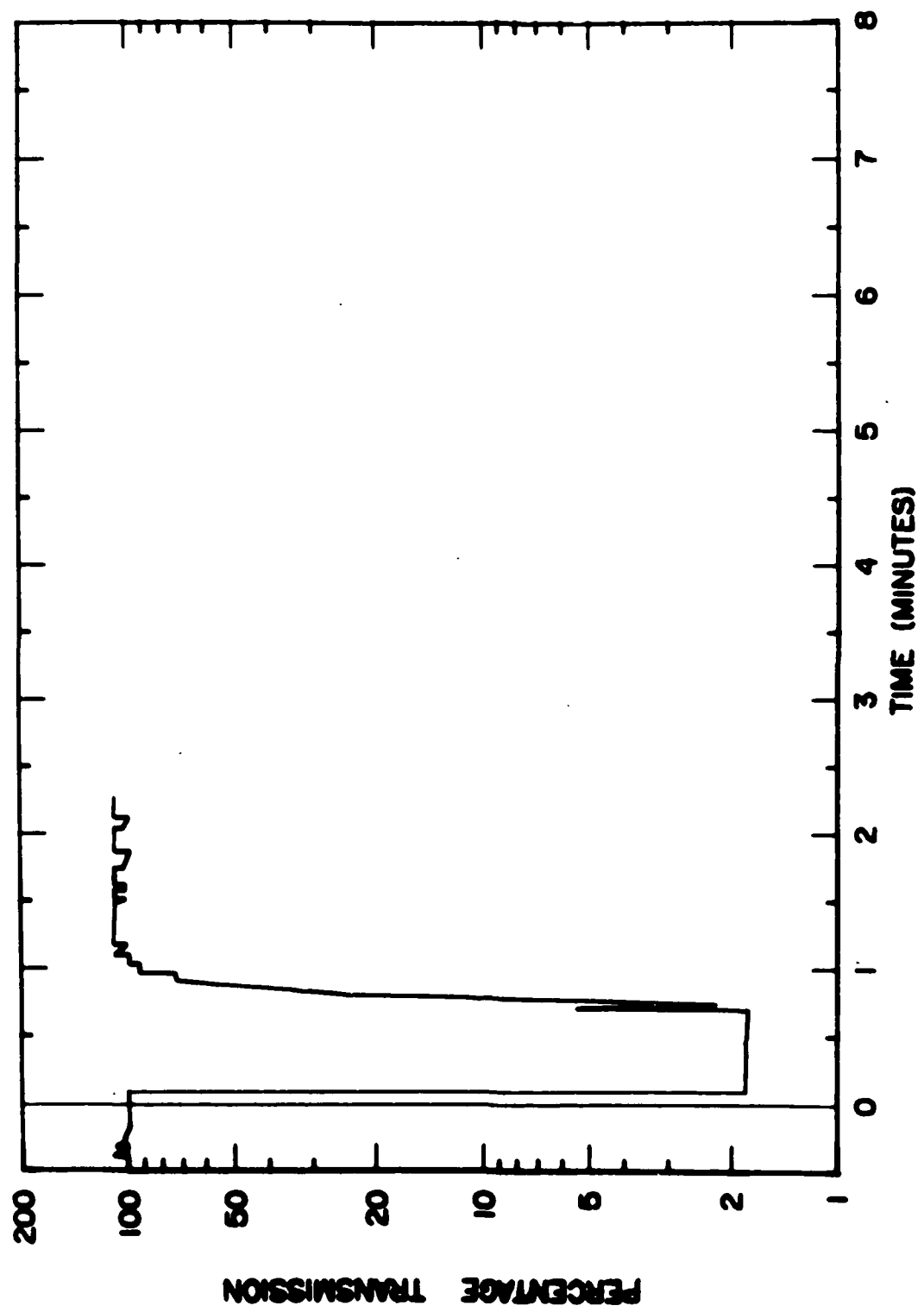


Figure 39. Event E-4  $10.6\mu\text{m}$  transmission.

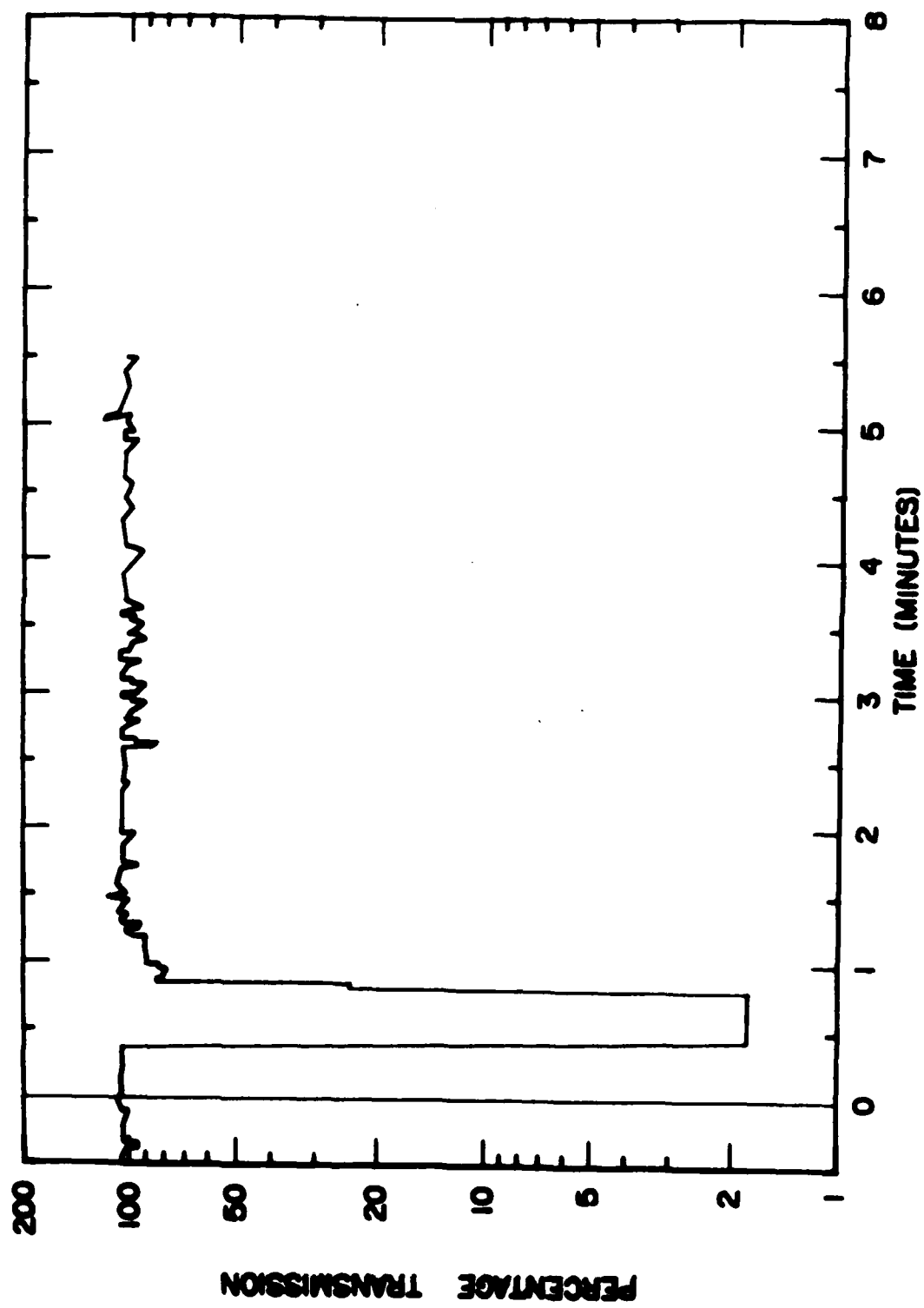


Figure 40. Event F-1 10.6 $\mu$ m transmission.

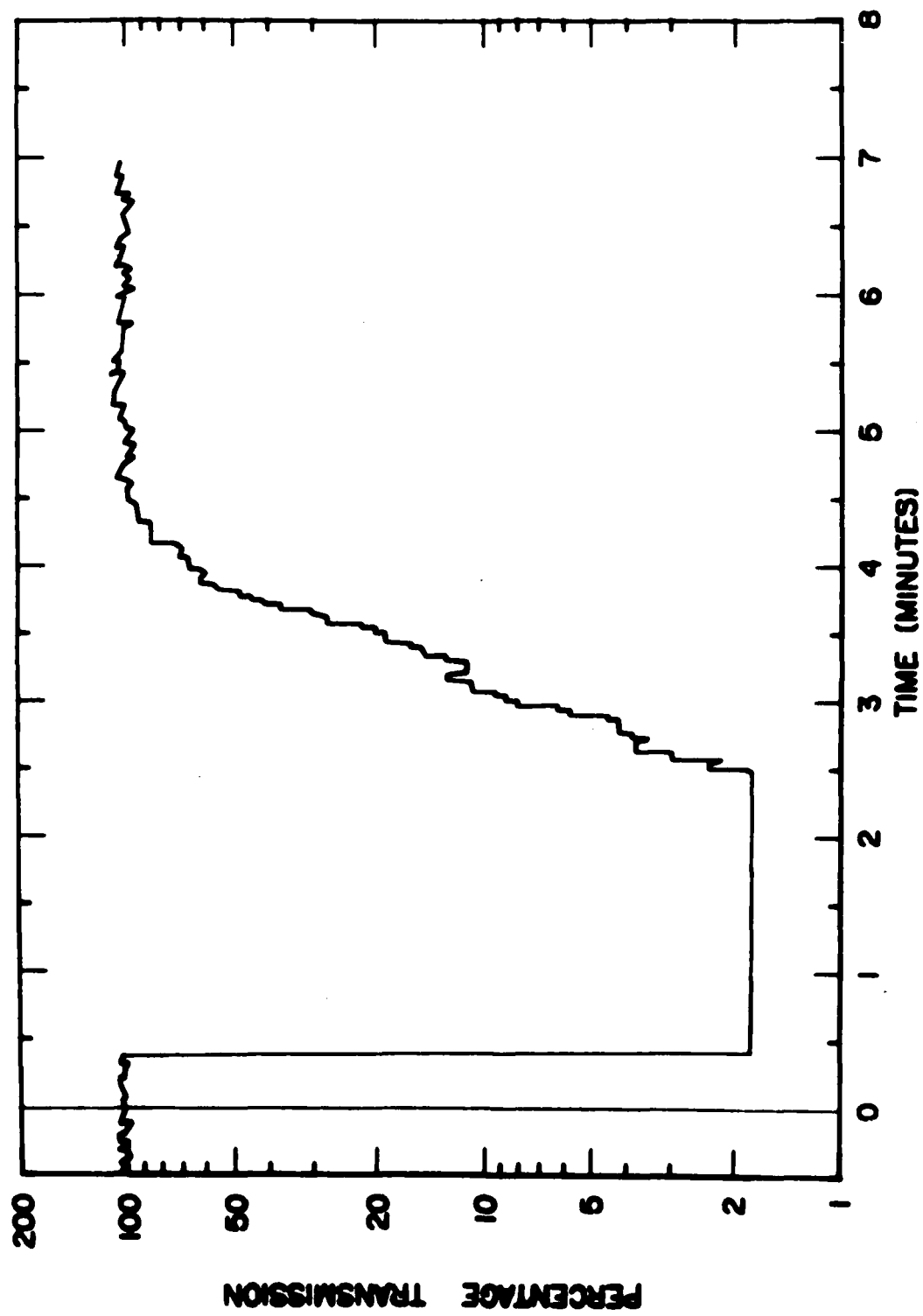


Figure 41. Event F-2 10.6 $\mu$ m transmission.

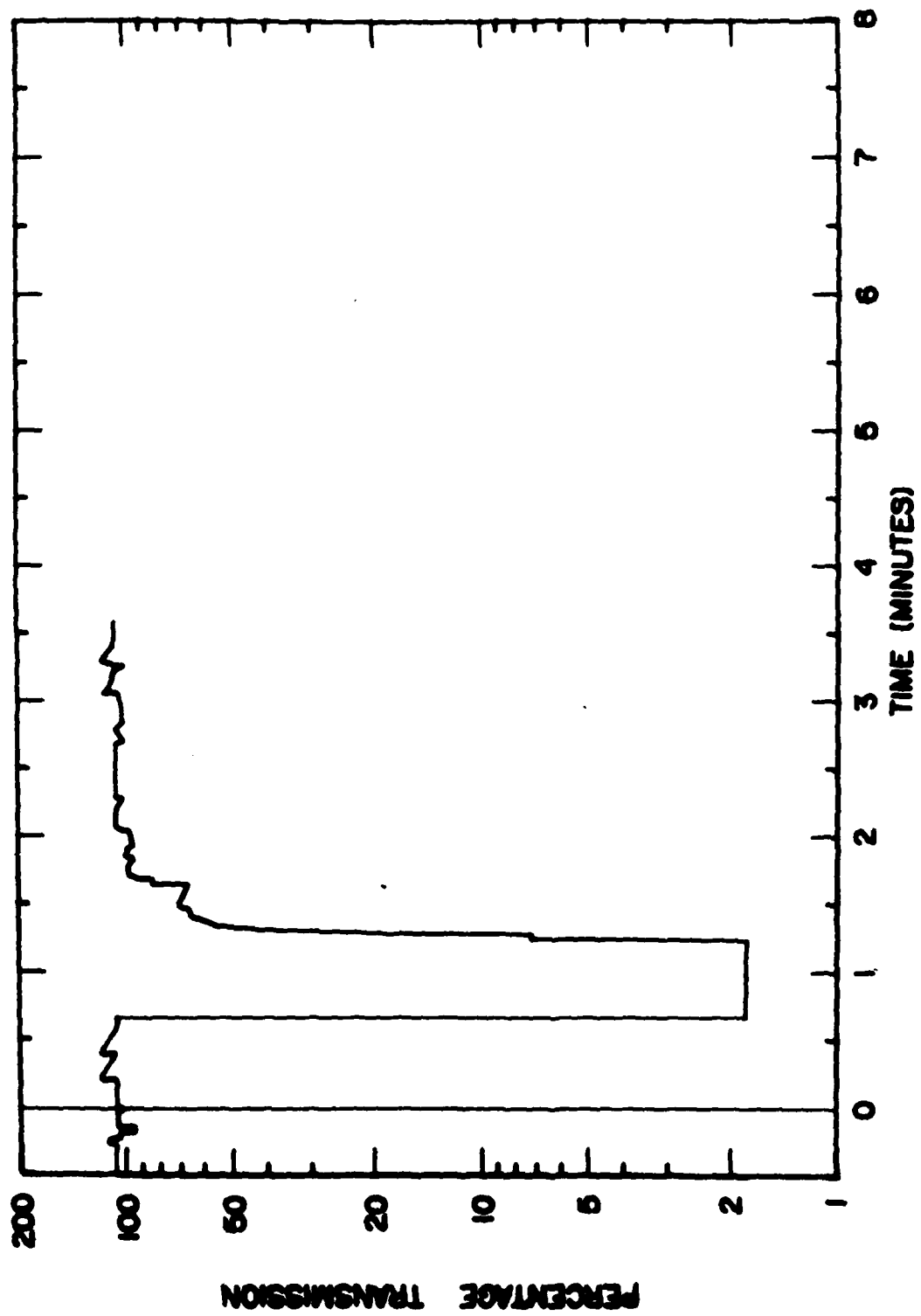
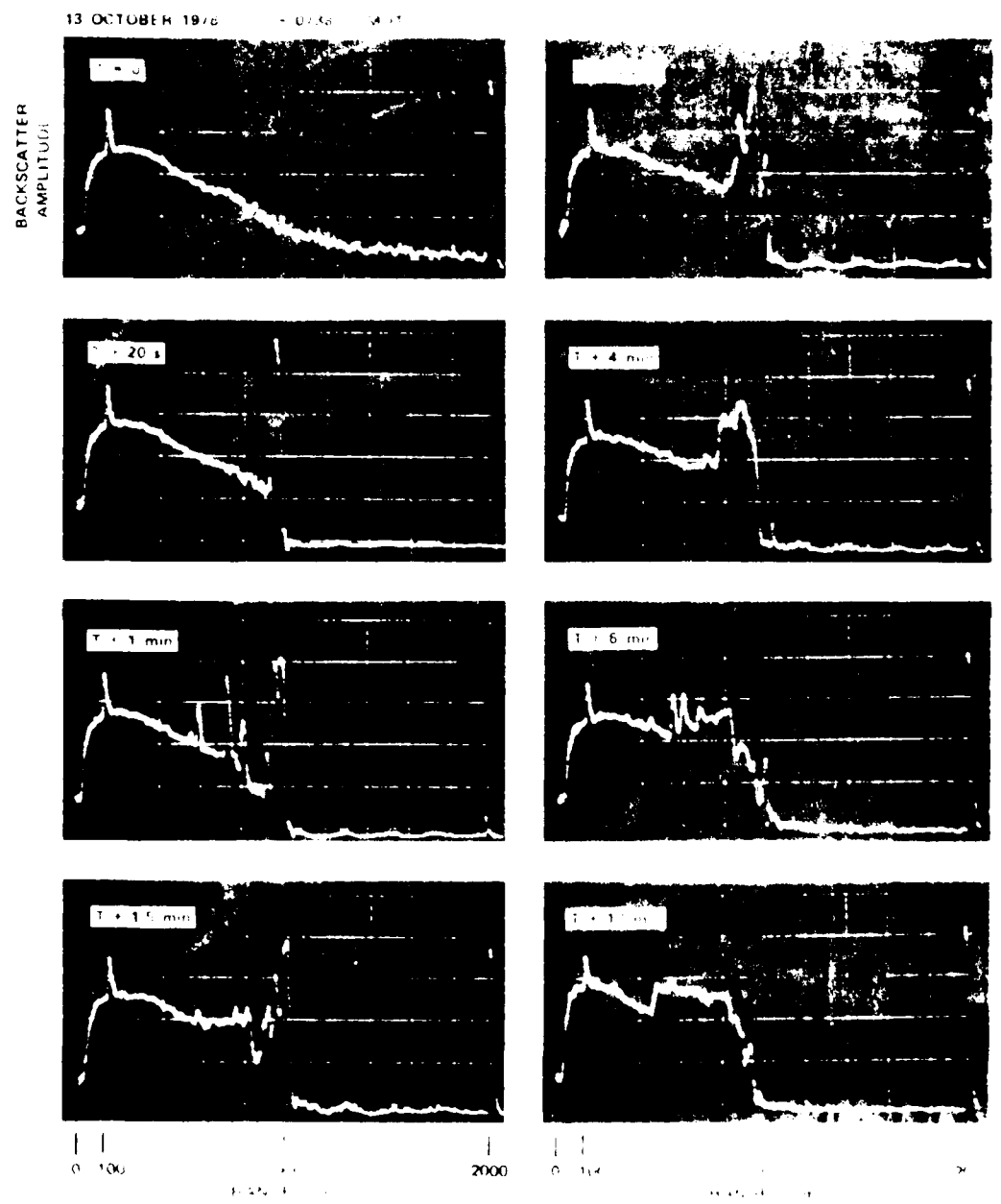


Figure 42. Event F-3  $10.6\mu\text{m}$  transmission.



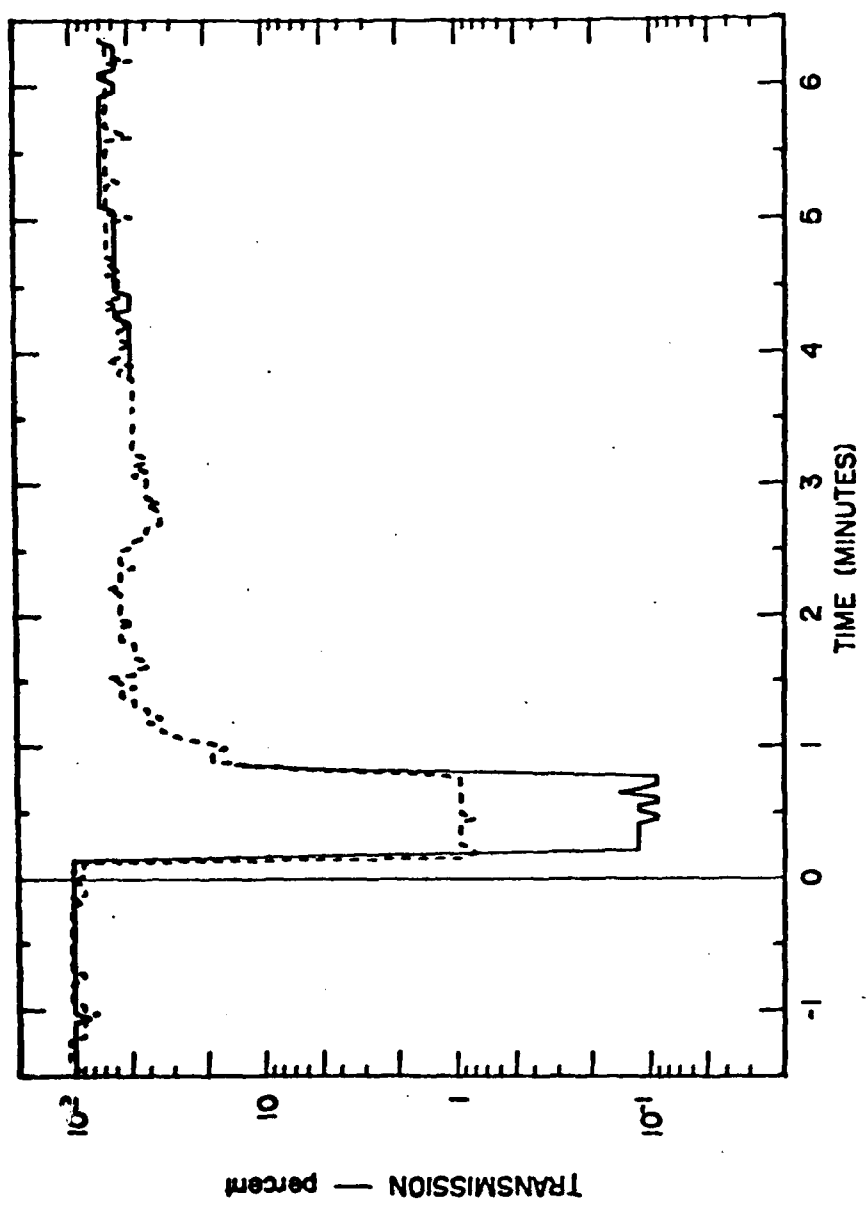


Figure 44. Transmission observed by the two-wavelength lidar system (F-5).

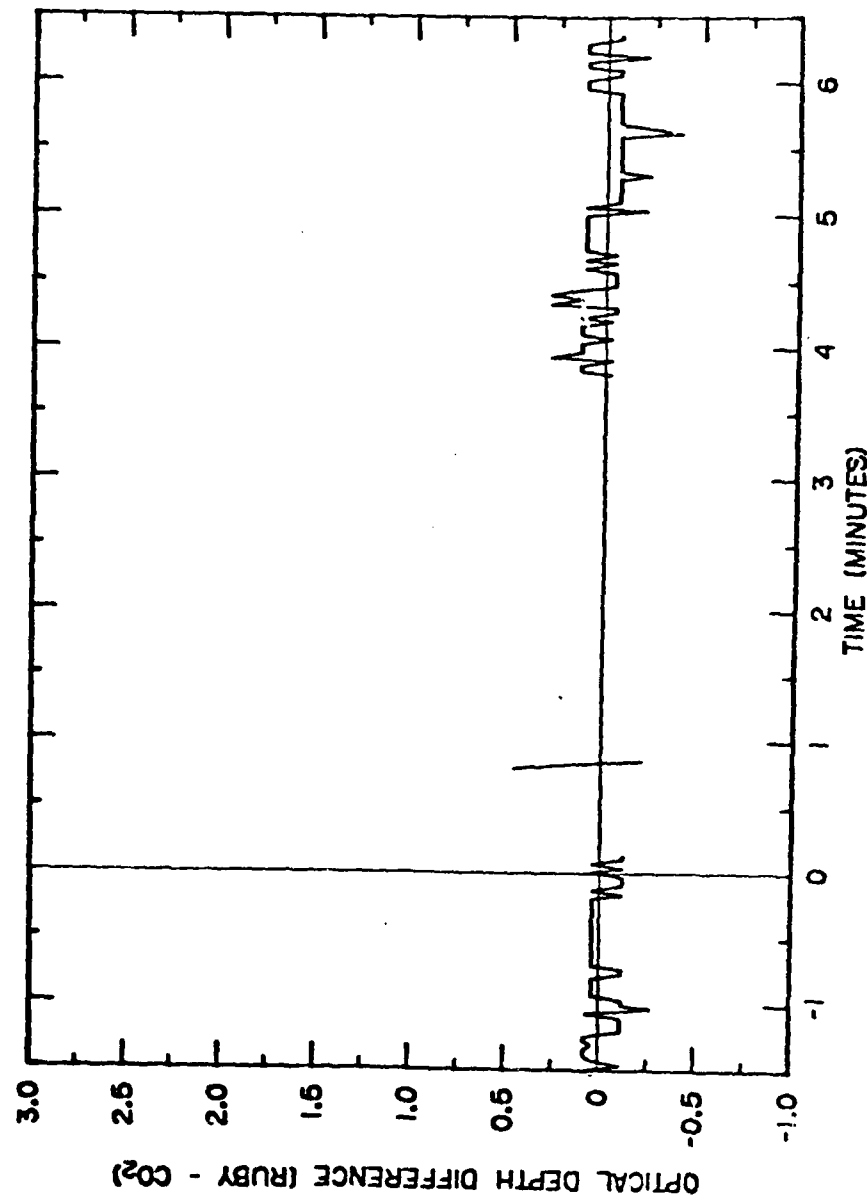


Figure 45. Difference between Ruby and CO<sub>2</sub> optical depths ( $\gamma_1 - \gamma_2$ ).

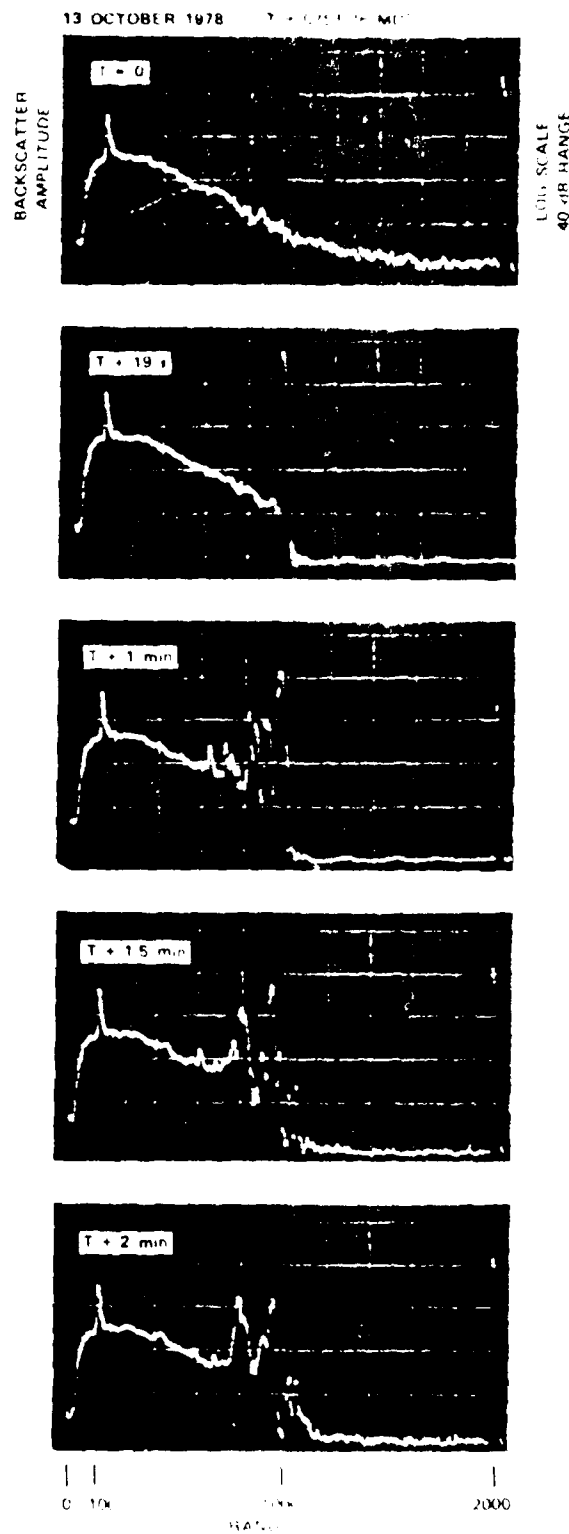


Figure 16. Examples of backscatter data.

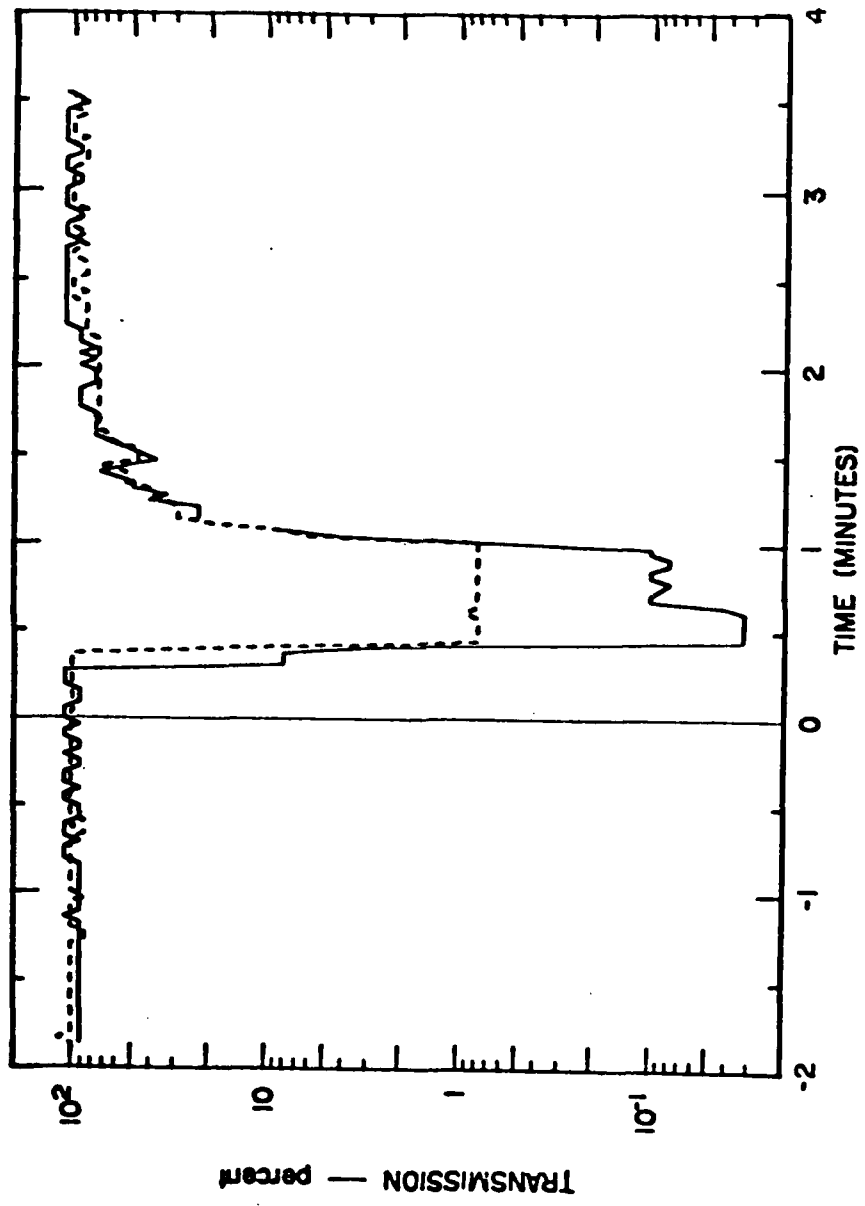


Figure 47. Transmission observed by the two-wavelength lidar system (F-6).

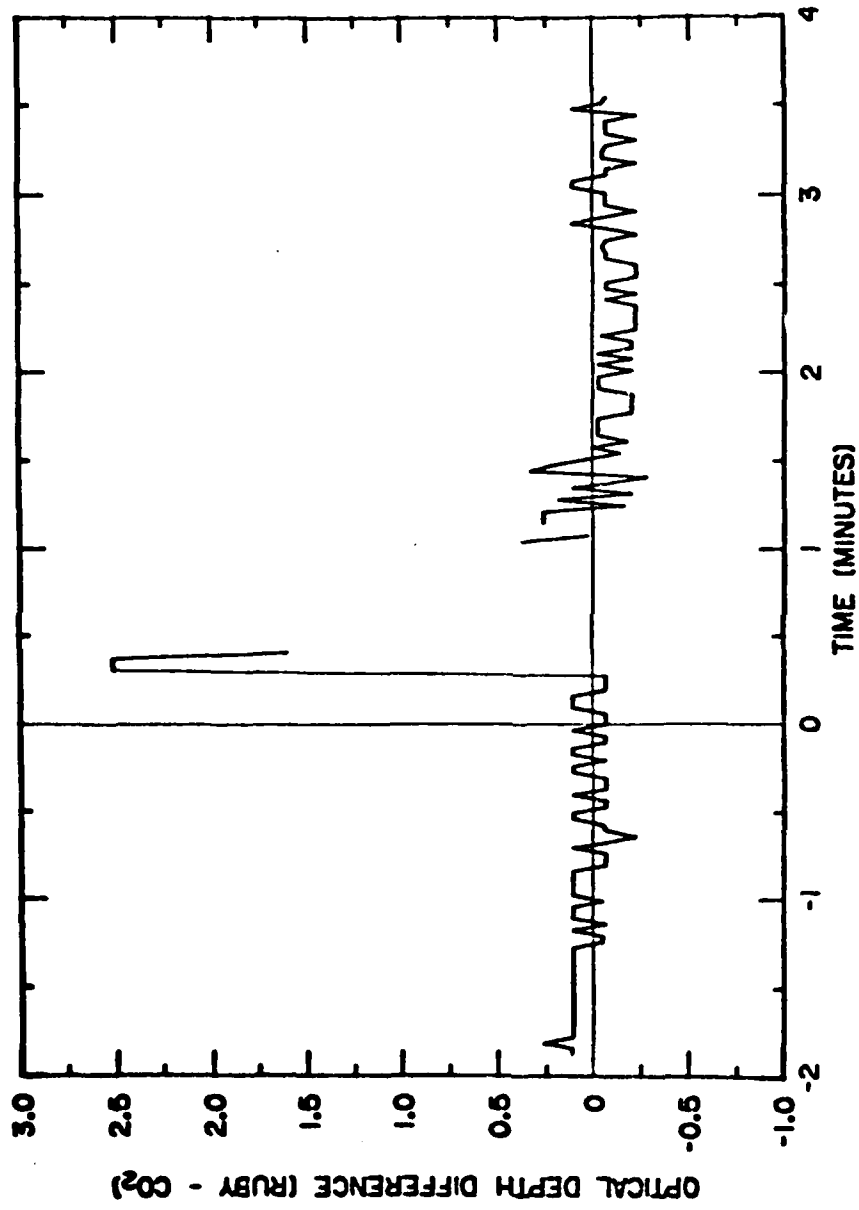


Figure 48. Difference between Ruby and  $\text{CO}_2$  optical depths (F-6).

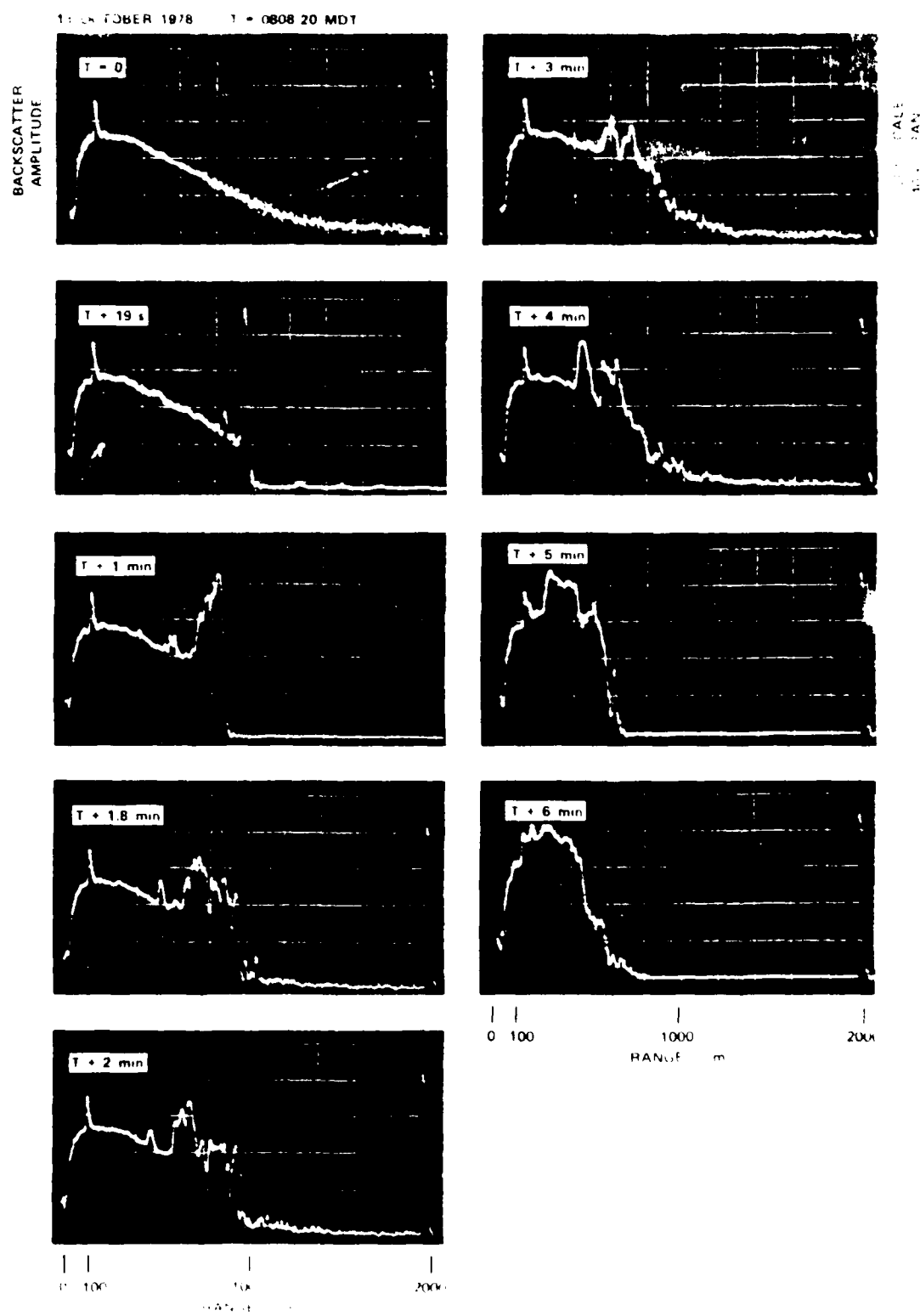


Fig. 4. Radar images at 10.7 GHz during the event.

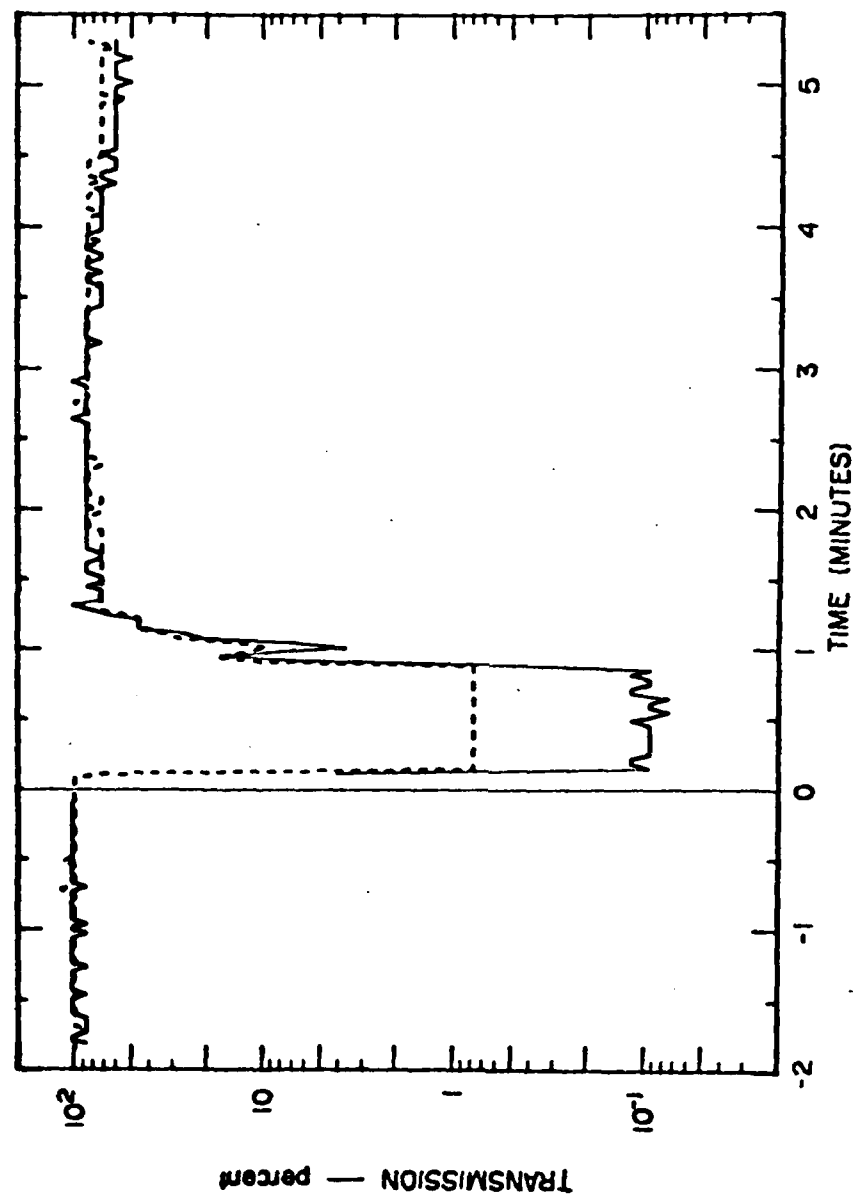


Figure 50. Transmission observed by the two-wavelength lidar system (F-7).

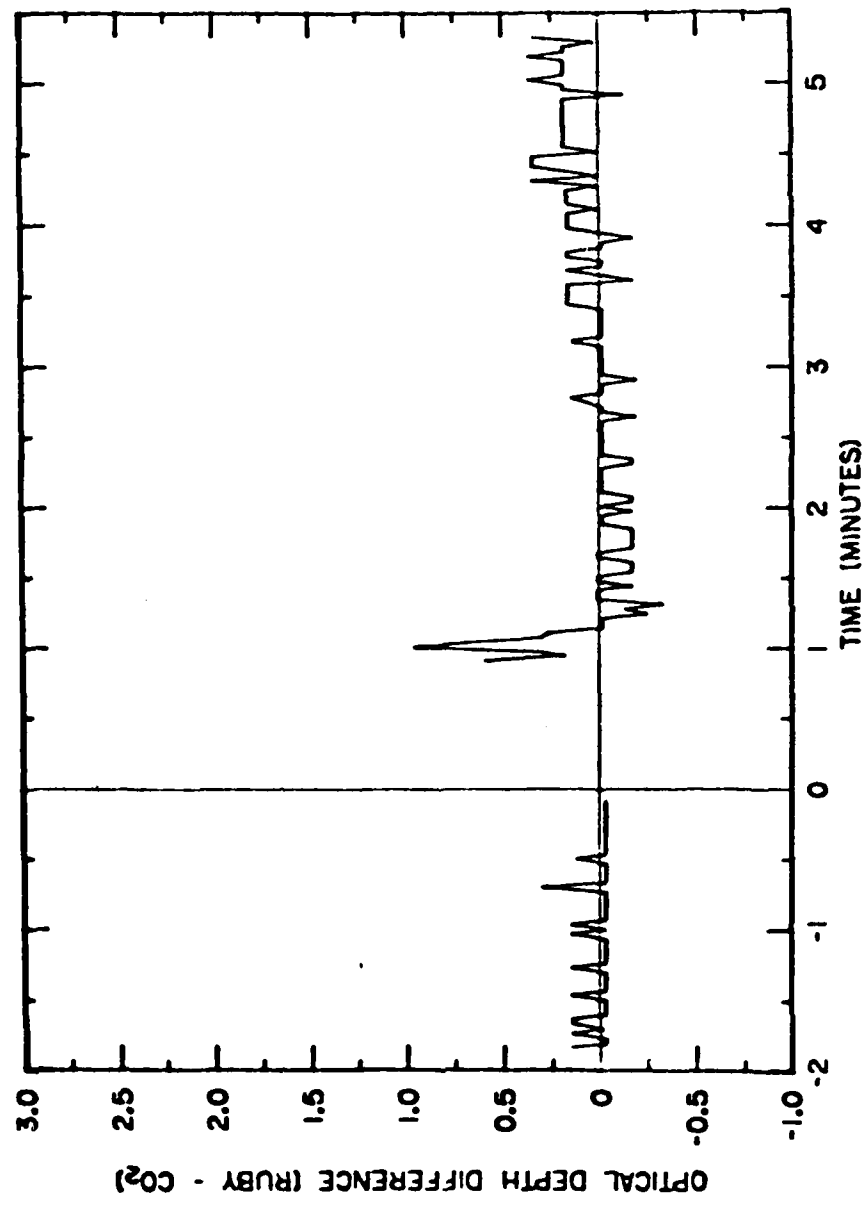
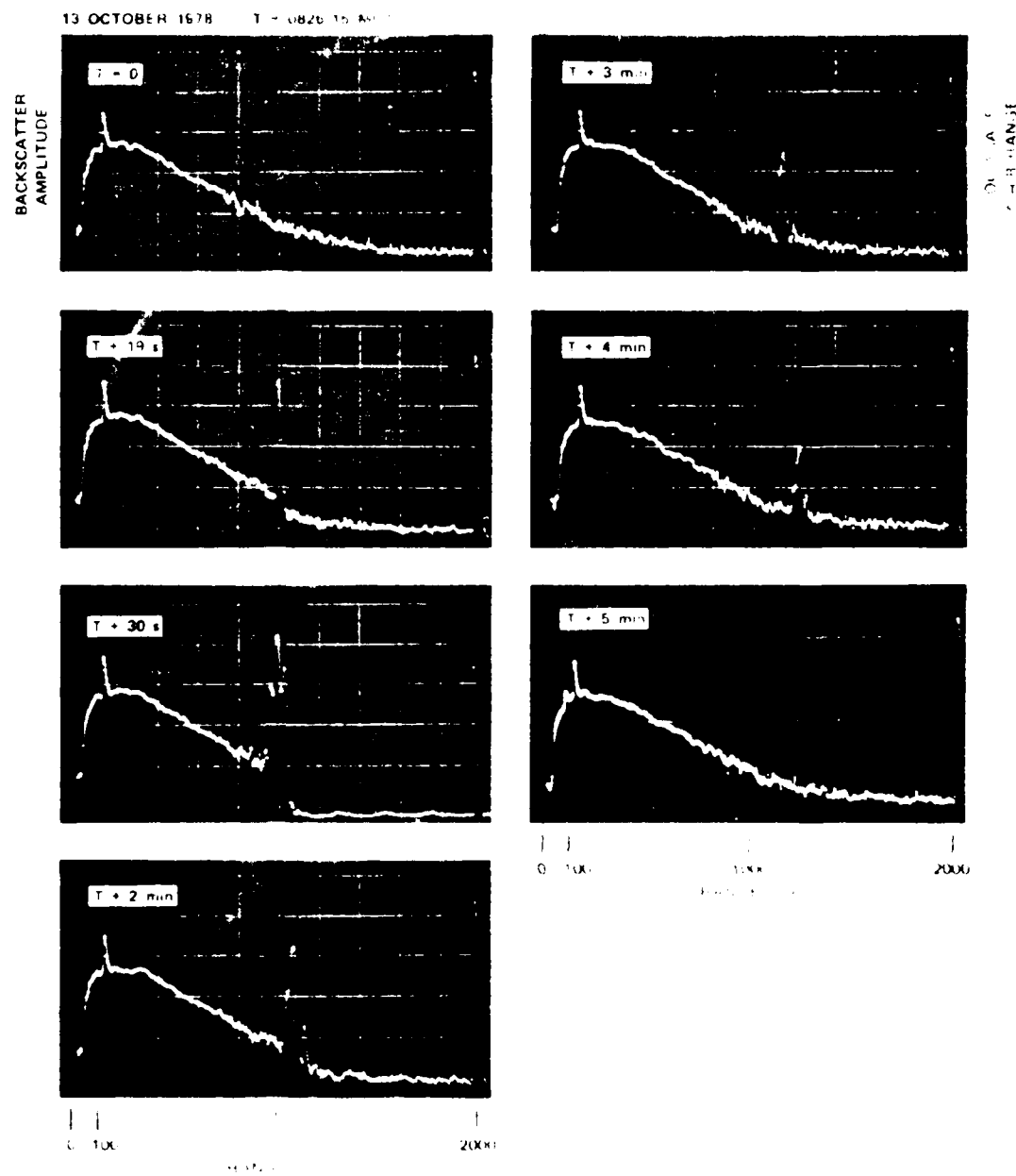


Figure 51. Difference between Ruby and CO<sub>2</sub> optical depths (F-<sup>-7</sup>).



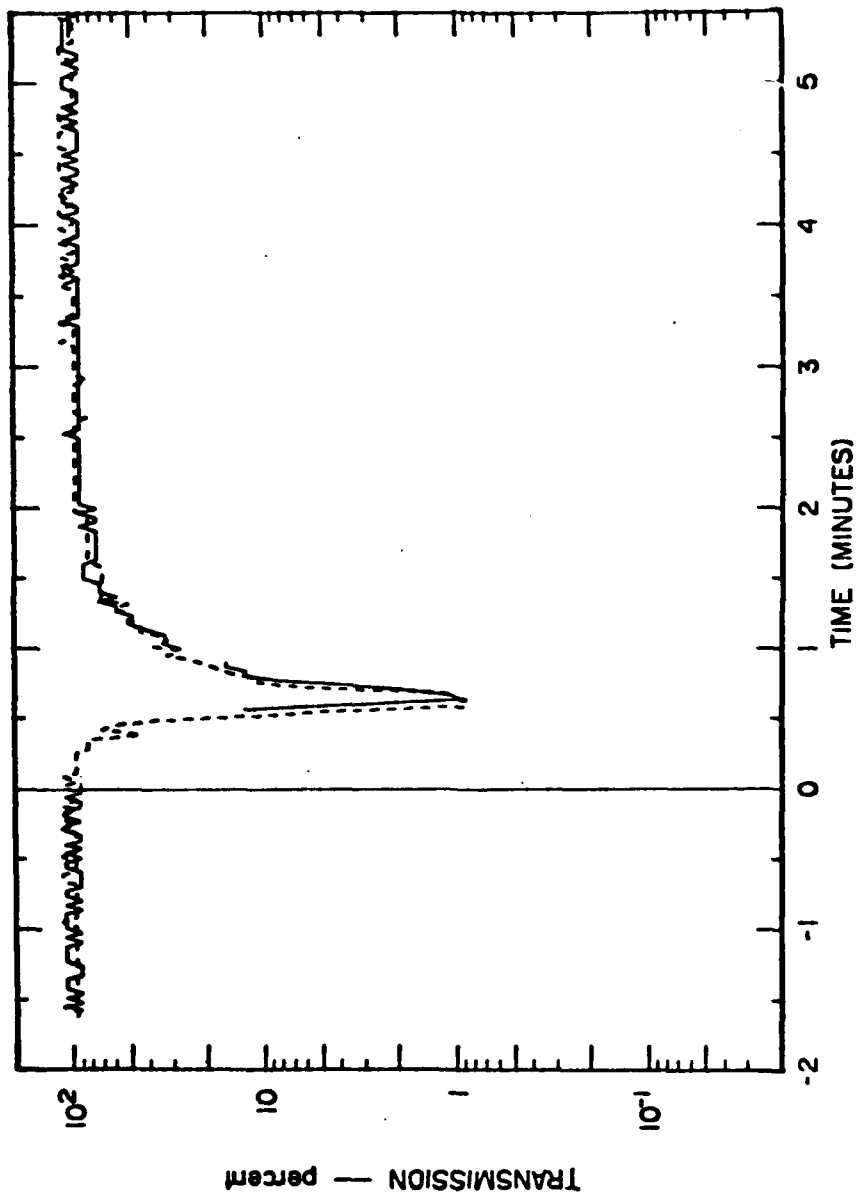


Figure 53. Transmission observed by the two-wavelength lidar system (1-8).

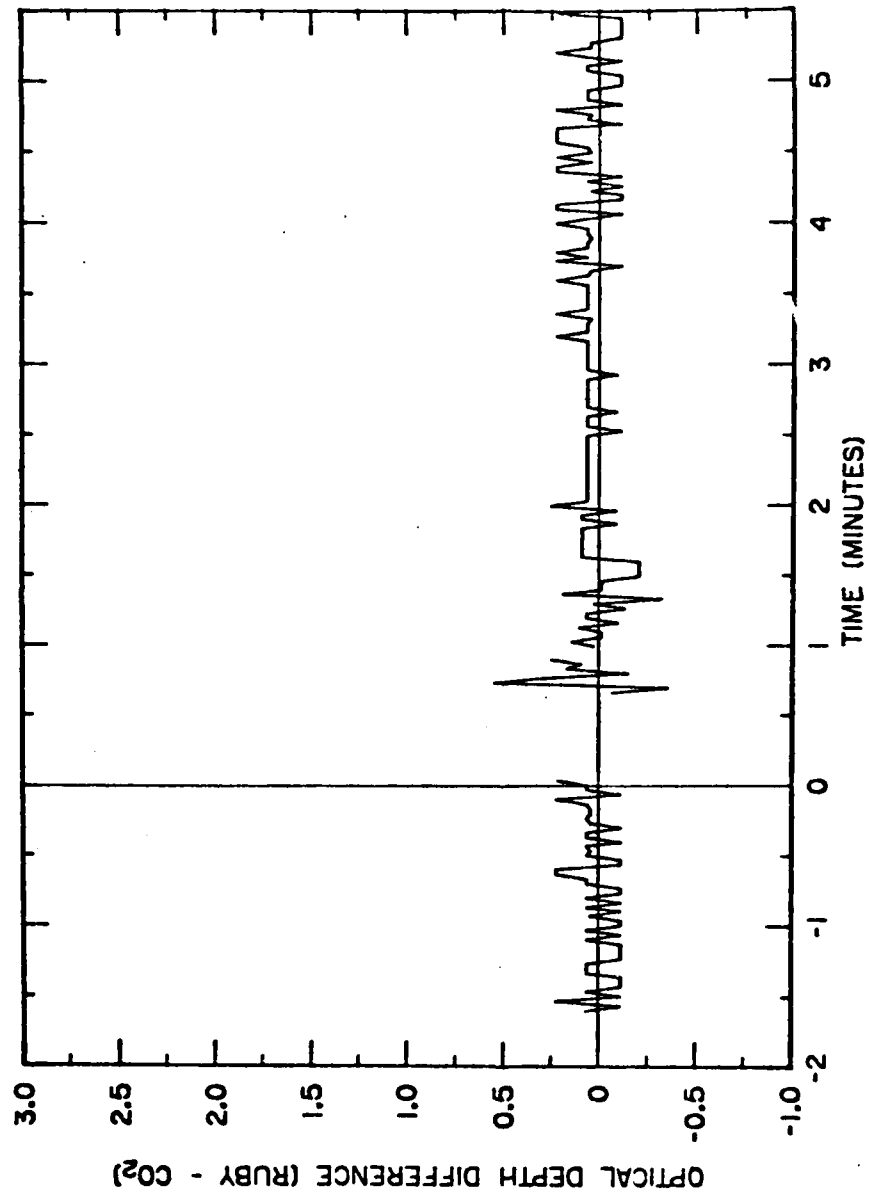


Figure 54. Difference between Ruby and CO<sub>2</sub> optical depths (F-8).

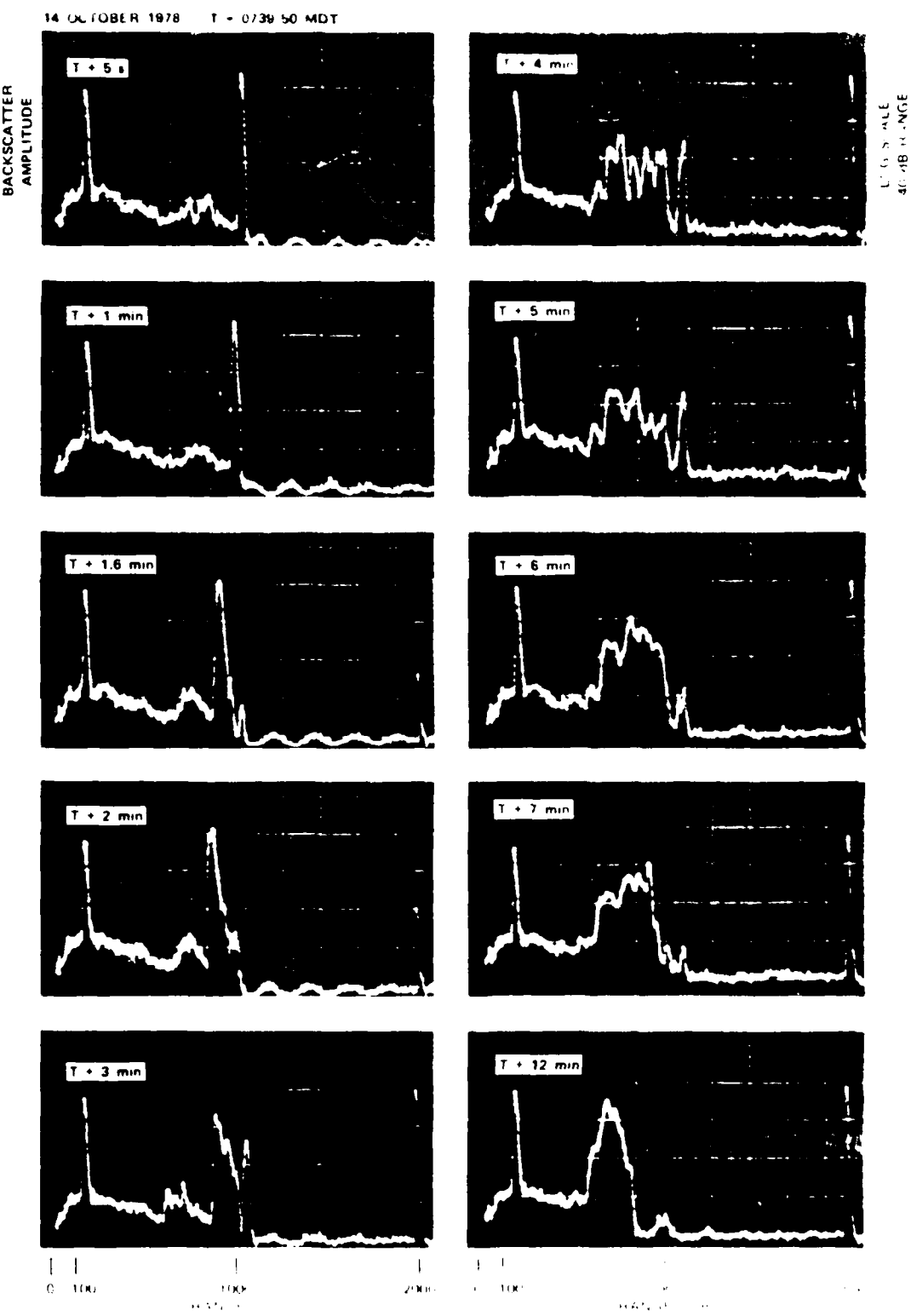


FIG. 1. A plasma event (L = 10, R = 10 m) in the E region.

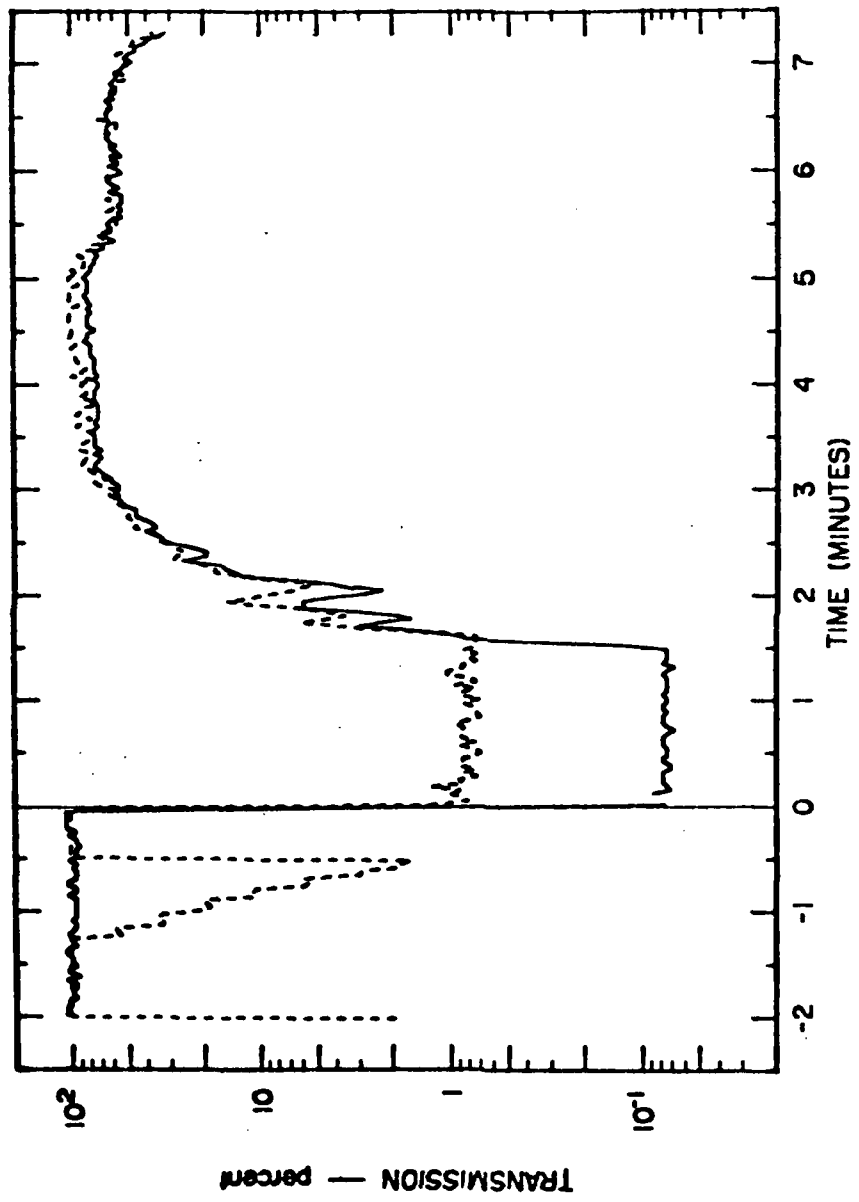


Figure 56. Transmission observed by the two-wavelength lidar system (E-5).

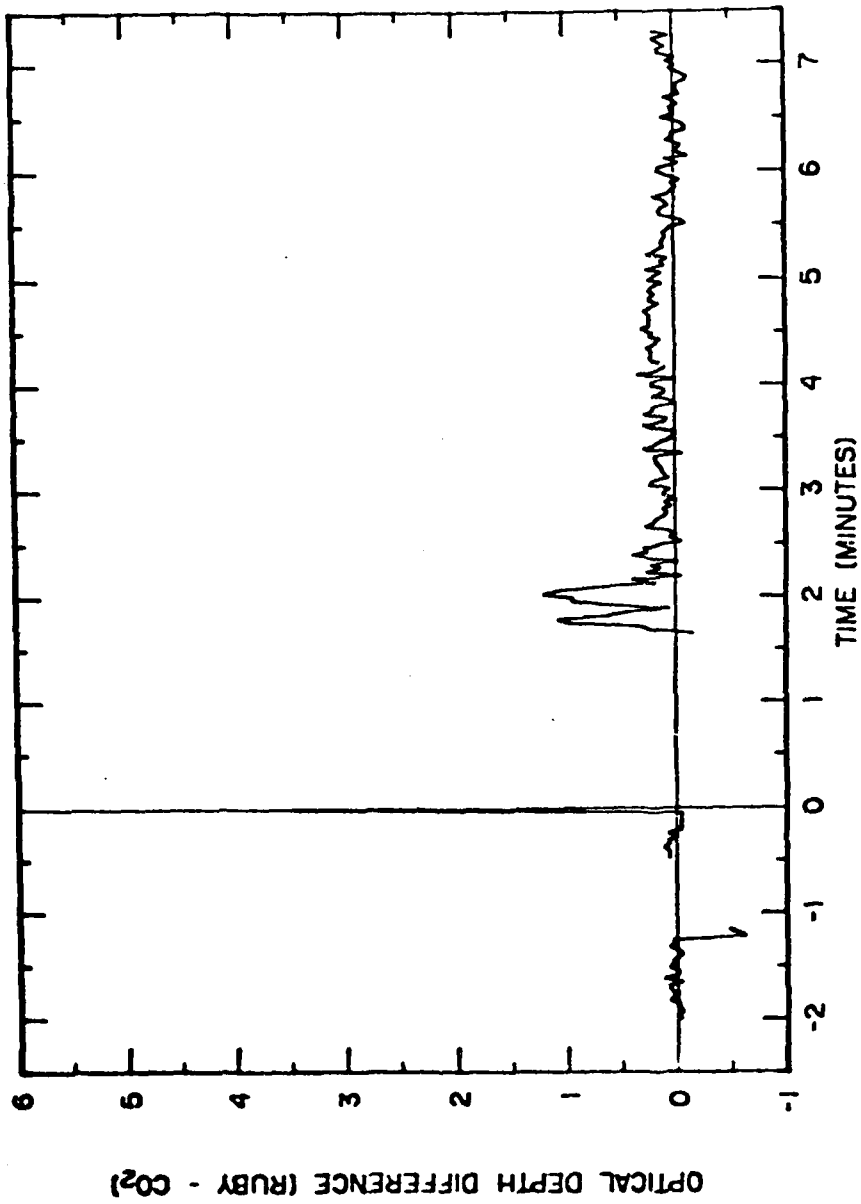


Figure 57. Difference between Ruby and CO<sub>2</sub> optical depths (E-1).

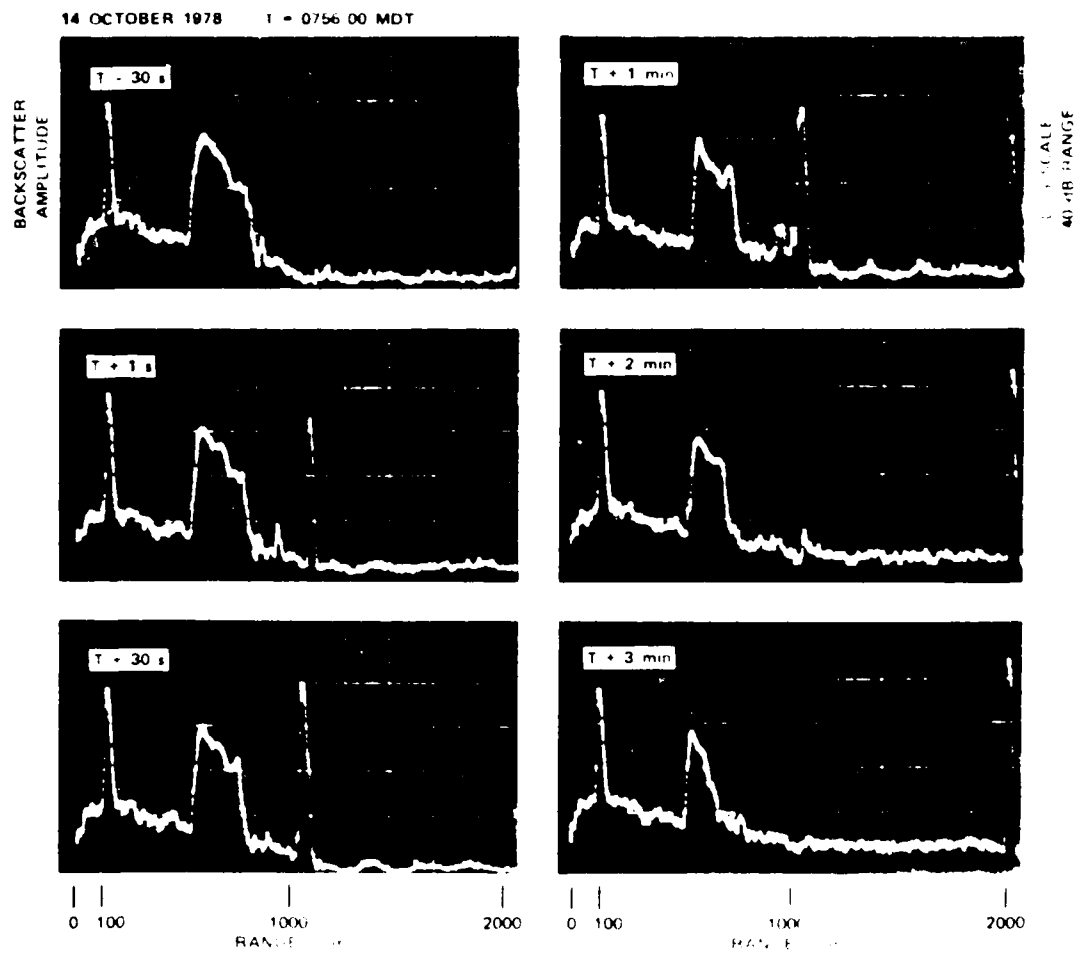


Fig. 1. Ionospheric event (Ref. 11, October 1978).

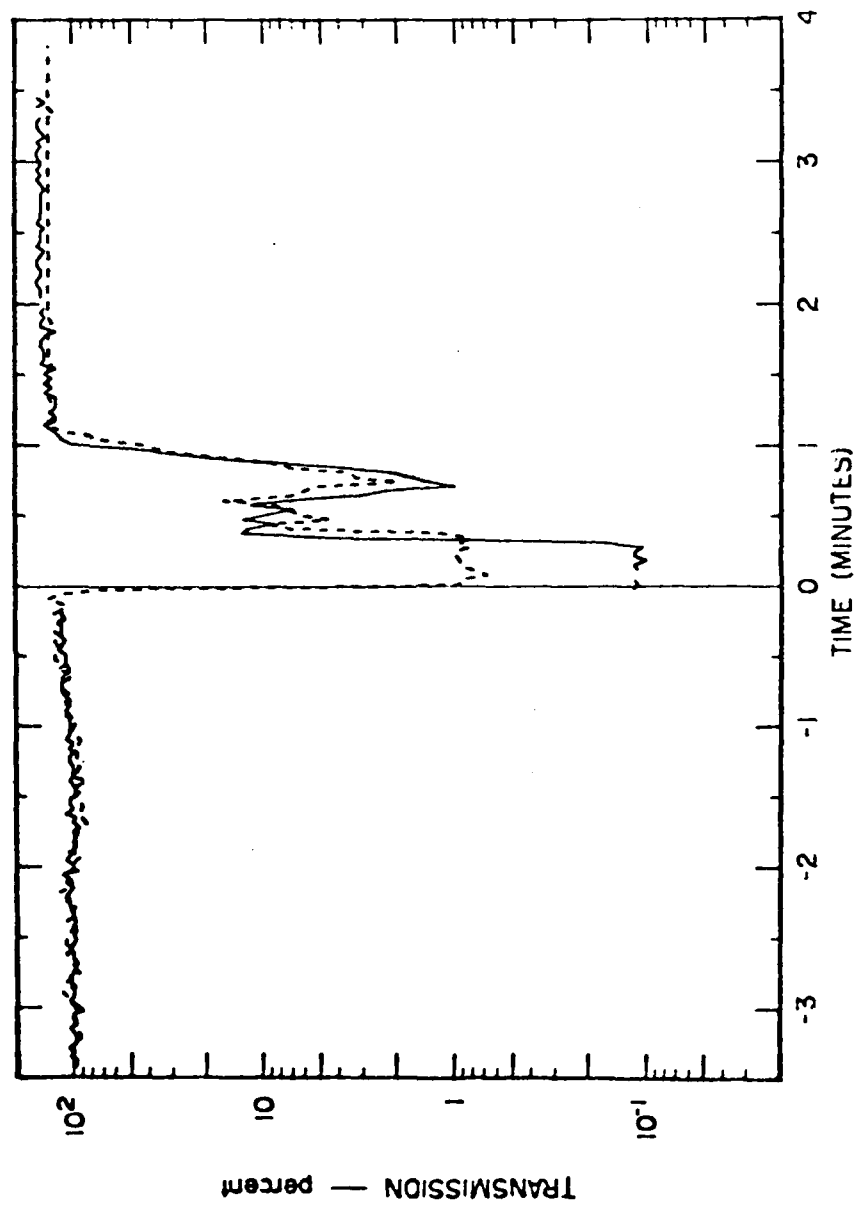


Figure 59. Transmission observed by the two-wavelength lidar system (L-6).

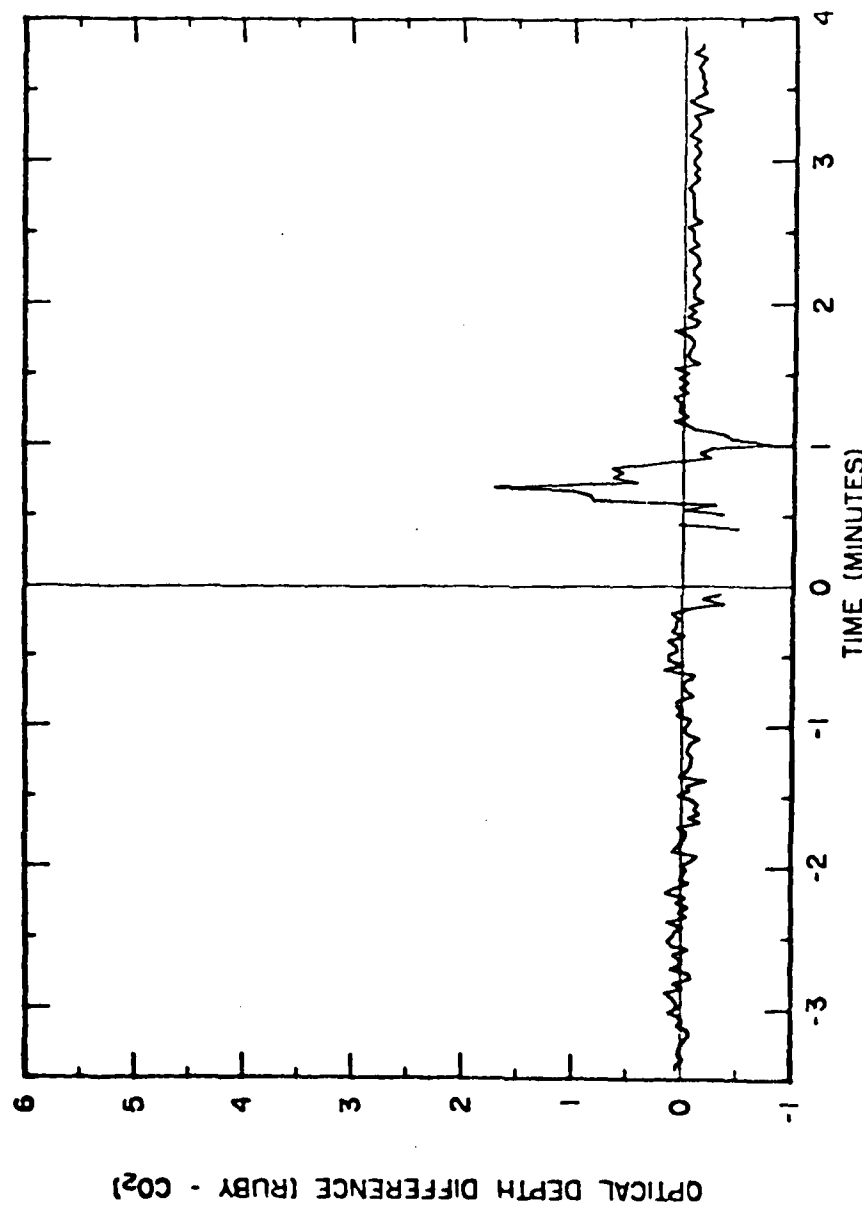


Figure 60. Difference between Ruby and CO<sub>2</sub> optical depths (E-6).

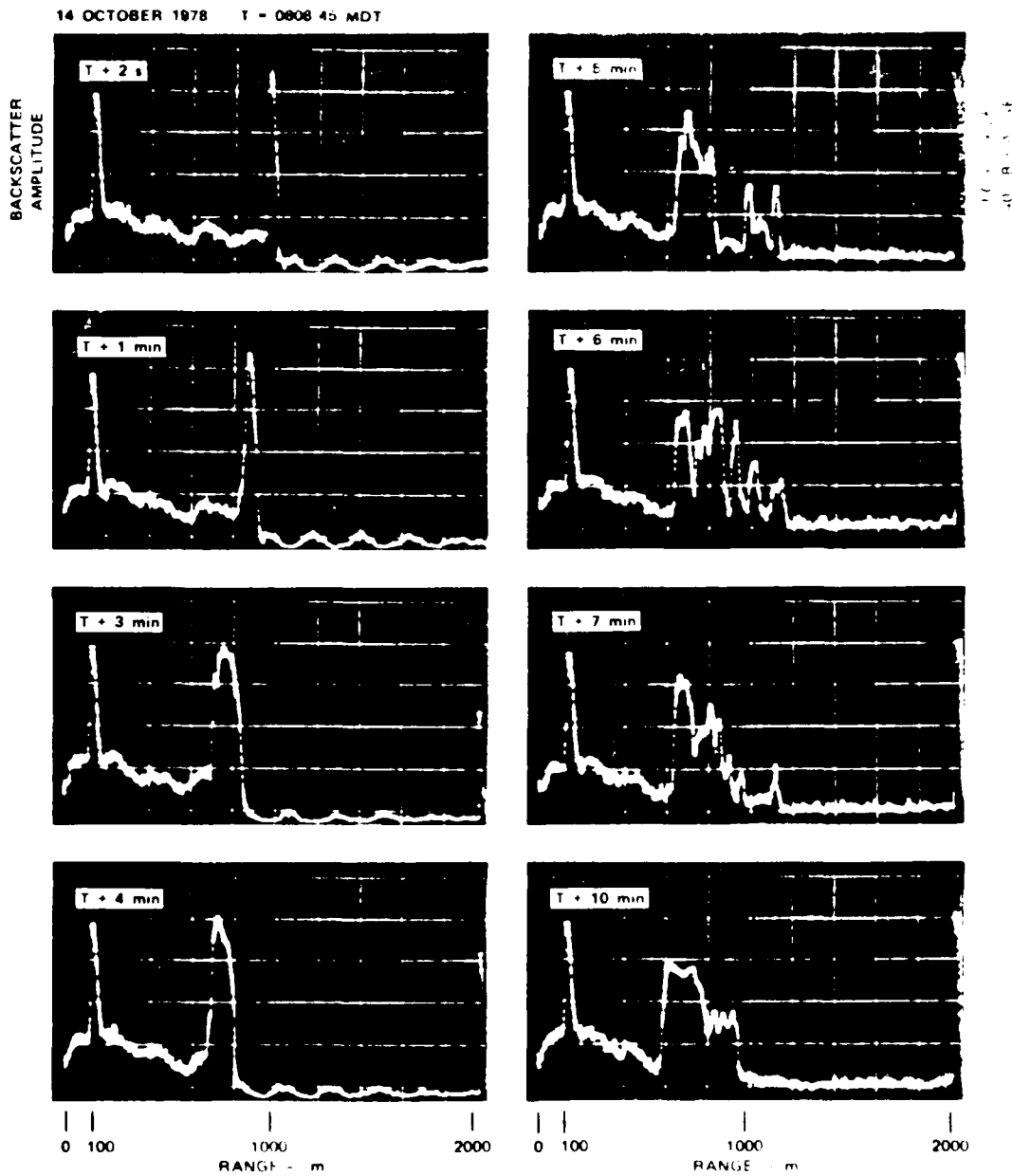


Figure 10. Radar event line 10.

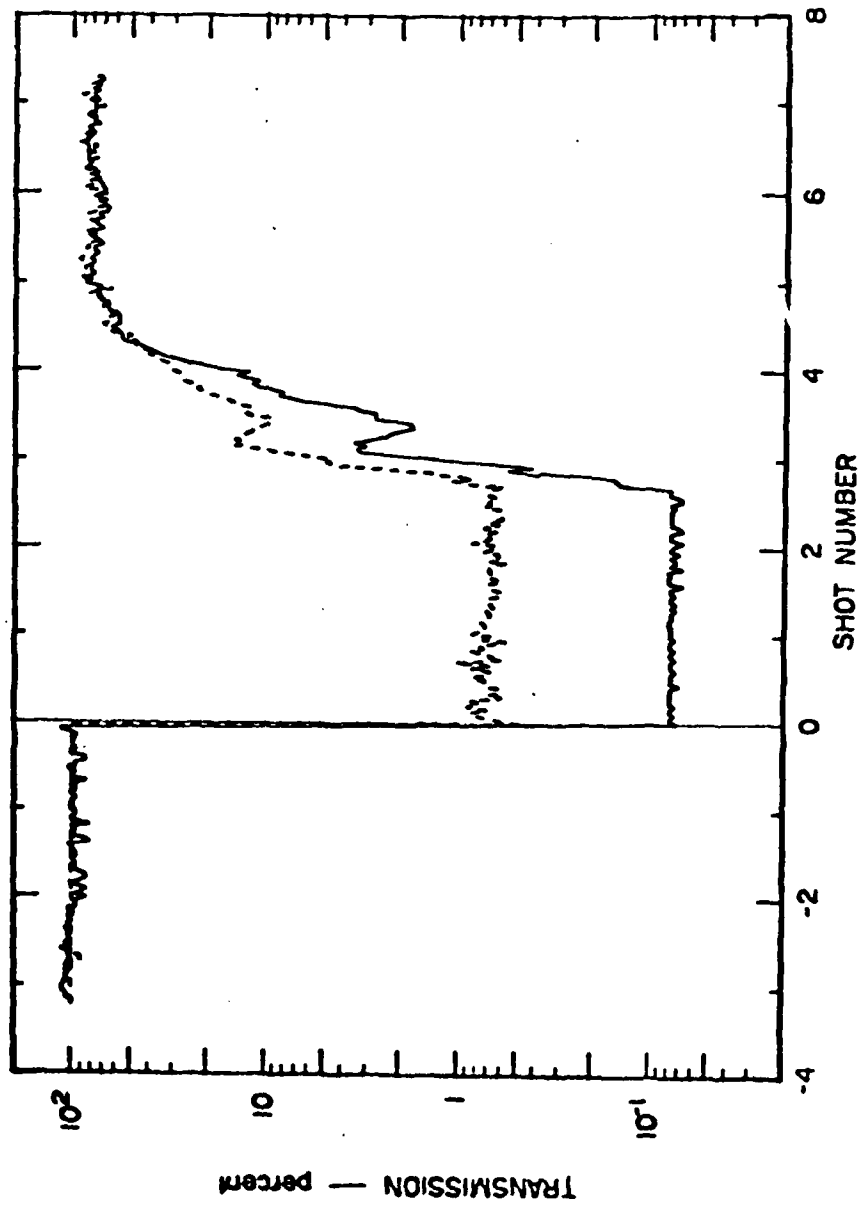


Figure 62. Transmission observed by the two-wavelength lidar system (E-7).

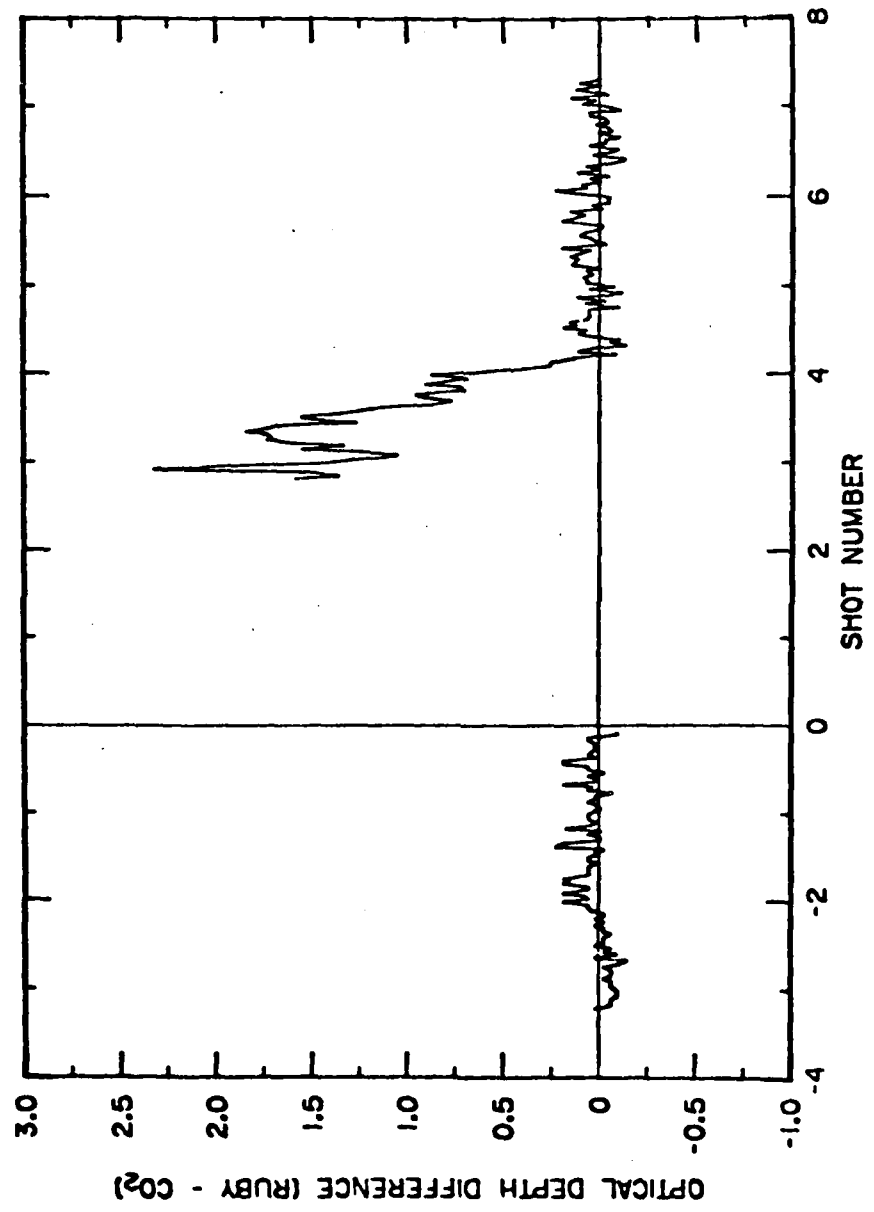


Figure 63. Difference between Ruby and  $\text{CO}_2$  optical depths (E-7).

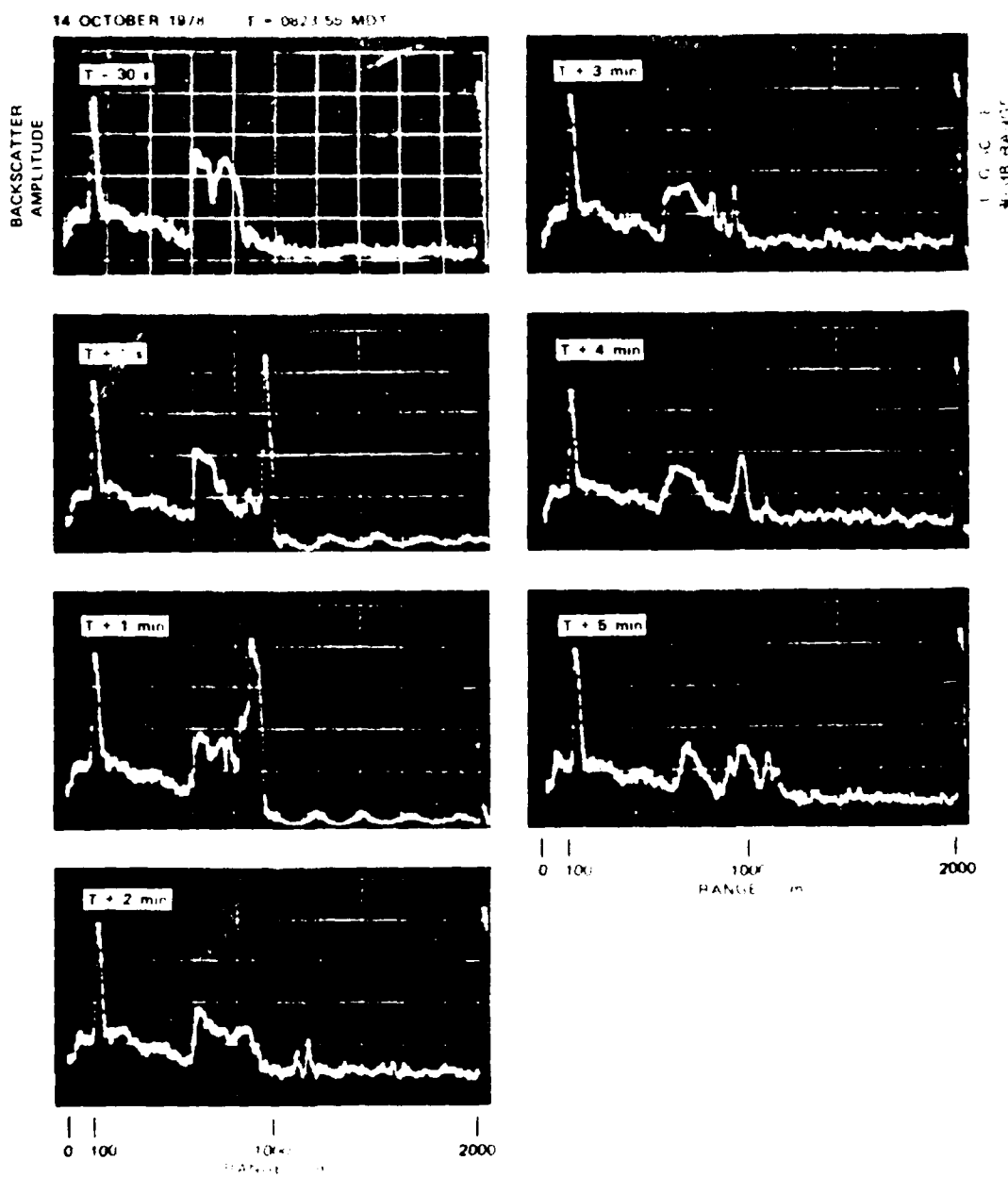


FIG. 1. Six panels of 14 October 1978 10.6  $\mu$ m backscatter data.

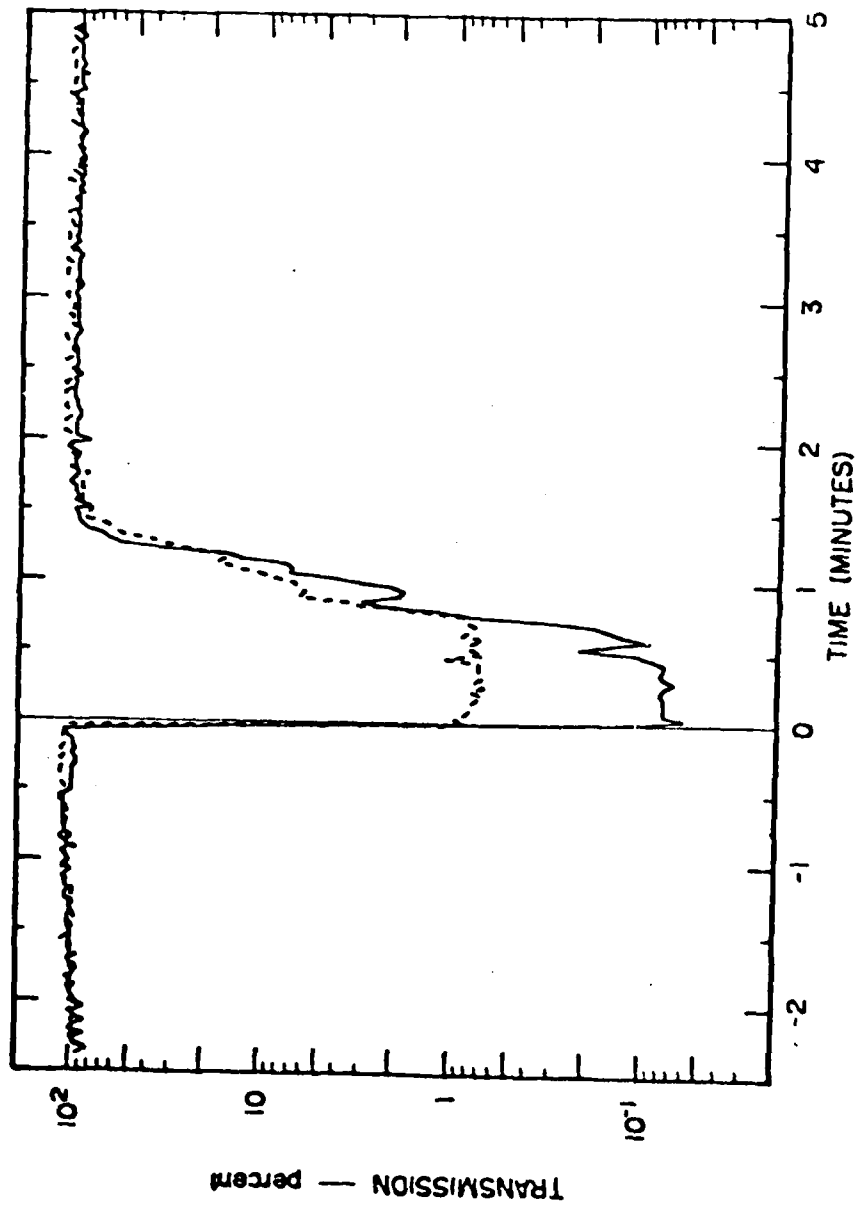


Figure 65. Transmission observed by the two-wavelength lidar system (E-8).

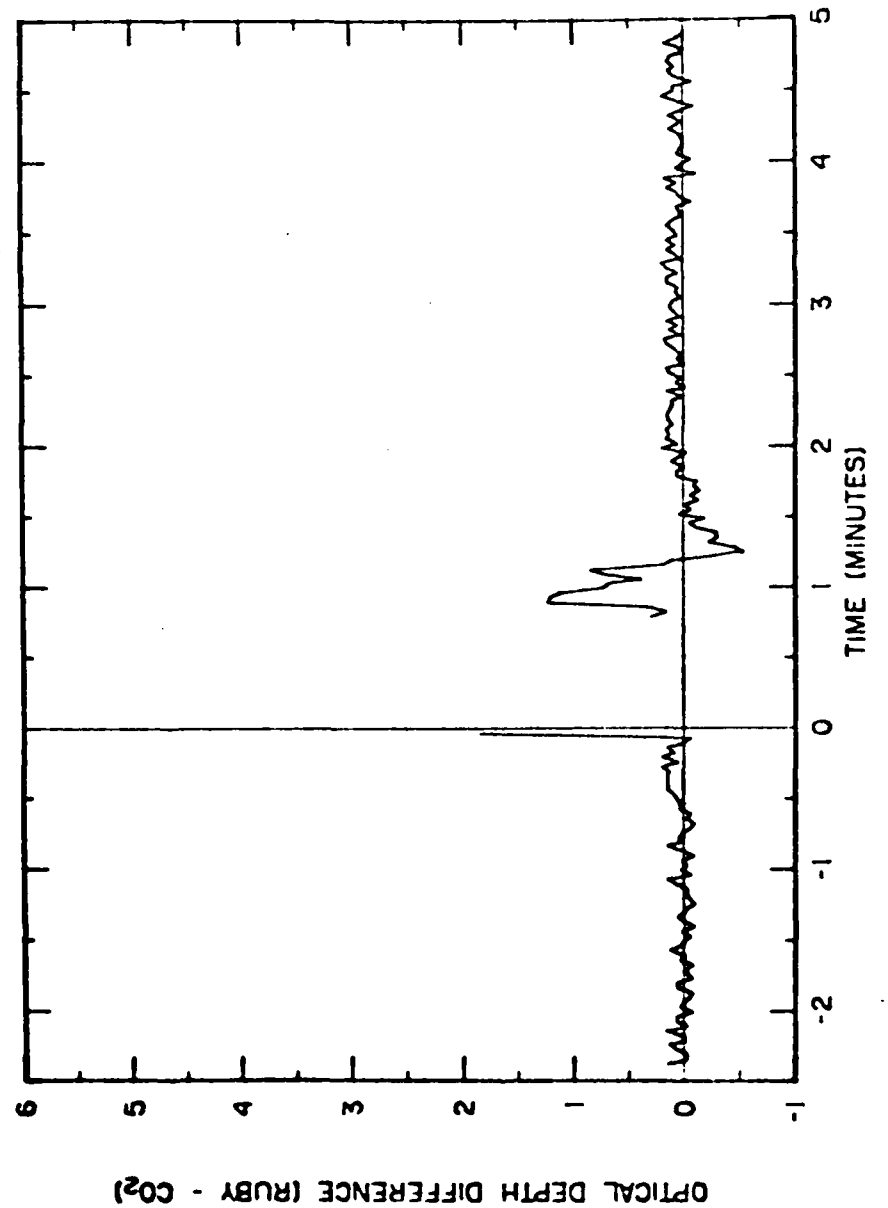


Figure 66. Difference between Ruby and CO<sub>2</sub> optical depths (E-8).

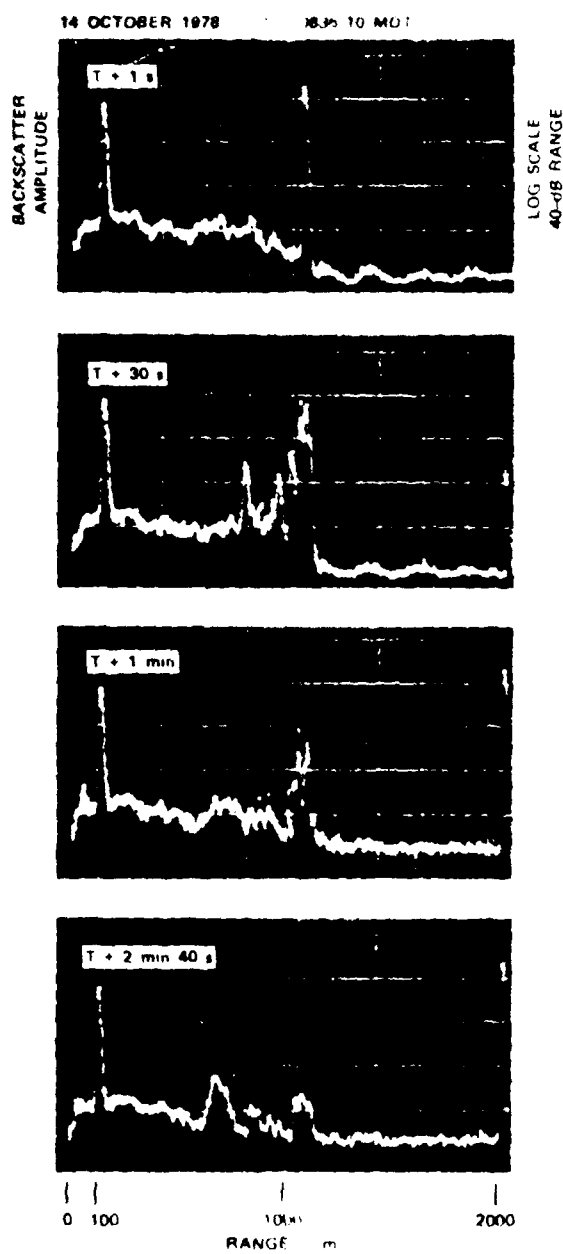


Figure 67. Event 1978-11-14-1835 backscatter data.

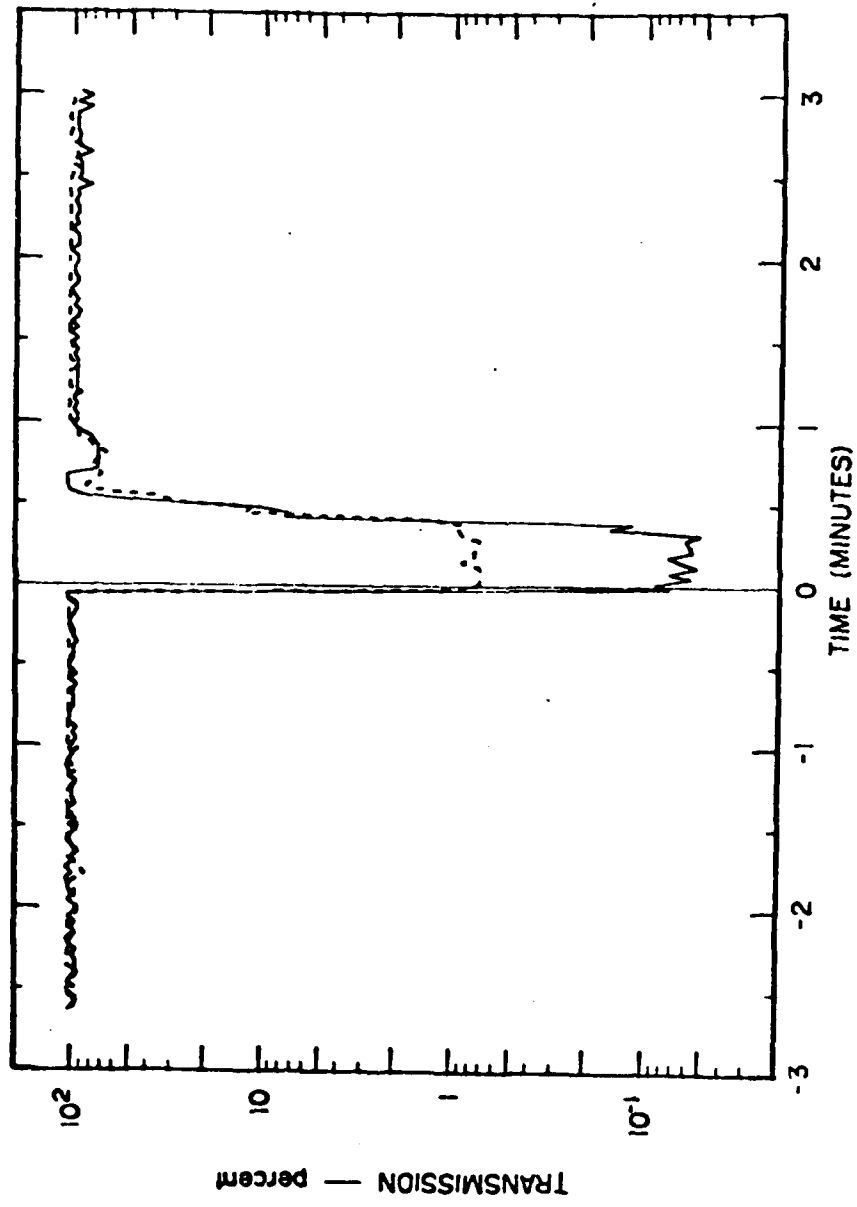


Figure 68. Transmission observed by the two-wavelength lidar system (E-9).

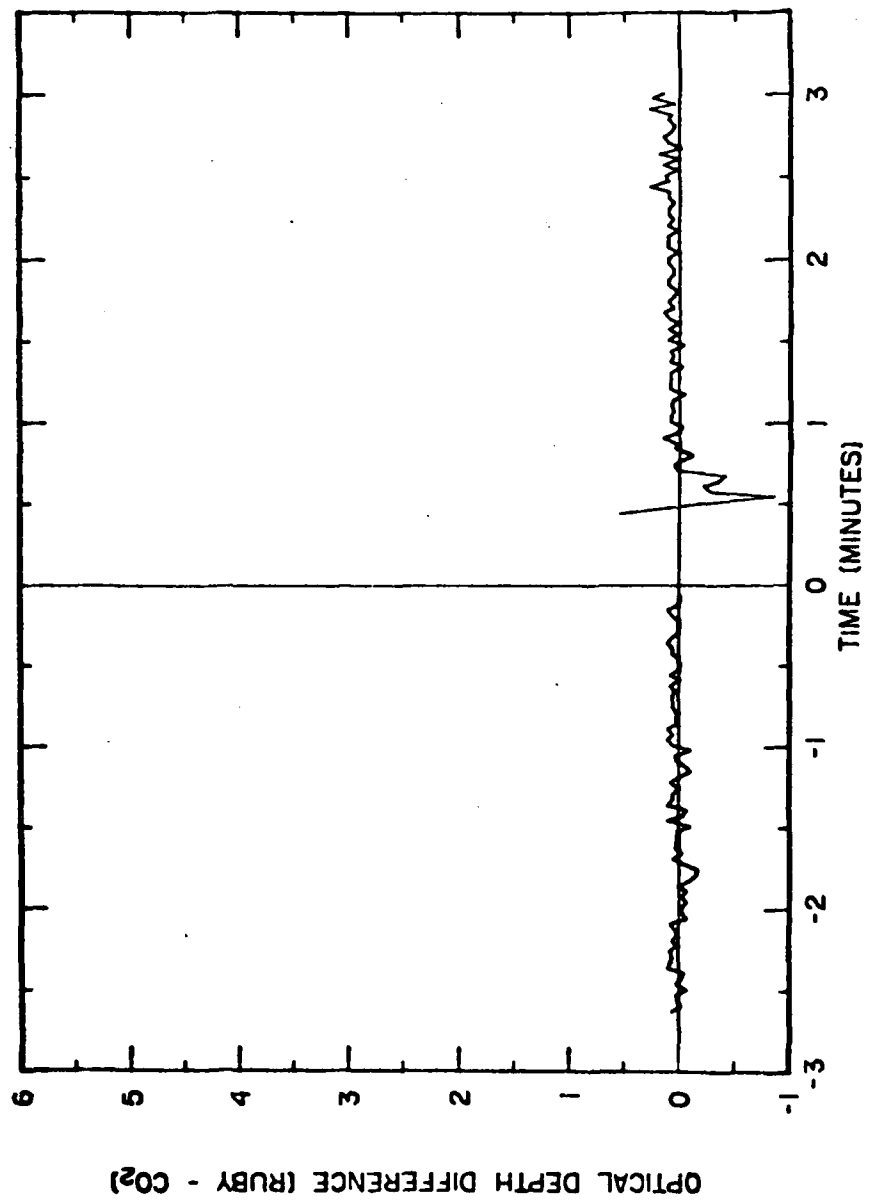
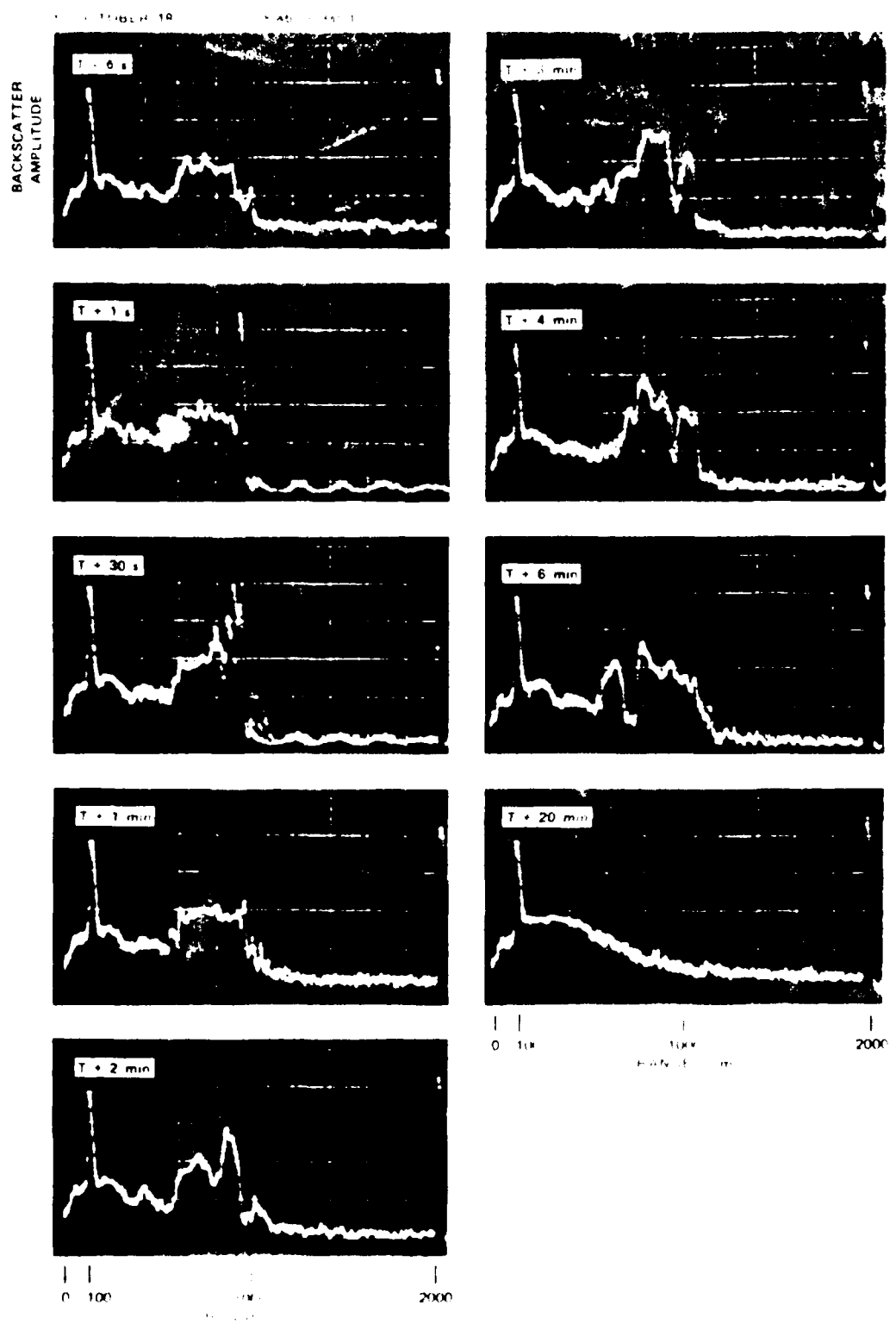


Figure 69. Difference between Ruby and  $\text{CO}_2$  optical depths (E-9).



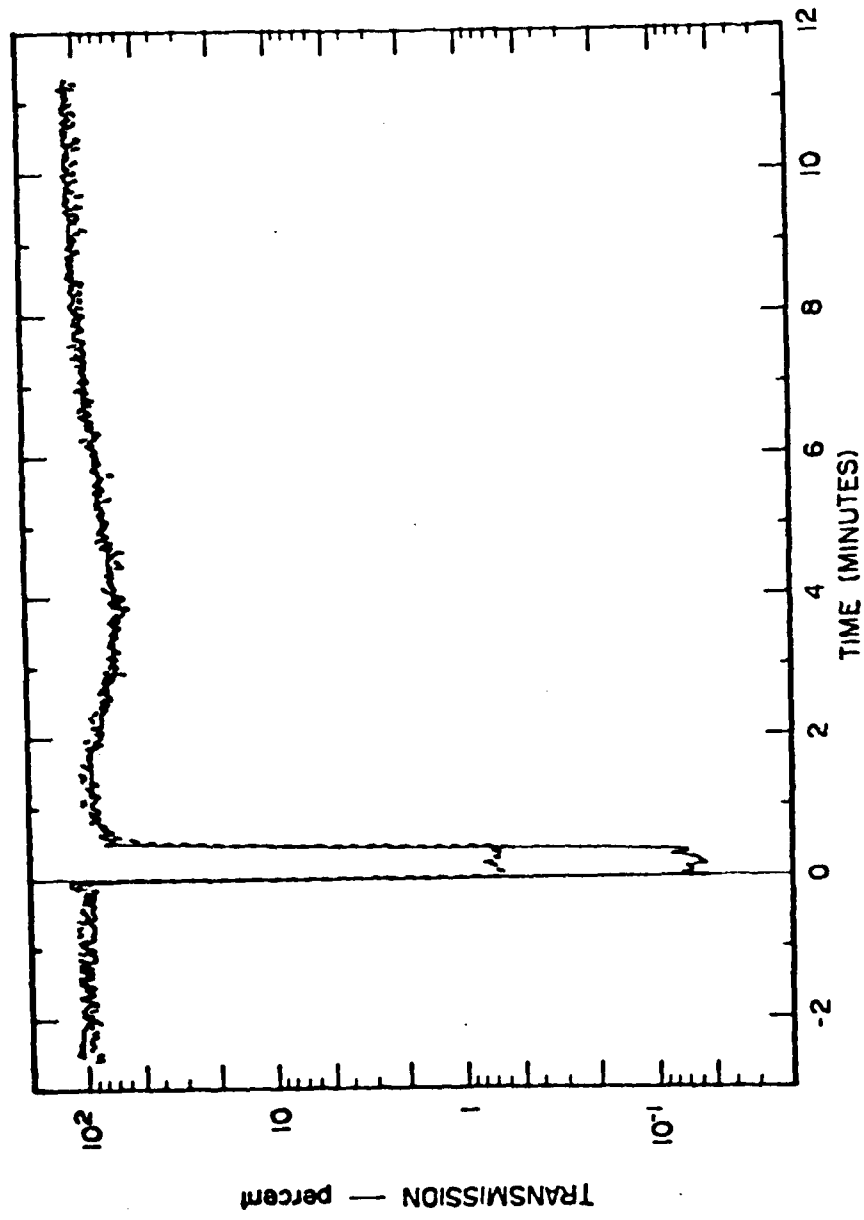


Figure 71. Transmission observed by the two-wavelength lidar system (E-10).

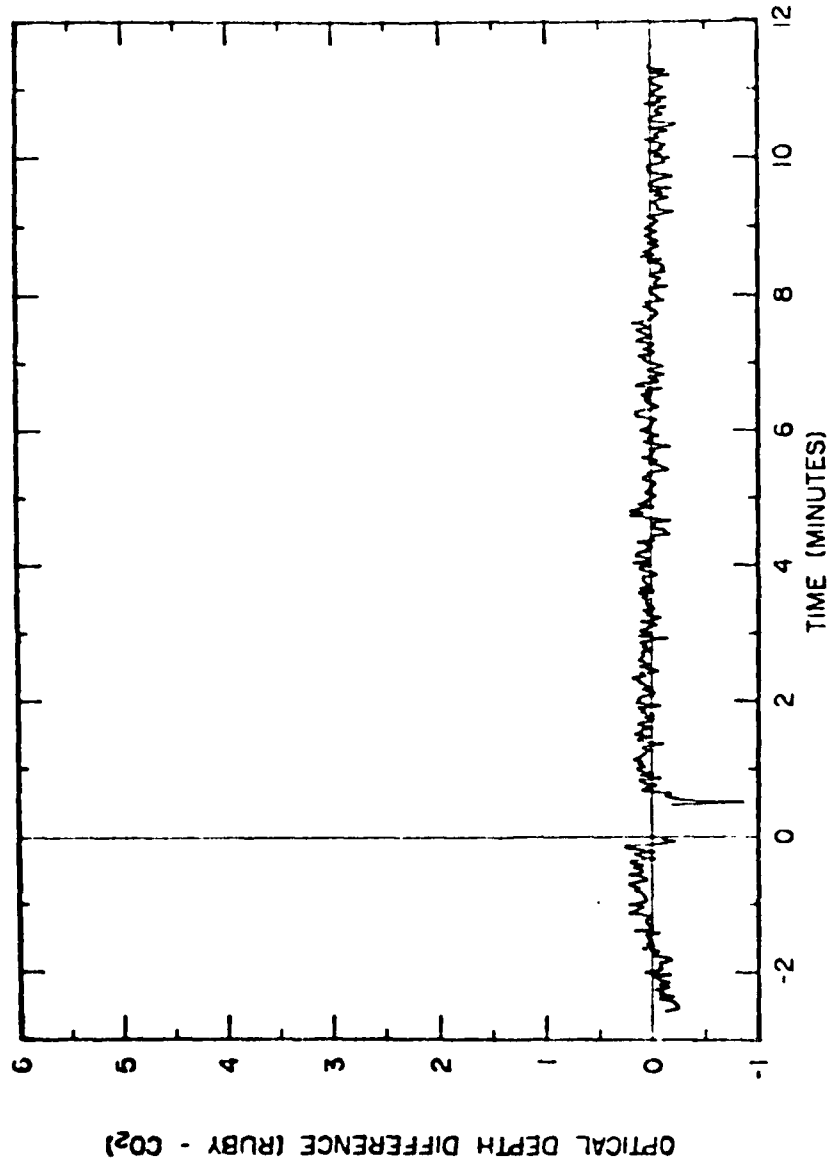
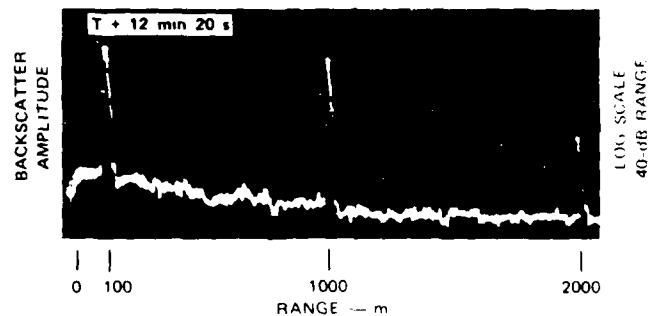


Figure 72. Difference between Ruby and CO<sub>2</sub> optical depths (E-10).

14 OCTOBER 1978 T = 1056 MDT



LOG SCALE  
40-dB RANGE

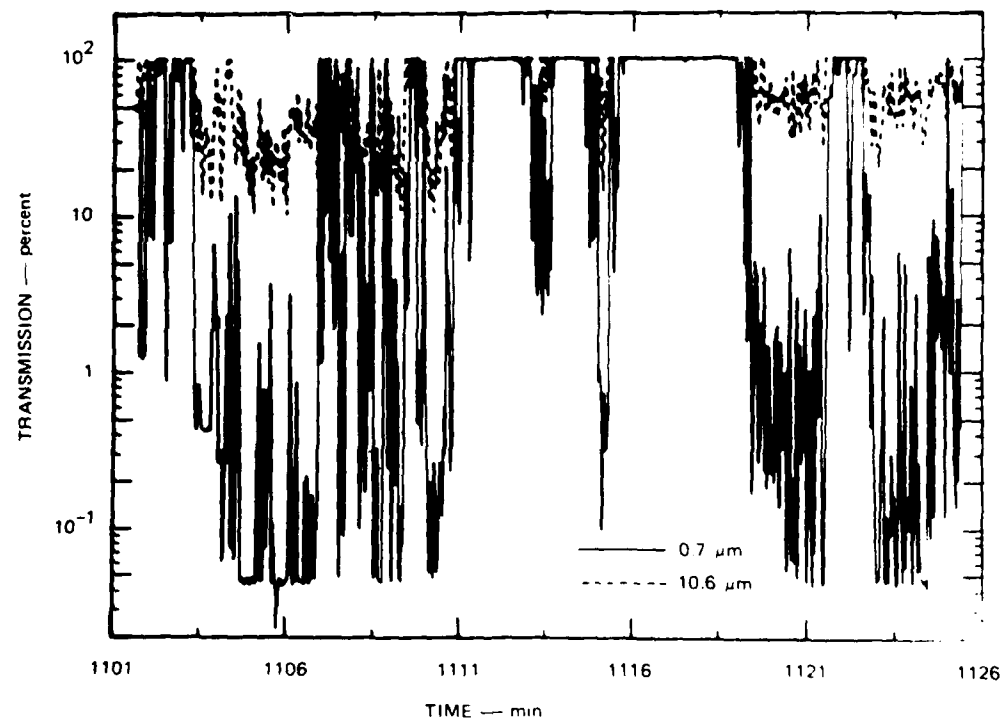


Figure 73. Event G-1 10.6  $\mu$ m backscatter data and two-wavelength transmission.

14 OCTOBER 1978

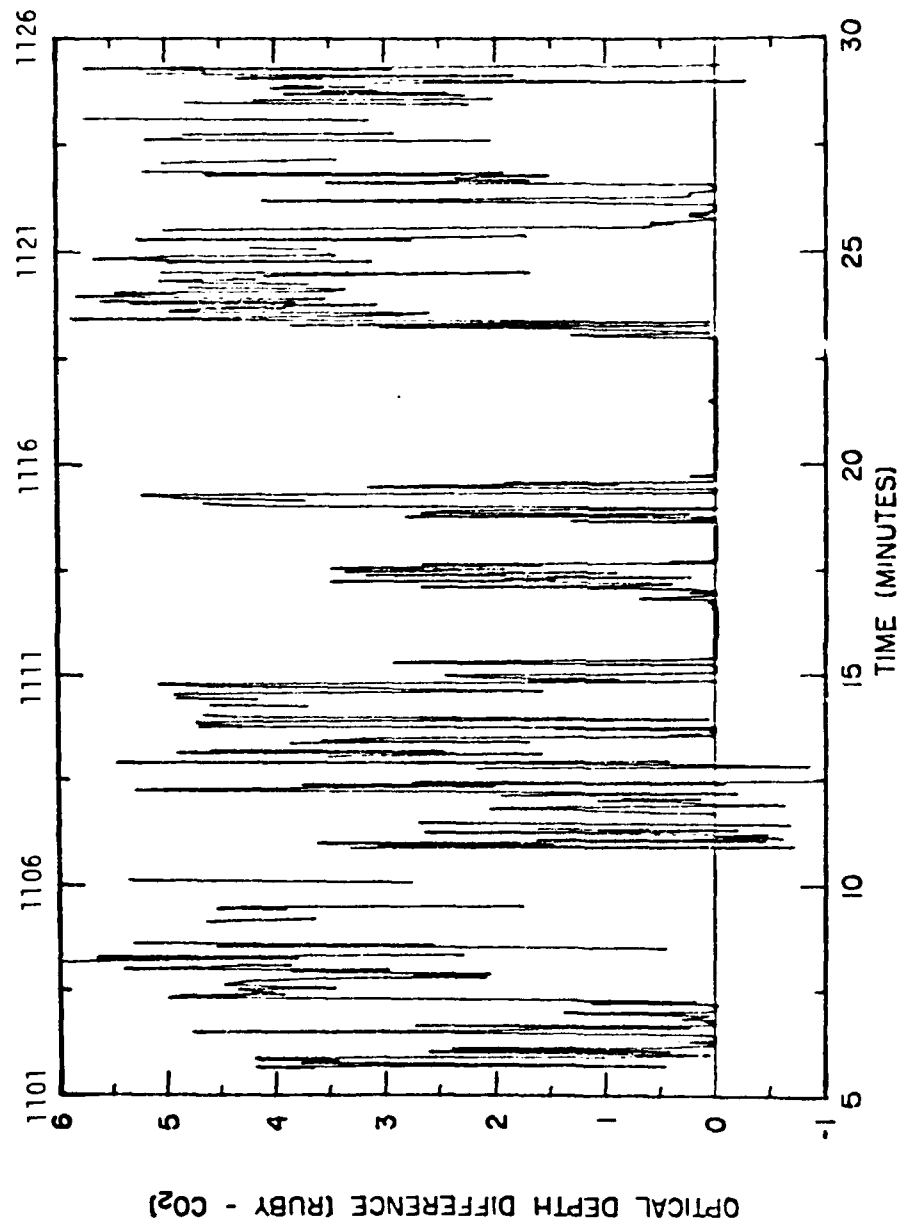


Figure 74. Difference between Ruby and CO<sub>2</sub> optical depths (G-1).

#### REFERENCES

1. Uthe, E. E., and R. J. Allen, 1975, "A Digital Read Time Lidar Data Recording, Processing, and Display System," Optical and Quantum Electronics, 7:121.
2. Van der Laan, Jan E., 1979, Lidar Observations at  $0.7\mu\text{m}$  and  $10.6\mu\text{m}$  Wavelengths during Dusty Infrared Test-I (DIRT-I), ASL-CR-79-0001-2, US Army Atmospheric Sciences Laboratory, White Sands Missile Range, NM.
3. Lindberg, James D., 1979, Measured Effects of Battlefield Dust and Smoke on Visible, Infrared and Millimeter Wavelength Propagation: A Preliminary Report on Dusty Infrared Test-I (DIRT-I), ASL Technical Report 0021, US Army Atmospheric Sciences Laboratory, White Sands Missile Range, NM.

